Retrofitted Solar Thermal System for Domestic Hot Water for Single Family Electrically Heated Houses

Development and testing

Ricardo Bernardo

Division of Energy and Building Design
Department of Architecture and Built Environment
Lund University
Faculty of Engineering LTH, 2010
Report EBD-T--10/13

Lund University

Lund University, with eight faculties and a number of research centres and specialized institutes, is the largest establishment for research and higher education in Scandinavia. The main part of the University is situated in the small city of Lund which has about 110 000 inhabitants. A number of departments for research and education are, however, located in Malmö. Lund University was founded in 1666 and has today a total staff of 6 000 employees and 46 000 students attending 274 degree programmes and 2 000 subject courses offered by 63 departments.

Division of Energy and Building Design

Reducing environmental effects of construction and facility management is a central aim of society. Minimising the energy use is an important aspect of this aim. The recently established division of Energy and Building Design belongs to the department of Architecture and Built Environment at the Lund University, Faculty of Engineering LTH in Sweden. The division has a focus on research in the fields of energy use, passive and active solar design, daylight utilisation and shading of buildings. Effects and requirements of occupants on thermal and visual comfort are an essential part of this work. Energy and Building Design also develops guidelines and methods for the planning process.

Retrofitted Solar Thermal System for Domestic Hot Water for Single Family Electrically Heated Houses

Development and testing

Ricardo Bernardo

Licentiate Thesis

Keywords

Domestic hot water, photovoltaic thermal concentrating hybrids, PVT, parabolic reflectors, CPC thermal collector, high solar fraction, retrofitting tank heaters, single family electrically heated houses.

The English language corrected by L. J. Gruber BSc(Eng) MICE MIStructE.
Layout: Hans Follin, LTH, Lund.
Cover photo: Ricardo Bernardo

Printed by Tryckeriet i E-huset, Lund 2010

Report No EBD-T--10/13
Retrofitted Solar Thermal System for Domestic Hot Water Single Family Electrically Heated Houses. Development and testing.
Department of Architecture and Built Environment, Division of Energy and Building Design, Lund University, Lund

ISSN 1651-8136
ISBN 978-91-85147-47-2

Lund University, Lund Institute of Technology
Department of Architecture and Built Environment
Division of Energy and Building Design
P.O. Box 118
SE-221 00 LUND
Sweden

Telephone: +46 46 - 222 73 52
Telefax: +46 46 - 222 47 19
E-mail: ebd@ebd.lth.se
Home page: www.ebd.lth.se

Abstract

In Sweden, there are more than half a million single family houses that use direct electric heating for both domestic hot water production and space heating. These were typically built around the 70s with relatively low insulation levels and large thermal bridges, resulting in poor energy performance. Hence, there is a great need to reduce electricity consumption in these houses. Installing a high solar fraction solar thermal system for domestic hot water production together with an air-to-air heat pump for space heating can significantly decrease energy use. Furthermore, changing windows and adding extra insulation can further contribute to this decrease. When the new solar thermal system is installed, the existing water tank heater can be retrofitted. Hence, the system investment cost can be significantly reduced since solar storage tanks are one of the most expensive components of a solar thermal system. A one-axis tracking PV/T concentrating hybrid and a CPC thermal collector were analysed in connection with the solar thermal system. The PV/T collector produces both hot water and electricity. The CPC collector design aims to adapt the solar production to the yearly consumption profiles. Hence, higher annual solar fractions can be achieved.

Outdoor measurements were carried out to characterise the PV/T concentrating hybrid and the CPC collector. Afterwards, the measured parameters were used in specially created TRNSYS models validated against the measured data. As regards the retrofitted system, simulations were carried out to determine what is the system configuration achieving the highest annual performance. A prototype with such configuration was built at the laboratory for continuous performance monitoring.

Measurement results showed that the efficiency values of the PV/T tracking concentrating hybrid are significantly lower than those of conventional flat plate collectors and PV modules. Also, the usable incident irradiation on a one-axis tracking concentrating surface is lower than the usable irradiation incident on a flat tilted surface. Even though the studied hybrid has margin for improvement, the combination of low efficiencies with low usable irradiation levels makes it difficult for concentrating PV/T hybrids to compete with conventional alternatives, especially in countries

where the annual beam irradiation values are low. On the other hand, the studied CPC collector system achieves a higher annual solar fraction than a conventional flat plate collector system. Also, it makes use of less absorber surface, one of the most expensive components in the collector. Hence, the decrease in absorber area together with the performance increase must compensate for the cost of extra materials such as reflectors, glass and frames.

Finally, several different configurations for the retrofitted solar thermal system were analysed. The best performing retrofitted system achieves an annual solar fraction comparable with that of a conventional solar thermal system. This means that, if the retrofitting proves to be cost-effective, it can be a very interesting solution since it can be used in almost any kind of thermal storage. Moreover, thermal collectors can be connected not only with existing tanks but also with new water heaters, accessing a world-wide, well developed industry.

Future research work aims to validate the retrofitting system models against measured data of the prototype built at the laboratory. An economical assessment for the retrofitted solar thermal system will be included. A new simulation model of a conventional Swedish single family house, including the validated retrofitted system, will also be built. Finally, the influence of every renovation measure on the house energy performance will be assessed.

Contents

Acknowledgments

This Licentiate thesis was written as part of my Ph.D. degree supported by Swedish Energy Authority and the Marie Curie program, SolNet - Advanced Solar Heating and Cooling for Buildings - the first coordinated international PhD education program on Solar Thermal Engineering.

I wish to thank my supervisor Björn Karlsson for valuable work discussions and positive attitude. He is one of the best I have met in the solar energy field when it comes to interpretation of results and creative solutions.

For being a present co-worker and a friend since I arrived at the department, I am grateful to Henrik Davidsson. He has been one of the great contributors in teaching me Swedish especially at the very beginning. I am especially grateful to Johan Nilsson for valuable discussions and close support during challenging times of the project. Åke Blomsterberg was very helpful providing a critical view of the work and proof reading this manuscript. I would like to thank Håkan Håkansson for the support with measurements. His capability to come up with new solutions and ideas is notable. Bengt Perers is acknowledged for the help I got in my practical work. I can probably say that he was one of the persons from whom I have learned the most concerning practical work. His help on the simulation software and interpretation of the results was also important. Peter Krohn is acknowledged for helping to properly install and control the data monitoring system. I also would like to thank Gunilla Kellgren for all the help and support.

For everyone at the Division of Energy and Building Design I wish to express my gratitude for making me feel welcome since the very beginning. The biggest reward of working abroad is, without a doubt, the culture and social experience which they are an important part of.

Finally, it is with particular pleasure that I express my gratitude to my supporting family for all the help during this period. My wonderful grandparents have been tireless in keeping me in touch with home despite the distance. They have mailed me a bit of everything from Portugal such as newspapers, Porto wine and even my favourite cake. They have been very interested in hearing me refute many of the Swedish myths so common

in south Europe. Some of their favourites are the non existence of polar bears, that fruit does exist in Sweden and that the temperature reaches 25°C in the summer. I am especially grateful also to my parents and grandfather for being a constant and active source of information related to the research subject.

Nomenclature

Latin

A_c	Collector area	m^2
$A_{active\ elect.}$	Electric active glazed area of the hybrid	m^2
$A_{active\ thermal}$	Thermal active glazed area of the hybrid	m^2
A_{Hybrid}	Total glazed area of the hybrid	m^2
$b_{0\_electric}$	Electric incidence angle modifier coefficient	-
$b_{0\_thermal}$	Thermal incidence angle modifier coefficient	-
C	Geometrical concentration ratio	-
C_p	Heat capacity	J/(kg°C)
dT_m/dt	Mean time derivate of the average fluid temperature during the time step	°C/s
dV/dt	Flow rate	m^3/s
FF	Fill Factor	-
F'	Collector efficiency factor	-
F'U	Heat loss coefficient	W/(m^2°C)
$F'U_0$	Heat loss coefficient when $(T_m-T_{amb})=0$	W/(m^2°C)
$F'U_1$	Temperature dependence of the heat loss coefficient	W/(m^2°C^2)
$F'U_u$	Wind speed dependence of the heat loss coefficient	Ws/(m^3°C)
$F'(\tau\alpha)_n=\eta_0(\theta=0)$	Zero loss efficiency for beam radiation at normal incidence angle	-
$F'(\tau\alpha)_\theta$	Zero loss efficiency for beam radiation at incidence angle θ	-
G	Global solar radiation	W/m^2
Gb	Beam solar radiation	W/m^2
G_d	Diffuse solar radiation	W/m^2
I	Current	A
I_L	Light generated current	A
I_{mp}	Current at maximum power point	A
I_{sc}	Short circuit current	A
I_0	Diode leakage current in the absence of light	A
k	Boltzmann's constant	J/K

$K_b(\Theta)$	Beam incidence angle modifier	-
$K_{b\_electric}(\Theta)$	Electric beam incidence angle modifier	-
$K_{b\_thermal}(\Theta)$	Thermal beam incidence angle modifier	-
K_d	Diffuse incidence angle modifier	-
K_T	Beam electric efficiency dependence on temperature	%/°C
n	Idealist factor of the diode	-
q	absolute value of the electronic current	C
Q	Power	W
$Q_{electric}$	Electric power	W/m^2
$Q_{thermal}$	Thermal power	W/m^2
r	Reflectance coefficient of the reflector	-
RRR	Resources/Reserves Ratio	-
R_L	Load resistance	Ω
R_s	Series resistance	Ω
R_{sh}	Shunt resistance	Ω
T	Temperature	°C
T_{amb}	Ambient temperature	°C
$T_{auxiliar}$	Preset temperature of the auxiliary heater	°C
T_{in}	Inlet fluid temperature	°C
T_m	Mean fluid temperature in the absorber	°C
T_{out}	Outlet fluid temperature	°C
T_{solar}	Solar hot water temperature in the upper part of the retrofitted tank	°C
u	Wind speed near the collector	m/s
V	Voltage	V
V_{mp}	Voltage at maximum power point	V
V_{oc}	Open circuit voltage	V
$(mC)_e$	Effective thermal capacitance including piping for the collector array	$J/(m^2°C)$

Greek

α	Absorptance coefficient	-
η	Efficiency	-
$\eta_{b\_electric}$ (25°C)	Beam electric efficiency at 25°C outlet fluid temperature	-
$\eta_0(\theta = 0)$	Zero loss efficiency for beam radiation at normal incidence angle	-
$\eta_0(\theta)$	Zero loss efficiency for beam radiation at incidence angle θ	-
Θ	Angle of incidence of the beam radiation with the normal to the collector plane	°

Θt	Angle of incidence of the beam radiation projected transversely to the collector plane	°
ρ	Density	kg/m^3
τ	Transmittance coefficient of the glass	-
$(\tau\alpha)$	Effective transmission-absorption of the radiation	-
$(\tau\alpha)_n$	Effective transmission-absorption of the beam radiation at normal incidence angles	-

Abbreviations

CPC	Compound parabolic concentrator
DHW	Domestic hot water
IPCC	Intergovernmental Panel for Climate Change
PV/T	Photovoltaic/Thermal hybrid

List of articles

I. Bernardo, L. R., Perers, B., Håkansson, H. and Karlsson, B., 2008. Evaluation of a Parabolic Concentrating PVT System. Proceedings of Eurosun 2008, Lisbon, Portugal.

II. Bernardo, L. R., Perers, B., Håkansson, H. and Karlsson, B., 2010. Performance Evaluation of Low Concentrating Photovoltaic-Thermal Systems - a case study from Sweden. Submitted to Solar Energy in July 2010.

III Bernardo, L. R., Davidsson, H. and Karlsson, B., 2010.Performance Evaluation of a High Solar Fraction CPC-collector System. Submitted to Renewable Energy in November 2010.

IV Bernardo, L. R., Davidsson, H. and Karlsson, B., 2010. Retrofitting Domestic Hot Water Tanks for Solar Thermal Collectors - a theoretical analysis. Submitted to Energy and Buildings in November 2010.

1 Introduction

In this section the background and main objectives of the research work are addressed. The latest developments regarding the availability of conventional fuels and climate change issues are briefly presented. The climate and energy policies of the European Union and Sweden are also discussed. The background of the energy use in Swedish buildings is described with the focus on electrically heated single family houses. Previous related research is also revised and the main objectives of this work are presented. Finally, the methodology used to achieve the objectives is described.

1.1 Background

1.1.1 Conventional fuels, climate change and solar energy

Climate change and the scarcity of energy resources are two of the biggest challenges we will face in a near future (European Renewable Energy Council, 2010). Growth and implementation of renewable energies depend directly on the conclusions arrived at concerning these issues. In order to avoid misinterpretations and consequent wrong conclusions many interesting and relevant statements from official entities are quoted in this sub-chapter.

Two of the main conventional fuels which play major roles in our energy supply are oil and nuclear energy. Probably the central questions regarding these fuels concern their costs and availability in the future. Fossil fuel prices have drastically increased especially in the last decade (see Figure 1.1). The vertical axis represents the price in U.S. dollars per energy equivalent to one oil barrel. In Figure 1.2 and Table 1.1 data is shown concerning the present and predictable future availability of non-renewable fuels. Figure 1.2 represents the historical production profile of oil and gas liquids since 1930 including a forecast scenario up until 2050. In Table 1.1, the estimated available resources/reserves ratio at the end of

2005 is presented. A large ratio means that a large amount of resources has the potential to be converted into reserves. All these indicators point out a clear conclusion. J. Peter Gerling (Federal Institute for Geosciences and Natural Resources, Germany) wrote the following in the Survey of Energy Resources of the World Energy Council in 2007:

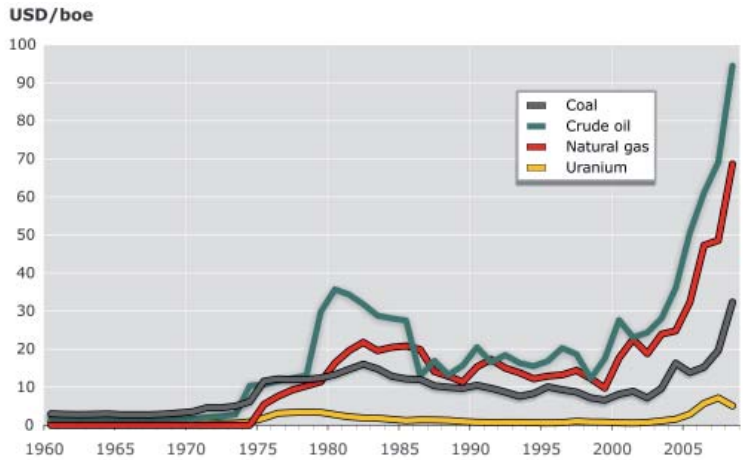

Figure 1.1 *Nominal fossil fuel prices development in the last decades (Federal Institute for Geosciences and Natural Resources, 2009).*

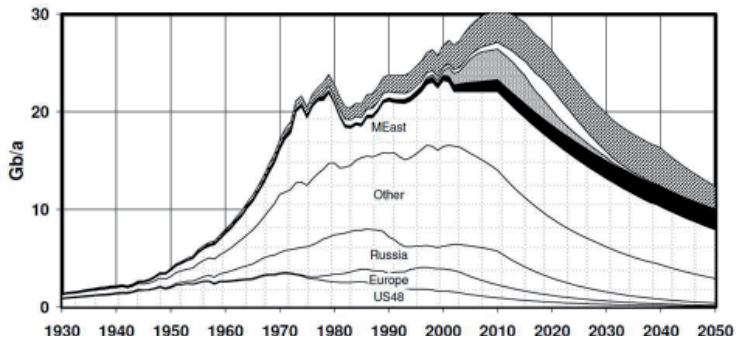

Figure 1.2 *Production profile of oil and gas liquids (World Energy Council, 2007).*

Table 1.1 Resources/Reserves Ratio - an indicator of the future availability of conventional geo-fuels at the end of 2005 (World Energy Council, 2007).

Fuel	Resources		Reserves		RRR
Conventional oil	82	billion tones	162	billion tones	0.5
Conventional natural gas	207	trillion m^3	179	trillion m^3	1.2
Hard coal	4079	billion tones	746	billion tones	5.5
Brown coal/lignite	1025	billion tones	207	billion tones	5
Uranium	12.8	million tones	1.9	million tones	6.7

> "The evidence suggests that the peak of world discovery was in the 1960s, meaning that the corresponding peak of production for 'Conventional Oil' is approaching. The world started using more than it found in 1981 and that gap has widened since. From a geological point of view, the remaining potential for conventional oil can provide for a moderate increase in oil consumption over the next 10 to 15 years. Demand will then have to be met by other fuels. The timing of the peak currently attracts much debate, but is considered less important than the vision of the long decline that comes into view on its far side. Certainly, countries that begin to address the issue and implement the necessary changes will find themselves enjoying huge advantages over those which continue to live in the past and have blind faith in unspecified technological solutions, or the ability of an open market to deliver.
>
> The world will not finally run out of oil for very many years, if ever, but the onset of decline may prove to be a discontinuity of historic proportions, given the key role oil plays in modern economies. The transition to decline threatens indeed to be an age of great economic and geopolitical tension."

When it comes to uranium availability for nuclear power the conclusion is different. Assuming that the future electricity consumption levels would be the same as that in 2005 and that nuclear power would continue using the same type of technology, the available resources would last at least 85 years. If investment was made to exploit undiscovered resources the time limit could be pushed ahead by many hundreds of years. Hence, it is estimated that nuclear power development will not be directly constrained by uranium resources in the next generations. If such a thing happens it is more likely to be related to political decisions taking into account radioactive wastes and possible industrial accidents (Holger Rogner - International Atomic Energy Agency – in Survey of Energy Resources for the World Energy Council, 2007). Other points of view consider that the costs of treating radioactive wastes for the next generations and the risk for public health should also be taken into account when calculating

the cost per energy produced by this technology (European Renewable Energy Council, 2010).

When it comes to climate change the biggest reference for information today is the Intergovernmental Panel for Climate Change (IPCC). This organization was created in 1988 by the United Nations Environment Programme and the World Meteorological Organization to provide a reliable and impartial investigation of the facts concerning worldwide climate change. The last assessment report was released in 2007 (IPCC, 2007). Some of the main conclusions from that report are: *"Warming in the climate system is unequivocal..."; "Most of the observed increase in global average temperature ... is very likely due to ... increase in greenhouse gas concentrations"; "Continued greenhouse gas emissions ... would induce many changes ... that would very likely be larger than those observed..."* Figure 1.3 shows a comparison between observed changes in surface temperature and simulated results by climate models. The models take into account either natural or both natural and anthropogenic factors. The results indicate the influence of human activity on the surface temperature rise.

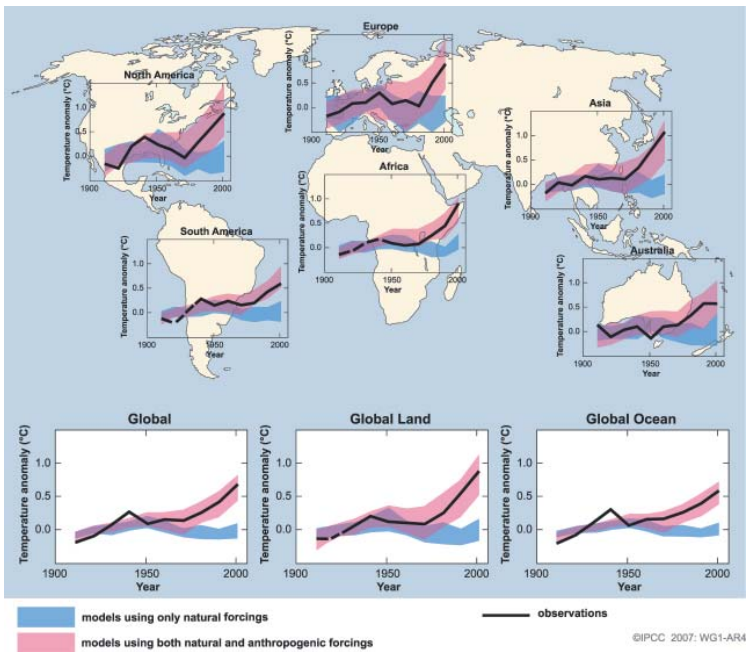

Figure 1.3 *Comparison between measured data and model results on the global and continental surface temperature change (IPCC, 2007).*

Many questions were raised in this report which resulted in continuous scientific investigations. The next assessment report is currently under development. However, some of the latest findings that will be assessed by that report have already been released. The main conclusion is that the new data stands behind the conclusions of Assessment Report 4 (2007). Moreover, they indicate that the current CO_2 concentration levels are higher and increased more rapidly than expected; measured sea-level rise is slightly higher than previously estimated; emitted CO_2 remains in the atmosphere for thousands of years causing irreversible changes in the climate and in ocean chemistry (IPCC Working Group I, 2010). Very recently, in August of 2010, IPCC proffered the following statement (Dr Rajendra Pachauri, chairman of the IPCC at a press conference at the United Nations in New York):

> "By overwhelming consensus, the scientific community agrees that climate change is real. Greenhouse gases have increased markedly as a result of human activities and now far exceed pre-industrial values."

After discussing the latest developments concerning two of the most important non-renewable fuels it seems that climate change adds up to what was already clear. The energy sector is a major concern today. Profound changes need to be made not only to reduce our energy use but also to change the way it is produced.

Recent figures show that all renewable energy sources provide 3078 times the current global energy needs. The energy potential of every source is shown in Figure 1.4. These are the theoretical potentials, i.e., the total available energy of each source at the earth's surface. They are calculated according to the available scientific data and correspond to the upper limit of what can be exploited. All the renewable energy sources depend in one way or another on the constant solar energy incident on the sun's surface. Solar energy is the renewable energy that has by far the largest potential. By itself it is enough to ensure 2850 times the annual global energy needs. In just one day the solar energy incident on the earth's surface equals the global energy needs during eight years.

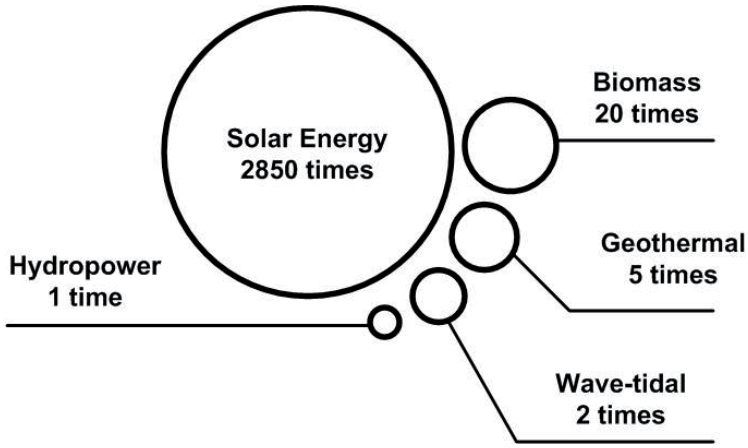

Figure 1.4 *Theoretical potential of renewable energy sources compared with the global energy needs (European Renewable Energy Council, 2010).*

Taking into consideration only the theoretical potential of solar energy can be misleading. Together with the theoretical potential, it is also crucial to evaluate technical and economical potential as well (European Renewable Energy Council, 2010). The technical potential considers the general limitations of the existing technology necessary to exploit a certain energy source. Among others, it takes into account the available raw material, the geographical locations where the energy can be explored, general technical limitations and the final efficiency of energy conversion. The economic potential weights the price of exploring the renewable energy source with the total energy produced. It also accounts for future benefits of exploring renewable energy sources. These can be the decrease in greenhouse gases production, the value of energy supply independence, impact on the environment and consequent influence on the health and well being of society.

The technical potential and the economic potential must be evaluated in a dynamic way. Both these potentials can change significantly with time. Certain technical challenges today might be easily solved in a near future due to a steep learning curve of the technology used to explore an energy source. The same applies for the economic potential analysis. The present energy price that the renewable energy source replaces might change significantly in a near future. Also, factors like future introduction of direct costs per released quantity of greenhouse gases can be taken into account. When evaluated dynamically, solar energy is one of the sources

with bigger technical and economical potentials (European Renewable Energy Council, 2010).

In total, the estimated incident radiation on a horizontal surface in Lund during a year is around 1000 kWh/m^2/year. In Figure 1.5, the estimation of the distribution of the global incident irradiation on an optimally tilted south surface for the whole Europe is shown. If the same calculation is performed on a non optimal oriented surface the result will be different and dependent on the geographical location. This analysis is shown in Figure 1.6 for Lund, Sweden.

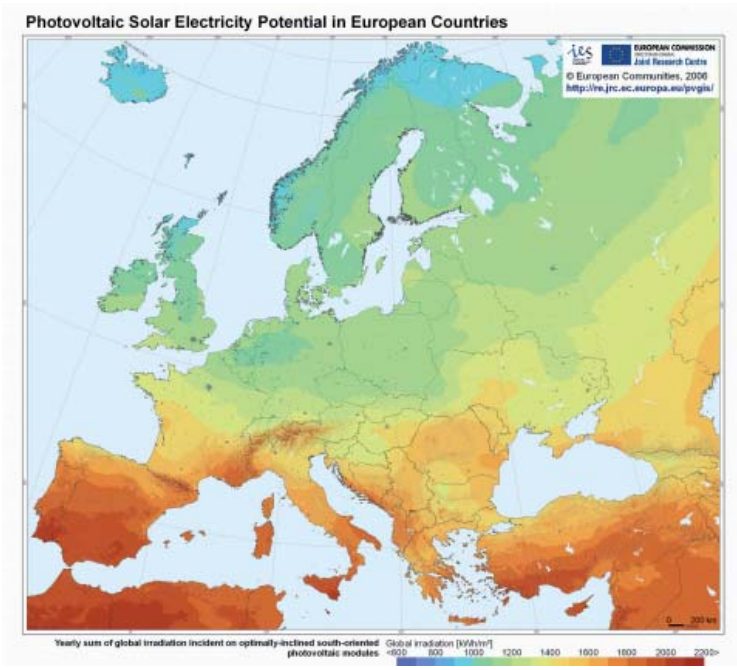

Figure 1.5 *Yearly sum of global irradiation incident on an optimally oriented surface kWh/m^2/year (European commission, 2006).*

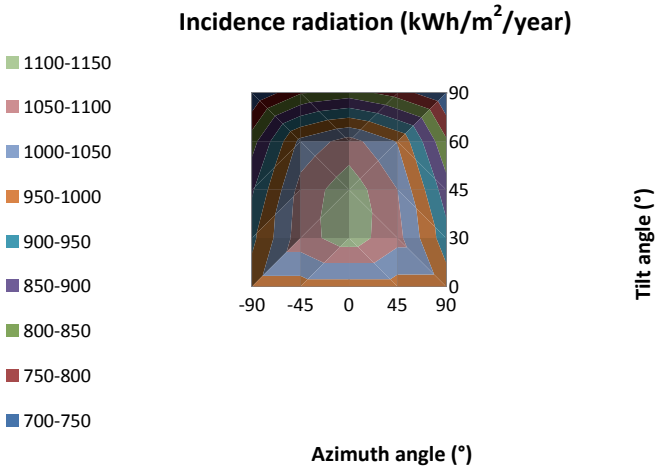

Figure 1.6 *Yearly global irradiation incident on a surface set at different tilts and orientations in Lund, Sweden.*

1.1.2 Single family electrically heated hoses in Sweden

In view of the previous discussed issues, in 2007 the European Union adopted an energy and climate change policy with ambitious targets for 2020. Among others, it aims to reduce greenhouse gas emissions by 20%, reduce energy use by 20% and meet 20% of our energy needs by means of renewable sources in comparison with the corresponding values in 2005 (European Union, 2007). Sweden went further and is aiming to meet 50% of its total energy need by renewable energy sources compared with 2008. Also, by 2020 the Swedish transport sector is aiming to cover 10% of its needs using renewable energy (Government Bill, 2008).

Building new energy efficient buildings has the potential to lower the future energy demand in the residential sector. However, the biggest energy savings potential lie in renovating the existing stock. The residential and service sectors represent 36% of the total energy use in Sweden where the biggest share is used for space heating and domestic hot water (Swedish Energy Agency, 2009a). In Sweden there are more than half a million single family houses which are electrically heated (Swedish Energy Agency, 2009b). The total electricity use in such houses is very high (Figure 1.7). It is interesting to verify that the electricity consumption did not decrease significantly in houses built between 1971 and 2000. This high number

of electrically heated houses combined with the Swedish cold climate and electricity driven industry leads to one of the highest electricity consumption per capita in the world. Actually, Sweden is the 4th biggest electricity consumer per capita in the world just behind Iceland, Norway and Canada (International Energy Agency statistics, 2009). This fact becomes even more relevant if one takes into account the electricity price and its trend. In Figure 1.8, the total energy prices in Sweden for several different sectors are presented. The final electricity price consists mainly of the price for producing electricity, profit for the network company and taxes. Taxes are primarily due to electricity certificates, energy tax, network taxes and value added taxes. Figure 1.8 shows that the most expensive energy fuel in Sweden during the year of 2009 was electricity used for heating.

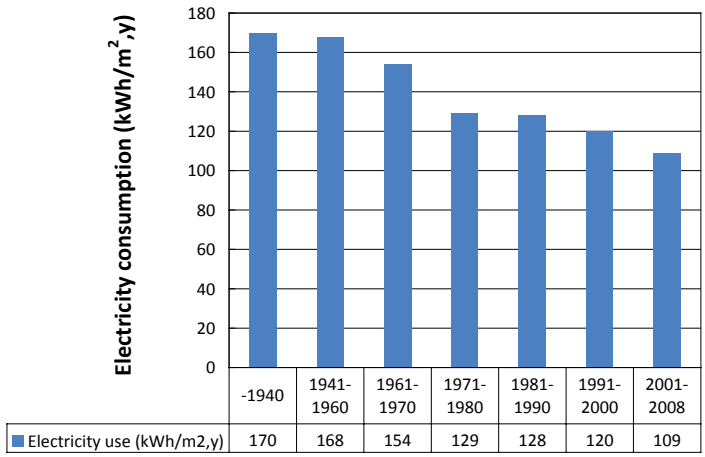

Figure 1.7 *Average electricity consumption per residential floor area, by year of construction of electrically heated single family houses in Sweden (Swedish Energy Agency, 2009b).*

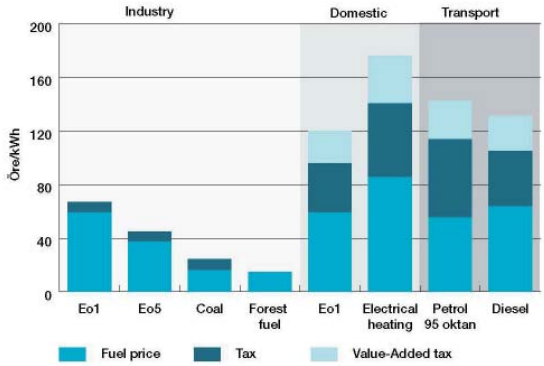

Figure 1.8 *The different fuel prices in Sweden, 2009. Eo1 and Eo5 are derivates of petroleum distillation and used for combustion (Swedish Energy Agency, 2009).*

It is important to look not only at the latest electricity price but also its trend during the last years and predictable future scenarios. Figure 1.9 shows the electricity price evolution for detached houses with electric heating between 2002 and 2009. As it is shown, the electricity price almost doubled in seven years.

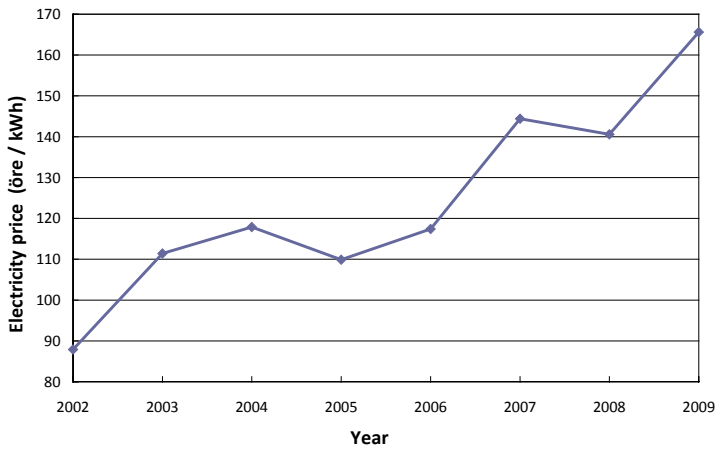

Figure 1.9 *Total price of electricity for detached electrically heated houses. Average price presented to the consumer by the network at January 1st of each year (Swedish Energy Agency, 2009a).*

The electricity market has become more international since trading is vital to ensure a stable and secure electricity supply. In 2008, 76% of the electricity used in the Nordic market was traded in the Nord Pool´s physical market (Swedish Energy Agency, 2009). Nord Pool is the Nordic power exchange market created to improve pricing transparency and exchange. This market is also increasingly trading with other countries like Poland, Germany and other central European countries. They produce a big share of their electricity with coal fired power plants. Hence, the Swedish electricity price is increasingly affected by the fuel prices and availability in the rest of Europe. Also, the policy of the European Union and Sweden to ensure that 10% of the energy use in the transport sector comes from renewable sources will predictably promote the implementation of electric vehicles. This means that a fraction of the fossil fuels energy demand may shift to electricity, increasing its consumption. Thus, it is likely that the electricity price will continue to rise. In summary, the current Swedish energy situation is a combination of the following factors, creating concerns for the future:

- more than half a million single-family houses consume electricity for domestic hot water production and space heating;
- Sweden is the 4th largest electricity consumer per capita in the world;
- electricity used for heating is the most expensive energy source in Sweden;
- electricity price has been rising at a high rate during recent years;
- due to its international market, the electricity price is increasingly dependent on fossil fuel availability and prices in other European countries;
- electricity price is generally expected to continue rising.

The accumulation of all these factors suggests that an intervention to decrease the electricity consumption in these houses is needed. Among others, some of the possible energy renovation measures are the installation of a solar thermal system, an air-to-air- heat pump, new low energy windows and extra insulation where it is most needed.

1.2 Objectives

The objectives of the present work are:

- to develop and test a solar thermal system for domestic hot water production where the existing water heater is retrofitted. This is the main focus of the research;
- to test and evaluate a photovoltaic/thermal (PV/T) concentrating hybrid. This way, not only heat but also electricity is produced. Concentrating hybrids aim to produce energy at a lower cost when compared with a conventional side-by-side system made of a flat plate collector and a PV module;
- to test and evaluate a compound parabolic concentrator (CPC) collector for use in the retrofitted system as well. This type of collector aims to achieve better annual performances than conventional collectors. A comparison with a flat plate collector system is included.
- to estimate what is the retrofitting configuration that achieves the best annual performance.

1.3 Method

The main challenge and focus of the presented work is to develop a solar hot water system for domestic hot water production. This is done by retrofitting the existing tank heater and connecting new solar collectors to it. Hence, no significant changes need to be carried out in the house when the new solar thermal system is installed. Also, since the solar hot water tank is one of the most expensive components of a solar thermal system, retrofitting the existing tank can lower the investment cost.

To be integrated in the system, a PV/T concentrating hybrid was evaluated. This concentrating hybrid aims to produce domestic hot water and electricity at a lower cost. For domestic hot water production, a high performance CPC-thermal collector adapted to Swedish climate was also analysed. These collectors were tested at the laboratory facilities and validated models were developed. These models make it possible to estimate the collector annual performance of both collectors compared with conventional alternatives. The hybrid performance was compared with conventional flat plate collectors and PV modules working separately side-by-side. The CPC-collector annual performance was compared with that of a conventional flat plate collector.

By means of TRNSYS simulations, different configurations for the retrofitted system design were analysed. The configuration achieving the highest solar fraction is described in this thesis. To combine the collectors with any normal storage tank, a special connection unit is under development. This unit makes it possible to retrofit almost any kind of storage tank making the system installation very flexible. Also, using this component, solar collectors can be combined with new standard domestic hot water tanks at new installations.

2 Simulations in TRNSYS software

All the simulation analyses performed in this work were carried out using TRNSYS (Transient Systems Simulation Software) (Klein et al., 2006). The software was developed by the University of Wisconsin, U.S.A. It has been commercially available since 1975 and increasingly used by the research community. It was originally developed for building analysis together with active solar thermal systems. Currently, among other applications, it is used for renewable energy systems, low energy buildings, HVAC systems, etc. One of the biggest advantageous of this software is its flexibility in connecting many different components available in the library. Consequently, one of the trade-offs is its complexity. The modular nature of the software together with the open source code of the components has been one of the reasons for its success among researchers. This means that all users can change the code of the components and modify the mathematical models. Moreover, if a certain component is not available in the software library, there is the possibility to create a new one that matches the user needs. To do so, most of the common programming languages can be used (TRNSYS, 2010).

The simulations performed on the PV/T hybrid collectors were carried out with Winsun (Winsun educational software, 2009). This is a TRNSYS based software, developed by Bengt Perers, which estimates energy outputs from any user-specified collectors. The user only needs to provide the collector parameters, the average temperatures running in the collector, the weather file and the simulation time period. The simulation model was then validated against measured outputs. The software only takes into account the collector and not the whole solar thermal system. The equations that compute these collector models are a simplification of the dynamic collector models described by Fisher et al. (2004) and are described in equation 2.1:

$$Q = F'(\tau\alpha)_n K_b(\theta) G_b + F'(\tau\alpha)_n K_d G_d - F'U_0(T_m - T_{amb}) - F'U_1(T_m - T_{amb})^2$$

(equation 2.1)

In addition to the PV/T hybrid collector analysis, the performance of a conventional flat plate collector system was compared with that of a CPC load adapted collector system. For this evaluation, a TRNSYS model of the whole solar thermal system was built but only the collector model was validated. The model includes detailed measured data on the incidence angle modifiers. This information was added in the collector model by means of high grade polynomial equations to avoid interpolations and consequently to increase its accuracy.

Finally, TRNSYS was used to create several solar thermal system models corresponding to different retrofitting configurations of existing water heaters (see chapter "Simulations of retrofitted solar thermal systems"). At this point, the evaluation was theoretical and no models were validated yet. These simulation results were used to compare different system performances. For this investigation, the important conclusion was which system performs best instead of focusing on the absolute value of the performance results. This kind of analysis is especially important when working with non-validated models. Since the systems were built with the same design guidelines and using the same component models, inaccuracies of one system will be taken into account in the same way in the other ones. This helps in ensuring the validity of such theoretical analysis.

One of the retrofitted systems built in TRNSYS is shown in a simplified way in Figure 2.1. The other solar thermal systems vary to some extent in their configuration but the analysis is mainly the same. All the main components used in the performed simulations are described below:

- Radiation processor – Type 109-TMY2. This model reads data from an external file at regular time intervals. It transports the data converting it to proper units and recalculates the solar irradiation values on different tilted or tracking surfaces. The external weather file can be created by different kinds of software such as Meteonorm (Meteonorm 5.0). Lund (Sweden) weather data created by this software was used in the simulations (latitude 55°44'N, longitude 13°12'E).
- Domestic hot water load profile – Type 14b. This is a model of a forcing function with repeated behaviour during the simulation period. This model was used since the output is already configured with appropriate units of flow draw-offs (kg/h). This makes it very simple to introduce a weekly pattern on the domestic hot water consumption. The profile used in this model is based on measured data described in detail in the annexed paper "Performance Evaluation of a High Solar Fraction CPC-Collector System". In total, according to the latest statistics (Swedish Energy Agency, 2009b), the domestic hot water

consumption in a typical single family house in Sweden is estimated to be 2050 kWh/year.

- Thermal collector – CPC dynamic collector type 832. This type was developed from the original type 132 created by Bengt Perers in TRNSYS 15. Later it was further developed by Hellström, Fisher, Bales, Haller, Dalibard and Paavilainen (Perers et al., 2002). This model was chosen since it is appropriate to separate the diffuse and direct efficiency when modelling a low concentrating collector (Fisher et al., 2004). Detailed information concerning measured incidence angle modifiers was added to the model. This is described in the annexed paper "Performance Evaluation of a High Solar Fraction CPC-Collector System". Previously, incidence angle modifiers were accounted for in the model as discrete measured values and interpolation was used. In practice, precision was lost around the collector optical axis since the incidence angle modifier changes very rapidly in that range. Hence, interpolations around these angles are very difficult to take into account and likely to decrease the model accuracy. In this model, high grade polynomial equations for the incidence angle modifiers were added. More than 90 measured incidence angle modifiers at different angles were used to build these equations in a very accurate way. These were accounted for in the model with a simple technique which externally "filters" the sun's direct irradiation before it is processed by the collector model itself. The model was validated against measured data with great accuracy.
- Storage tank – Type 534. This tank model is probably the most flexible tank model available. Among other features it is possible to define its external geometry, the inlet/outlet connections and the number and type of internal heat exchangers. Also very useful is the feature which allows the user to define in which section of the storage the auxiliary heat is provided. The degree of mixing and consequent de-stratification due to temperature inversions in the tank can also be specified. This model was chosen since different tanks are used in the retrofitting system analysis. These will be validated against measured data in future work. The retrofitted conventional tanks and the solar storage tanks with an internal heat exchanger were modelled by this type.
- Storage tank – type 4c, stratified storage with uniform losses and variable inlets. This storage model adjusts the location of inlets continuously in order to place the incoming fluid at a level as close to its temperature as possible. This improves greatly the stratification in the tank and consequently the annual solar fraction. This tank model was used for the comparison analysis between a conventional flat plate collector system and the CPC load adapted collector system. The main point

of such analysis was to determine which collector performs best in a solar thermal system rather than to determine its absolute value of annual performance. Hence, a simple model such as type 4c was used. Consequently, the time used to build the system model and to run the simulations was reduced.

- External heat exchanger – type 5b, counter flow. This model was chosen since it represents some of the most common external compact heat exchangers in the market. The heat exchanger mounted in the laboratory facilities for future validation is a brazed plate heat exchanger with counter flow and can be modelled by this type.
- Controller – type 2b. This model generates an ON/OFF control function. It monitors a high and low temperature sources and compares its difference with predefined dead-bands. Hence, the state of the control function at the next time-step is defined. This controller model was chosen since it represents the most common controllers in the market. These controllers were the ones used in the laboratory installations.
- Water pump – type 3b, single speed. This type models a pump with a fixed speed capacity. The flow can only be set to the predefined value or turned off. All the other components in the same loop will be assigned with this flow. Once again, this model was used since this is the most common type of pumps used in solar thermal systems.
- Pipe duct – type 31. This type models a pipe duct. In order to calculate the thermal losses it takes into account the section geometry, the length, insulation and surrounding temperature. This model was used in the retrofitting systems since they will be validated against measured data. Different components were used to model different pipe lengths at different surrounding temperatures (indoors and outdoors).

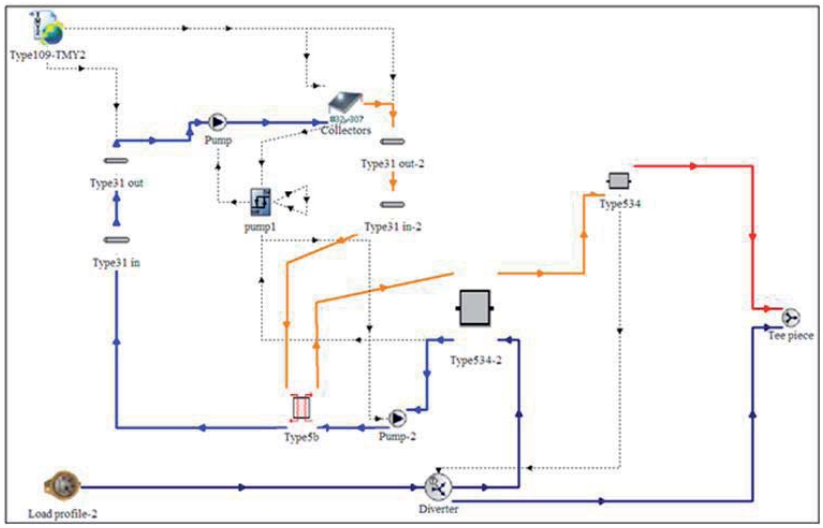

Figure 2.1 *Example of the simplified configuration of one retrofitting system model.*

3 Testing of the PV/T concentrating hybrid

A concentrating PV/T hybrid to be integrated in the retrofitted solar thermal system was tested. A comparison of the hybrid performance with that of conventional flat plate collectors and PV modules working side-by-side was also performed. In order to understand how to characterize a photovoltaic/thermal hybrid (PV/T) collector, both photovoltaic and solar thermal technologies should be understood separately.

In this chapter, a short description of the simplified working principles of solar cells and solar collectors is included. This will make it easier to better comprehend the effects of their combination and interaction in a hybrid. For further details concerning photovoltaics, the reader is referred to Wenham et al. (2007), Green (1998) and Fahrenbruch and Bube (1983). For details on thermal processes the reader is referred to Duffie and Beckman (2006).

3.1 Characterisation of solar cells

Photovoltaics is generally known as the process of converting solar radiation into electricity using solar cells. This is possible owing to the electronic properties of semiconductors. Photons with energy lower than the band gap energy pass through the semiconductor as if it was transparent. On the other hand, photons with energy greater than the band gap energy use their energy to break covalent bonds and create electron-hole pairs (Figure 3.1). Those electrons can then circulate around a circuit and produce electric power.

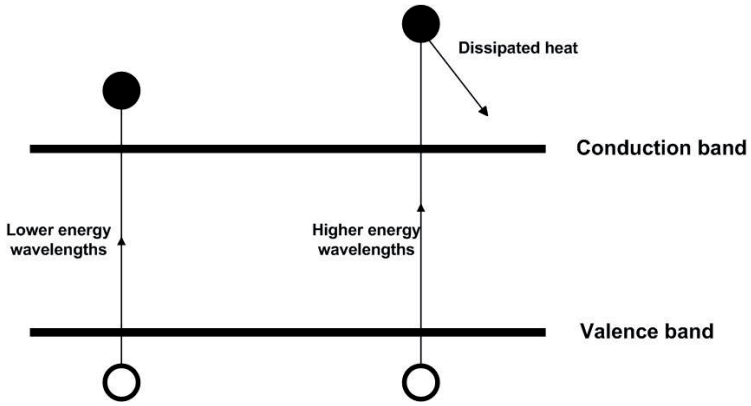

Figure 3.1 *Creation of electron-hole pairs and dissipation of energy for different energies of the wavelength (Wenham et al., 2007).*

Creating an electrically equivalent model which is based on separate electrical components whose performance is well known helps understanding the electronic behaviour of a solar cell. One of the simplest models consists of a current source in parallel with a diode. Since no solar cell is ideal, a shunt resistance and a series resistance are also included in the model. The result is the "one-diode equivalent circuit of a solar cell" shown in Figure 3.2.This model assumes that both the temperature and illumination are evenly distributed over the cell.

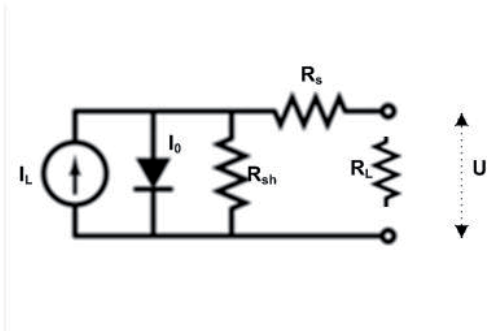

Figure 3.2 *Equivalent circuit of a solar cell (Wenham et al., 2007).*

A solar cell is characterised by its current-voltage characteristic curve (I-V curve). Using the following mathematical model that describes the previ-

ous equivalent electric circuit of a solar cell, one can generate theoretical I-V curves (Green, 1998):

$$I = I_L - I_0\left(e^{\left(\frac{q(U+IR_S)}{nkT}\right)} - 1\right) - \frac{U + IR_S}{R_{sh}} \qquad \text{Equation 3.1}$$

I represents the current, U represents the voltage over the load, I_L is the light generated current, I_0 is the diode leakage current density in the absence of light, n is the idealist factor of the diode, q is the absolute value of the electronic current, k is the Boltzmann constant, T is the absolute temperature, R_s is the cells series resistance, R_{sh} is the shunt resistance and the load is represented by R_L.

Using these I-V curves, three parameters can be estimated to characterise the performance of a solar cell for given irradiance, operating temperature and area. These are the short circuit current I_{sc}, the open circuit voltage V_{oc} and the Fill Factor FF. I_{sc} is the maximum current at zero voltage and is directly proportional to the available sunlight. V_{oc} is the maximum voltage at zero current while the Fill Factor FF is a measure of the quality of a cell. The higher the Fill Factor the higher is the cell's efficiency. The product of the current and voltage represents the power output for that operating condition. The Fill Factor is defined as (Green, 1998):

$$FF = \frac{V_{mp} I_{mp}}{V_{oc} I_{sc}} \qquad \text{Equation 3.2}$$

The product $V_{mp}I_{mp}$ represents the maximum power point of the solar cell while $V_{oc}I_{sc}$ represents the maximum power point if the cell was ideal. Hence, this coefficient corresponds to the fraction of the maximum efficiency that the cell can ideally reach. In order to take best advantage of the cells, the load should match this maximum power point regardless of the light conditions. This can be achieved with a maximum power point tracker normally built into the inverter.

A simple study of the cell's efficiency as a function of the incident irradiation, working temperature, series and shunt resistances was performed. This was carried out by generating I-V curves through varying the previous parameters and comparing them with the I-V curves of a reference case. The data used in the calculations for the reference case is shown in Table 3.1. The estimated I-V curve for the reference case is shown in Figure 3.3 while the other cases are illustrated in Figure 3.4 to Figure 3.7.

Table 3.1 Data used to generate the I-V curve for the reference case.

Reference case	
I_{sc} (A)	2
G (W/m^2)	1000
T (K)	293
U_0 (V)	0.65
R_s (Ω)	0.008
R_{SH} (Ω)	50
q (C)	1.6E-19
n (-)	1
k (J/K)	1.38E-23

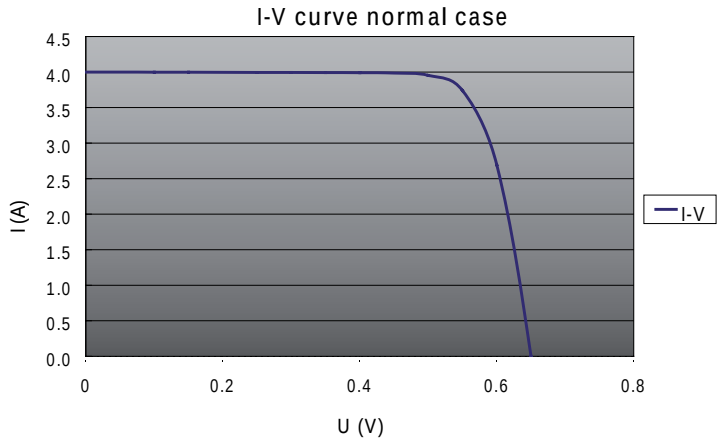

Figure 3.3 Estimated I-V curve corresponding to the reference case.

3.1.1 Effects of irradiation variation

The results for the different irradiation levels as well as the correspondent power outputs are shown in Figure 3.4.

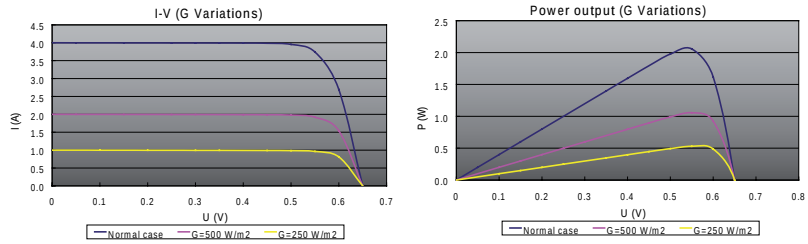

Figure 3.4 *I-V curves and corresponding power outputs for three different irradiation levels.*

As expected, higher irradiation levels imply an increase in the short circuit current since more electrons are collected into the circuit.

3.1.2 Effects of temperature variation

The I-V curves and the power output variation with temperature are illustrated in Figure 3.5.

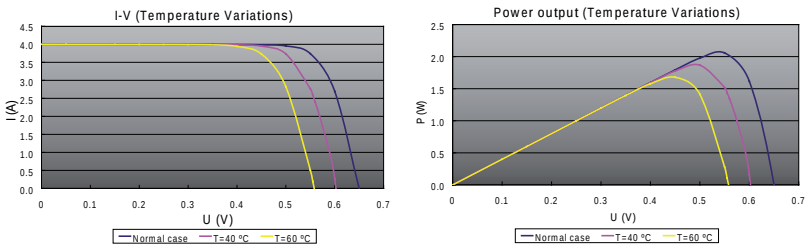

Figure 3.5 *I-V curves and corresponding power outputs for three different temperatures.*

The main effect of the temperature rise is the voltage drop which reduces the cell power output. With temperature increase more electrons escape through the p-n junction and recombine. For most types of solar cells one concludes that it is desirable to operate at as low a temperature as possible, since (Green, 1998):

- Cell output power is increased at lower temperatures;
- Thermal cycles and stress are reduced;
- Degradation rates approximately double for each 10^{o}C increase in temperature.

3.1.3 Effects of series resistance variation

The influence on the I-V curves using three different values of series resistance was estimated. The results are shown in Figure 3.6.

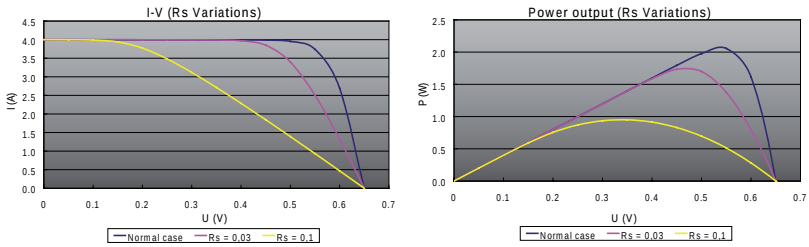

Figure 3.6 *I-V curves and corresponding power outputs for three different series resistances.*

The main contributors to the series resistance (R_s) are the bulk resistance of the semiconductor material, the metallic contacts, interconnections and the resistance between the metallic contacts and the semiconductor. This resistance represents all the non ideal connections in a solar cell. Thus, the higher the value of this resistance, less power is therefore extracted from the solar cell. As expected, the PV power decreases with higher series resistances.

3.1.4 Effects of shunt resistance variation

The shunt resistance (R_{SH}) corresponds to p-n junction imperfections and impurities near the junction. The ideal circuit should include an infinite shunt resistance that "forces" the current in the circuit and prevents its leakage through the joint. However, the shunt resistance has finite values and the smaller the shunt resistance is the bigger is the current drop (Figure3.7).

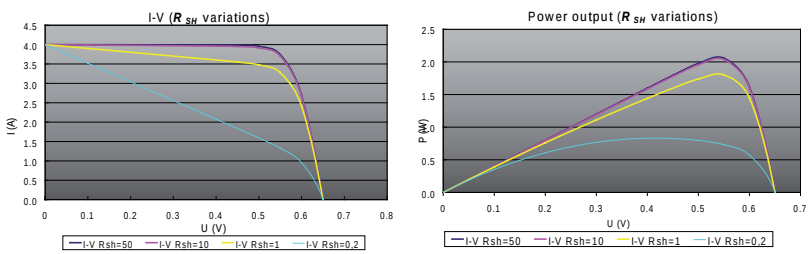

Figure 3.7 *I-V curves and correspond power outputs for three different shunt resistances.*

A PV cell cannot use all incoming photon energy to create electricity. It absorbs only radiation whose energy is higher than the band gap energy. For instance, a silicon solar cell absorbs roughly all radiation for wavelengths below the band gap of 1.1 µm (Green, 1998). This energy is used to produce electricity at variable efficiencies. Photons with higher energy than the band gap energy cannot be fully used as they will give off their excess energy as heat to the surroundings. For photons with energy below the band gap, the cell behaves as thought it were transparent. This means that all this radiation will be transmitted through the cell. Hence, most of the incident radiation is converted into heat. The part of the light spectrum that can be used to excite electrons and produce electricity is rather small. This explains why a conventional commercial solar cell has an efficiency of 10% to 15% for transforming all the available radiation into electric energy. Considering the high price of the solar cells it is attractive to use concentrating solar light modules which aim to achieve higher electric outputs per unit area.

3.2 Characterisation of solar thermal collectors

Solar thermal collectors use the incoming energy from the sun to produce heat. This heat can be used for several applications ranging from pool heating to electricity generation from steam. In steady state, the performance of a solar collector can be approximately described by a simple energy balance that indicates the distribution of incident solar energy into useful energy gain, thermal losses and optical losses. Hence, the useful energy output of a collector is then the difference between the absorbed solar radiation and the thermal loss which, divided by the incoming radiation at a normal angle to the collector plane, corresponds to the instantaneous steady-state collector efficiency. This relation is modelled in the following way (Duffie and Beckman, 2006):

$$\eta = \frac{Q}{G} = F'(\tau\alpha)_n - F'U_0\frac{(T_m - T_{amb})}{G} \qquad \text{Equation 3.3}$$

This equation is the basis standard for many test methods such as the one displayed in Figure 3.8.

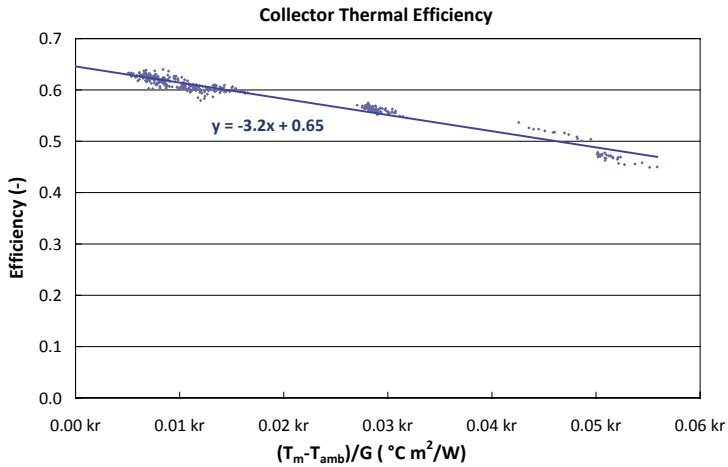

Figure 3.8 *Example of a collector thermal efficiency obtained by steady-state experimental testing.*

This thermal efficiency line can be seen as a classification of a thermal collector. It is obtained for a wide range of inlet temperature conditions. Each illustrated measurement point corresponds to the "instantaneous" steady state efficiency during a time interval. This was determined from the previous formula and plotted as a function of $(T_m-T_{amb})/G$. However, in reality, the performance line is not straight but a curve.The thermal losses are temperature dependent since the thermal losses do not increase linearly with temperature. Also, the previous efficiency equation does not take into account other factors such as variable wind speeds. Thus, more advanced dynamic models can be built (Fisher et al., 2002):

$$Q = F'(\tau\alpha)_n K_b(\theta) G_b + F'(\tau\alpha)_n K_d G_d - F'U_0(T_m - T_{amb}) - F'U_1(T_m - T_{amb})^2 - F'U_u u(T_m - T_{amb}) - (mC)_e \frac{dT_m}{dt} \quad (W/m^2)$$

Equation 3.4

Probably the most important component of a modern flat plate solar thermal collector is the selective absorber. The selective surface aims to increase the heat collection performance. Such surfaces used in solar technology are characterized by their high absorptance for short-wave radiation coming from the sun and low emissivity for long-wave heat radiation from the absorber. Thus, the energy absorbed from the sun is maximised and the heat losses from the absorber minimised.

Different solar collectors feature different performances. Theoretical collector performances are exemplified in Figure 3.9 for three different collector designs: an unglazed collector, a glazed collector with a selective surface and glazed collector with a selective surface and a Teflon insulator film. These were carried out using "Solar Collector" software (Solar collector, LTH). By analysing the figure one can conclude that the choice of the most appropriate collector depends on the application. If the application requires low temperatures, the least expensive collector, the unglazed collector, has the highest efficiency. On the other hand, if high temperatures are required by the load, the most expensive collector corresponding to the glass cover, selective absorber and Teflon film performs best. A detailed cost-performance analysis should be carried out in order to estimate the most suitable collector for a desired application.

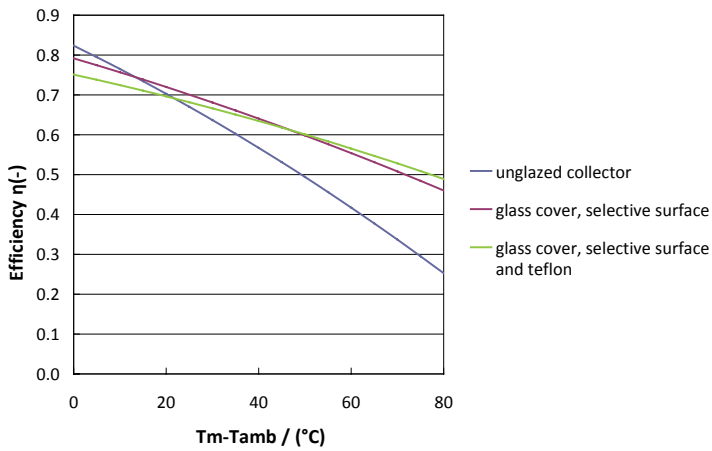

Figure 3.9 *Thermal efficiency curves obtained by theoretical simulations for three different collectors at a constant irradiation level and normal incidence angles.*

3.3 Concentrating Photovoltaic / Thermal (PV/T) technology

One of the most important aspects to take into account when studying photovoltaic/thermal hybrids is the interaction between electrical and thermal outputs. When an electric load is connected to the electric circuit, electric and thermal power is extracted. This means that part of the incoming irradiation is transformed into electricity by the PV cells instead of being absorbed by the thermal receiver. Hence, the thermal

output decreases as much as the electrical output is extracted. Figure 3.10 shows the measured power outputs of a hybrid when an electric load is connected to the PV modules during a period of the day. By analysing the figure, one can understand the interaction between the thermal and electrical outputs of a PV/T hybrid system.

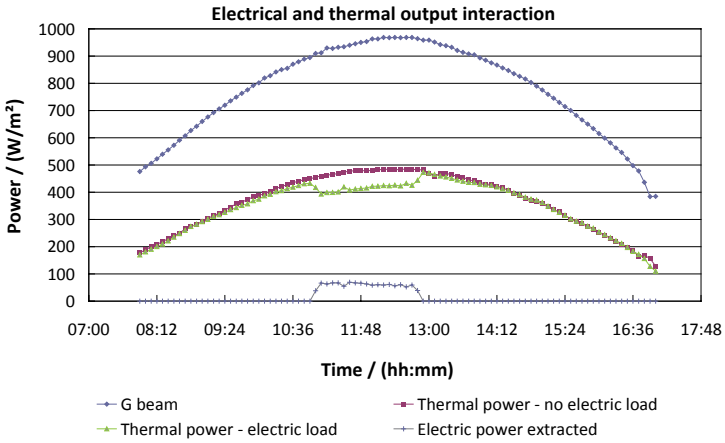

Figure 3.10 *Measured interaction of the hybrid electric and thermal outputs during two clear days with and without electric load. Power outputs expressed per glazed area (A_{Hybrid}=4.6 m²) (Bernardo et al., 2008).*

PV modules today convert light directly into electricity with a relatively low efficiency at a high cost. Replacing expensive solar cell material by cheaper reflectors offers the possibility of reducing the price per energy output unit. Above certain concentration factors, the use of reflectors generally requires cooling of the PV cells. This is vital in order to prevent permanent damage to the cells and maintain their efficiency (Nilsson et al., 2007). Usually, a photovoltaic/thermal (PV/T) concentrating hybrid tracks and concentrates light into a water/air-cooled photovoltaic module working as a thermal absorber (Figure 3.11). Hence, not only electricity is generated from the absorber but also heat. The thermal absorber uses the energy that the PV cells are not capable of transforming into electricity – both the excess energy used to excite the electrons when the photon energy is higher than the energy band gap and the photon energy that is not large enough to excite electrons.

Generally, the performance of a typical solar cell decreases by 0.4% per centigrade of temperature increase (Whenham et al., 2007). As discussed in the previous sub-chapter, the performance of a solar collector also

deteriorates with increasing operating temperature. This is because the thermal losses to the ambient are proportional to the temperature difference between the absorber and the surrounding temperature. Consequently, the production of both heat and electricity is favoured by lowering the operating temperature. However, different applications require different temperatures (Affolter et al., 2004). For instance, the minimum temperature for pool heating is typically 25°C whereas for domestic hot water it is around 70°C. Another issue to take into account is the higher temperatures of the cells compared to the temperature of the cooling medium at high irradiance. This is a result of the heat conduction resistance between cells and fluid. Therefore it is important for the absorber to have as high conduction as possible.

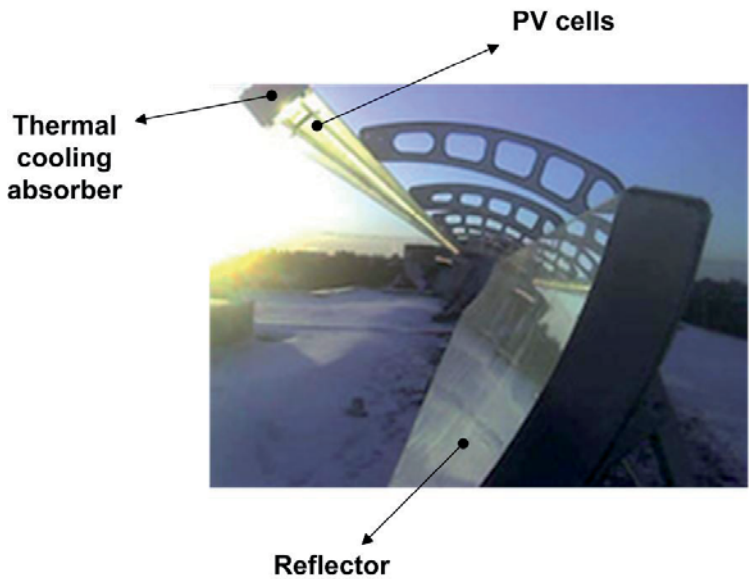

Figure 3.11 Concentrating PV/T hybrid (Menova Energy, 2010).

Concentrating PV/T hybrids aim to increase the cost effectiveness of the system but the impact of this combination on the heat and electricity production when compared with conventional systems is not obvious. In a PV/T hybrid, the absorber is made of solar cells instead of a selective surface as in conventional solar thermal collectors. This implies a higher thermal emittance and thereby a higher U-value and a lower optical efficiency. Also, the optical efficiency is reduced since the absorptance of the PV cells is lower than that of a selective surface, due to the reflector reflectance factor, light scattering and common shape imperfections. Logically,

when an electric load is connected to the PV cells, the heat production is lowered since part of the radiation is converted into electricity. The use of concentrators will also reduce the electricity production due to the non-uniform concentration profile of the irradiation. In the end, a life cycle cost analysis is necessary to determine whether the concentrating system reduces the unit cost of produced energy making the system more cost-effective (Arvind and Tiwari, 2010; Arvind et al., 2009).

3.4 Description of the PV/T concentrating hybrid design and experimental setup

This photovoltaic/thermal parabolic concentrating system tracks and concentrates light into a water-cooled photovoltaic module working as a thermal absorber (Figure 3.12). The PV/T system consists of a photovoltaic module, thermal absorber, parabolic reflector, tracking system, glazed protection and supporting structure (Figure 3.13). The photovoltaic cells, which are specially designed for concentrated light, are made of monocrystalline silicon and have a nominal efficiency of 16% at 25°C (Absolicon Solar Concentrator AB, 2008). The total surface area of the cells is 0.33 m². Water runs inside the aluminium thermal absorber where the cells are laminated. The parabolic reflector is made of a silver coated plastic film laminated on a steel sheet. The geometrical concentration ratio of the reflector is C=7.8 (Figure 3.12). It is important to notice that the reflector is 40 cm longer than the absorber at the edges to also make use of the irradiation in the morning and afternoon. The tracking is carried out by rotating the structure around an axis oriented in the east-west direction. The adjustment of the tilt angle is carried out periodically according to the calculated position of the sun. The parabolic trough is covered by a 4.6 m² glass pane with a measured transmission coefficient of 90% (Bernardo et al., 2008).

In this study, two hybrid areas were defined: total glazed area and active glazed area. For this particular hybrid the total glazed area (A_{Hybrid}) equals 4.6 m². Active glazed area was defined as the maximum glazed area that the system can make use of. This excludes surface areas where it is impossible for the incoming irradiation to reach the absorber such as frames and gaps between solar cells and reflector edges which are longer than the absorber (Figure 3.12). The electric and thermal active glazed areas are different since the thermal absorber is wider than the cells. The electric active glazed area ($A_{active\ elect.}$) is 3.5 m² while the thermal active glazed area ($A_{active\ thermal}$) is 3.7 m².

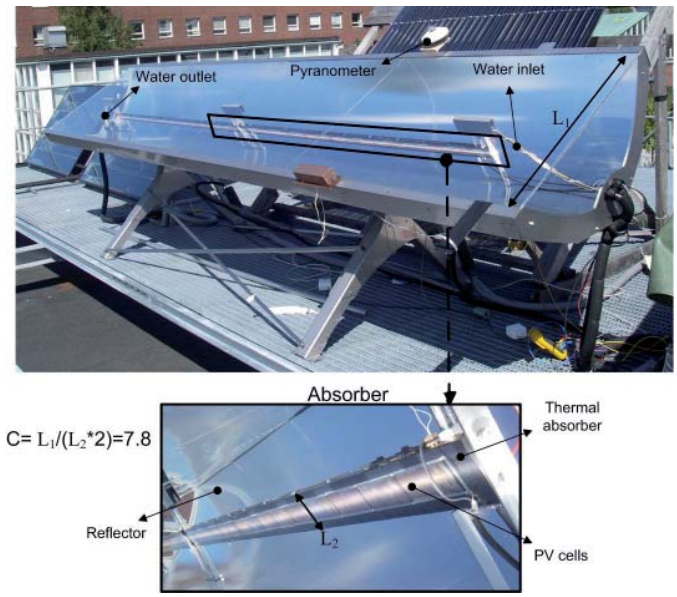

Figure 3.12 *PV/T concentrator trough and photovoltaic cells laminated on one side of the thermal absorber.*

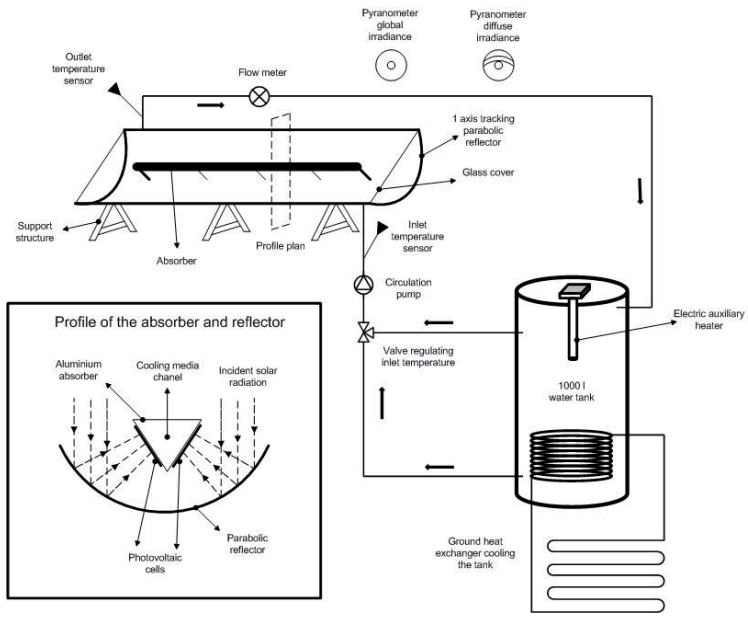

Figure 3.13 *Schematic diagram of the experimental setup system and its monitoring points.*

3.5 Evaluation method and model

The testing and characterisation method can be seen as a modified solar collector testing method described in the following steps:

a) Simultaneous monitoring of heat and power where the photovoltaic module operates continuously at maximum power point;
b) Characterisation of the thermal collector according to the steady-state test method (Fisher et al., 2004);
c) Characterisation of the photovoltaic module at high irradiances and variable working temperatures;
d) Description of the thermal and electrical incidence angle modifier during one day with stable high solar intensity;
e) Using the previous tested parameters to generate a mathematical steady-state model capable of accurately describing the thermal and electrical outputs;
f) Validation of the model by comparison between measurements and model outputs during days with varying weather conditions.

Both the electrical and thermal outputs were measured every six minutes for different temperature conditions in the collector. The maximum electric power output extracted by the hybrid was calculated based on periodical I-V curve measurements. Using this value together with the incident beam irradiation, the system electrical efficiency as a function of its working temperature was determined. In this specific case, since the structure is closed, it was not possible to measure the cell temperature directly. Instead, the temperature of the outlet water, running inside the thermal absorber at the moment of the electrical efficiency measurement, is presented. This is the temperature limiting the whole electric output since the cells are series connected.

Since there is no electric load continuously connected to the hybrid, all the incoming irradiation is used to produce heat. This output was calculated by equation 3.5 (Duffie and Beckman, 2006) where the monitored parameters are described in the nomenclature section.

$$Q = \rho \frac{dV}{dt} \cdot C_p \cdot (T_{out} - T_{in}) \quad \text{(W)} \qquad \text{Equation 3.5}$$

The thermal power was then obtained by subtracting the measured electric power from this heat output. The beam incidence angle modifier for the thermal and electric efficiency was calculated with equations 3.6 and equa-

tion 3.7, respectively (Duffie and Beckman, 2006). The thermal incidence angle modifier is the ratio between the measured zero loss efficiency at a certain incidence angle and the zero loss efficiency at normal incidence angle determined from the measurements. The electric incidence angle modifier is the ratio between the measured electric power at a certain incidence angle and temperature and the power at the same temperature but normal incidence angle estimated from the efficiency measurements.

$$K_{b\_thermal}(\theta) = \frac{\eta_0(\theta)}{\eta_0(0)} = \frac{\eta(\theta) + \frac{F'U(\Delta T)}{G_b}}{F'(\tau\alpha)_n} = \frac{\eta(\theta) + \frac{F'U_0(T_m - T_{amb}) + F'U_1(T_m - T_{amb})^2}{G_b}}{F'(\tau\alpha)_n} \quad (-) \qquad \text{Equation 3.6}$$

$$K_{b\_electric}(\theta) = \frac{Q_{electric}(\theta)}{G_b \cdot (\eta_{b\_electric}(25°C) - K_T \cdot T_{out})} \quad (-) \qquad \text{Equation 3.7}$$

The function commonly used to fit the incidence angle modifier data between 0° and 60° is given by equation 3.8 (Duffie and Beckman, 2006). The parameter b_0 shapes the curvature of the function, setting higher or lower incidence angle modifier values for the same incidence angle.

$$K_b(\theta) = 1 - b_0 * \left(\frac{1}{\cos(\theta)} - 1\right) \qquad \text{Equation 3.8}$$

The hybrid was continuously tested at the Energy and Building Design laboratory of Lund Technical University in Sweden (latitude 55°44'N, longitude 13°12'E) during the period 1/06/2008 – 13/09/2008.

By analyzing the measured data, one can determine the hybrid parameters and develop simple mathematical models capable of describing its behaviour and estimate its outputs for any geographic location. The monitored parameters and the model equations are presented in equation 3.9 to equation 3.12 (Duffie and Beckman, 2006).

$$Q_{thermal} = F'(\tau\alpha)_n K_{b\_thermal}(\theta) G_b + F'(\tau\alpha)_n K_d G_d - F'U_0(T_m - T_{amb}) - F'U_1(T_m - T_{amb})^2 \quad (\mathrm{W/m^2}) \qquad \text{Equation 3.9}$$

where $K_{b\_thermal}(\theta) = 1 - b_{0\_thermal} * \left(\frac{1}{\cos(\theta)} - 1 \right)$ (-) Equation 3.10

$$P_{electric} = \left[\eta_{b\_electric}(25°C) K_{b\_electric} \cdot G_b + \eta_{b\_electric}(25°C) \cdot K_d \cdot G_d \right] \cdot \left[1 - K_T \cdot (T_{out} - 25) \right] \quad (W/m^2)$$

Equation 3.11

where $K_{b\_electric}(\theta) = 1 - b_{0\_electric} * \left(\frac{1}{\cos(\theta)} - 1 \right)$ (-) Equation 3.12

The hybrid parameters were then fed into Winsun (Winsun Villa Software, 2009), a TRNSYS based simulation software which estimates the annual thermal and electrical outputs using the described models.

In order to compare the hybrid performance with a conventional side-by-side system made of standard thermal collectors and photovoltaic modules, simulations were also carried out for these standard components. It was assumed that the produced hot water should be used for domestic hot water applications since this can represent 90% of the potential market for these hybrids (Affolter et al., 2004). Therefore, the output temperature from the collectors should be around 65-70°C which was assumed to imply 40°C of mean absorber temperature. Consequently, the hybrid solar cells, but not the individual PV module, would work at 65°C to 70°C. As the PV module is independent of the flat plate collector it was assumed that it could work at around 25°C to 30°C. In order to understand how the performance would change if the hybrid were used for low temperature applications, simulations were also carried out for pool heating. For this application it was assumed that the required outlet temperature would be around 30°C which was estimated to imply 20°C average water temperature in the hybrid since the cold water inlet is around 10°C. The diffuse incidence angle modifier (K_d) was calculated as being the inverse of the geometrical concentration ratio (1/C where C=7.8) (Winston et al., 2005). All the parameters for the side-by-side system were assumed to be common values for standard components.

The relative uncertainties of the measuring instruments stated by the manufacturers are estimated for ideal measurement and installation conditions. In practice, somewhat higher relative uncertainties were assumed in order to take into account a safety margin that includes inaccuracies related to the installation and operation of those instruments in our laboratory. The pyranometer relative uncertainty was assumed to be +-2%, the flow meter +-1% and the Pt100 temperature measurement +-2%. The temperature

dependence of the heat capacity and specific mass of the water was taken into account in the calculations. Hence, using the standard method of the square root of the quadratic sum for the uncertainty propagation, the global uncertainty of the efficiency measurements was estimated to be 3%.

3.6 Measurement results and PV/T concentrating hybrid characterization

3.6.1 Electrical performance

In Figure 3.14 the system electrical beam efficiency as a function of the water outlet temperature is presented. The measured electrical efficiency is 6.4% at 25°C water outlet temperature while the temperature dependence of the electric efficiency is -0.3%/°C. The measured total peak power was 61 W/m² of total glazed area at 28°C inlet and 39°C outlet water temperature and 997 W/m² incident beam radiation.

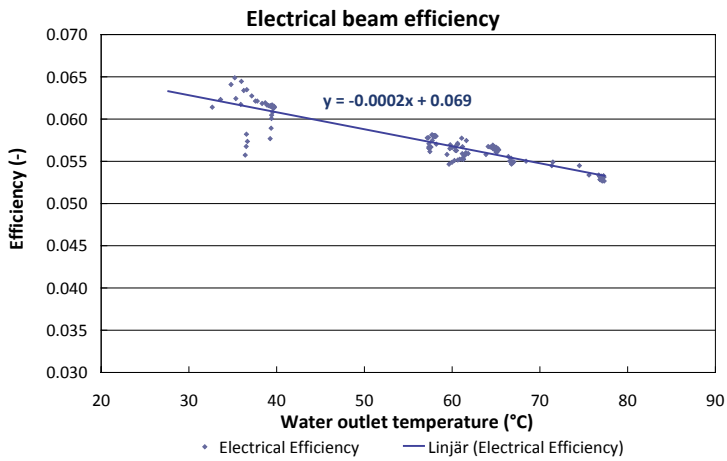

Figure 3.14 *Measured electrical beam efficiency per total glazed area for different working temperatures and beam irradiation higher than 900 W/m².*

3.6.2 Thermal performance

The measured thermal beam efficiency as a function of the working temperature and incident radiation is presented in Figure 3.15. Using linear

approximation, the hybrid beam zero loss efficiency $F'(\tau\alpha)_n$ and the heat loss coefficient $F'U_0$ were determined. They are equal to 0.45 and 1.9 W/ºC/m² of total glazed area. The measured thermal peak power was 435 W/m² of total glazed area at the same conditions described above.

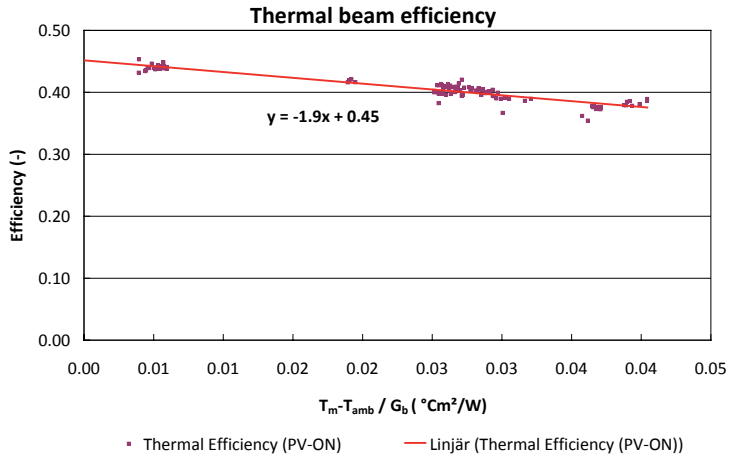

Figure 3.15 *Measured thermal beam efficiency per total glazed area for different working temperatures and beam irradiation higher than 900 W/m².*

3.6.3 Incidence angle modifier

During the morning and afternoon, the reflection losses at the glass cover and absorber increase due to higher angles of incidence. This effect causes a drop in the thermal and electrical outputs. The measured sensitivity of the thermal and electrical efficiency as a function of the angle of incidence is presented in Figure 3.16. The measured b_0 fitting the thermal and electric data was 0.14 and 0.28 respectively showing that higher angles of incidence have a greater impact on the electrical performance.

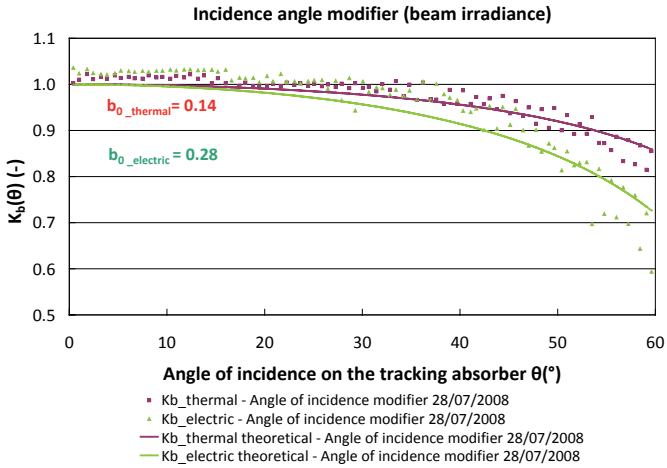

Figure 3.16 *Measured thermal and electrical incidence angle modifier for beam radiation during one clear day and θ<60°.*

3.7 Model validation

The hybrid measured parameters and the presumed parameters corresponding to conventional PV modules and thermal collectors are summarized in Table 3.2 and Table 3.3. The corresponding generated thermal and electric power outputs illustrated in Figure 3.17 and Figure 3.18 show that good agreement between the hybrid model and measurements was achieved even during unstable days, validating the models.

Table 3.2 Parameters for electricity production used in the simulations, expressed by total glazed area. The hybrid parameters were measured while the ones for the PV module were assumed.

Model electrical parameters	$\eta_{b\_electric}$ (25°C)	Kd (-) (-)	K_T (%/°C)	$b_{0\_electric}$ (-)
Hybrid Electric PV module	0.064 0.16	0.13 0.9	0.3 0.4	0.28 0.10

Table 3.3 Parameters for hot water production used in the simulations, expressed by total glazed area. The hybrid parameters were measured while the ones for the flat plate collector were assumed.

Model thermal parameters	$F'(\tau\alpha)_n$ (-)	K_d (-)	$F'U_0$ (W/m²°C)	$F'U_1$ (W/m²°C²)	$b_{0\_thermal}$ (-)
Hybrid Thermal (PV-ON)	0.45	0.13	1.9	0.0	0.14
Flat plate collector	0.8	0.9	3.6	0.014	0.15

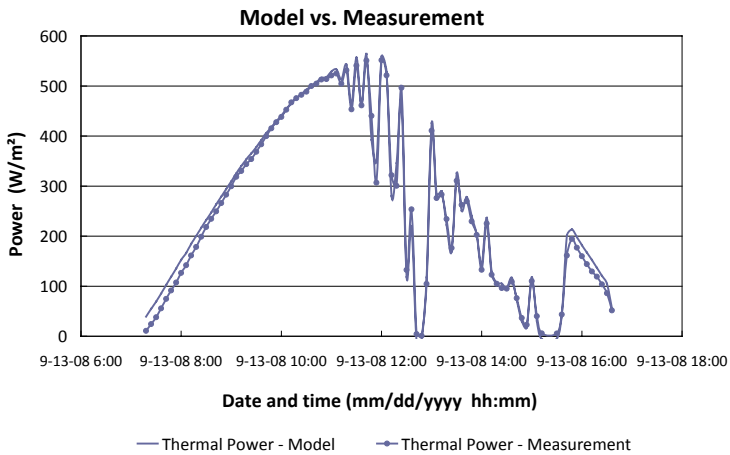

Figure 3.17 Thermal model and measurements during unstable irradiation day.

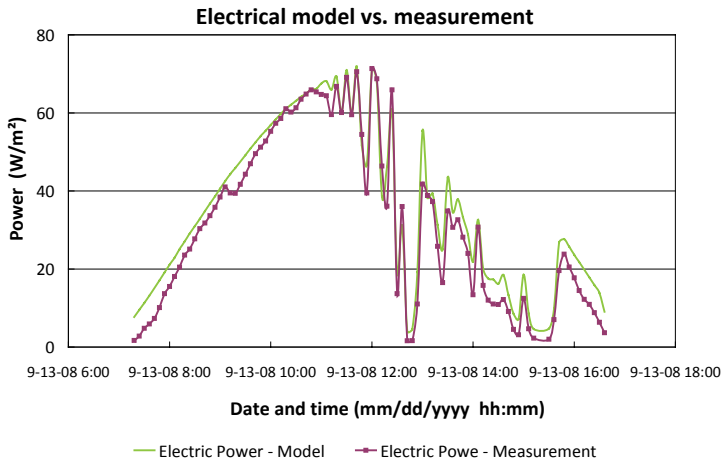

Figure 3.18 *Electrical model and measurements during unstable irradiation day.*

3.8 Performance analysis and discussion

Following the measurement test method described above, a performance analysis procedure is proposed in this section. This consists of estimating the hybrid annual performance for different latitudes and comparing it with separate conventional PV modules and thermal collectors.

3.8.1 Tracking system

The tested hybrid system is thought to work with its tracking axis oriented in the east-west direction. Simulations were carried out to estimate the received irradiation by a tracking surface with the axis horizontally oriented in both the east-west and north-south directions for several climates at different latitudes. The results are given in Table 3.4. Analysing the results, one can conclude that it is always better to track the sun around an axis in the north-south direction, independently of the geographical position. (10% to 20% better) This effect is even more relevant when the system is moved closer to the equator where the sun reaches higher altitudes. All the following simulations take into account this result, estimating the annual outputs as if the hybrid were tracking the sun in a more productive way with its axis in the north-south direction.

As it is known, concentrating solar systems can only make use of a fraction of the incident diffuse light. In contrast, non-concentrating systems like standard PV modules and flat plate collectors use the global irradiation. The concentrator can make use of the incoming beam irradiation plus $(1/C)$ of the diffuse irradiation (G_b+G_d/C) on the collector plane (Winston et al., 2005). This comparison is presented in Table 3.4. The conclusion is that the global irradiation incident on a static surface is higher than the beam irradiation on a one-axis tracking concentrating surface. This means that, independently of its location, a non-concentrating fixed collector receives more usable irradiation than a tracking concentrating one like the studied hybrid (roughly 20% to 40% in this case). Closer to the equator, the beam irradiation values are higher and this result becomes less accentuated. This is even clearer as the concentration ratio increases.

Table 3.4 Annual output ratio between a north-south and a east-west oriented tracking axis; annual output ratio between the usable irradiation incident on a static and north-south tracking concentrating surface. (Optimal static surface inclination from horizontal corresponds to 40º in Stockholm, 30º in Lisbon and 20º in Lusaka.)

Annual output ratio	Stockholm (lat=59.2°N)	Lisbon (lat=38.7°N)	Lusaka (lat=15.4°S)
Output ratio N-S/E-W tracking axis	1.10	1.14	1.19
Output ratio static/tracking concentrating surfaces	1.41	1.24	1.18

3.8.2 Annual performance

Based on the system parameters previously presented in Table 3.2 and Table 3.3, the total annual performance for the hybrid and the traditional side-by-side system was calculated for the three different climates. These results are presented in Table 3.5. For Stockholm, the hybrid electric and thermal annual output is 45.1 kWh/m^2,yr and 187.6 kWh/m^2,yr, respectively. The PV module produces 164.5 kWh/m^2,yr while the thermal collector generates 401.6 kWh/m^2,yr.

Table 3.5 Electric and thermal outputs of the hybrid and conventional side-by-side-system for domestic hot water application expressed per square metre of total glazed area.

Annual outputs per total glazed area (kWh/m^2,yr)	Stockholm (lat=59.2°N)	Lisbon (lat=38.7°N)	Lusaka (lat=15.4°S)
Hybrid electric annual output	45.1	83.3	102.5
Hybrid thermal annual output	187.6	456.7	612.6
(Side-by-side system) PV module annual output	164.5	264.8	308.3
(Side-by-side system) thermal collector annual output	401.6	887.7	1143.8

3.8.3 Hybrid concentrator vs. standard PV module based on cell area

One of the most common arguments in favour of PV/T concentrating systems is their higher electric output when compared with a regular PV module with the same cell area. According to this point of view, the expensive cell area can be reduced and the thermal application can be considered just a plus on cooling down the cells. Hence, if the thermal output is neglected, the hybrid can even work at a high flow rate, making the cells colder and more efficient. The production per cell area of the hybrid and the traditional PV module is presented in Table 3.6 and the ratio between the two annual electric outputs is shown in Figure 3.19. The results show that the concentrating hybrid cells produce 3.6 to 4.4 times more electricity than a PV module with the same cell area. This kind of analysis provides very useful information concerning the real extra electricity production one gets with the use of the reflector in different climates. For this simulation it was considered that the conventional PV module cells have 16% efficiency at 25°C.

Table 3.6 PV/T north-south concentrating hybrid and traditional PV module electric output comparison based on cell area. PV module inclination from the horizontal is set to optimum values of 40º in Stockholm, 30º in Lisbon and 20º in Lusaka. A_{cells_hybrid}=0.33m^2.

Electric annual output per cells area (kWh/m^2,yr)	Stockholm (lat=59.2°N)	Lisbon (lat=38.7°N)	Lusaka (lat=15.4°S)
Hybrid tracking N-S (65°C)	626.5	1156.1	1422.2
Traditional static PV module (25°C)	173.2	278.7	324.5

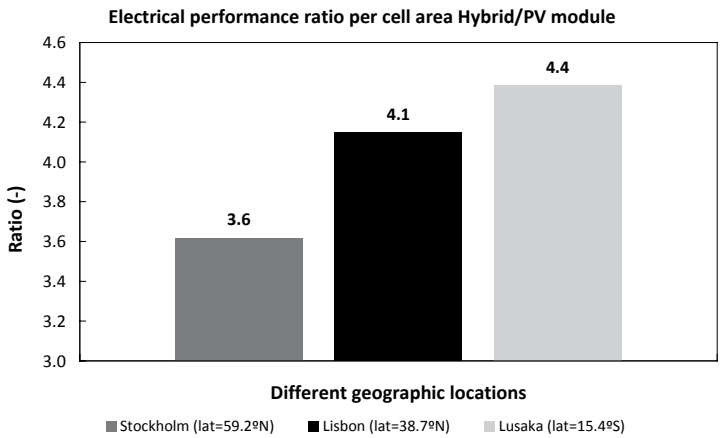

Figure 3.19 Ratio between the hybrid and standard PV module annual electric production per cell area.

3.8.4 Hybrid concentrator vs. standard side-by-side system based on glazed area

In another point of view, since heat is the largest energy fraction produced by the hybrid, it should be considered as a valuable output taken into account when the concentrating hybrid is compared with a conventional system. Hence, the hybrid outputs were compared with an individual PV module and a solar thermal collector working separately for both domestic hot water production and pool heating. The parameters used in the simulation were presented in Table 3.2 and Table 3.3. The hybrid

comparison with the traditional side-by-side system based on their power outputs per total glazed area is presented in Figure 3.20. This is particularly useful for areas where the available space is a strong limitation. As it is generally accepted, probably the most expensive part of these two systems is the solar cells. Hence, it makes sense to compare them taking into account that the hybrid and the PV module in the traditional system have the same cell area. This is not the only way to compare the systems but it seems to be the more reasonable one. The results show that, regardless of whether the produced hot water is used for domestic hot water application or for pool heating, the area by the traditional side-by-side system, which generates the same electrical and thermal outputs as the hybrid, is almost the same. This result is not obvious and is further considered in the discussion section.

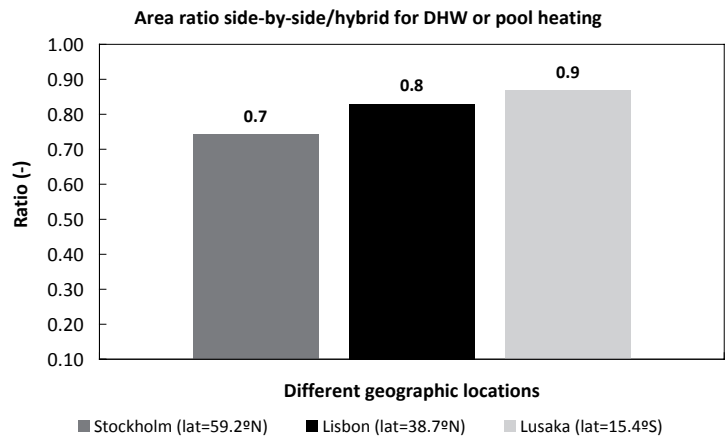

Figure 3.20 *Ratio between side-by-side system and hybrid total glazed areas producing the same electrical and thermal annual outputs for domestic hot water or pool heating.*

3.8.5 Discussion

In this section the implication of the results concerning the measured hybrid parameters, the annual performance and the comparison with conventional systems is discussed.

Using the efficiency per total glazed area one can estimate how much space one needs to reach the energy demand. It is then possible to determine, between several different hybrids, which one has the best performance for the space it uses and which hybrid is a reasonable choice for the

available space. The efficiency per active glazed area may be said to be a more scientific indicator that allows a technical comparison between hybrids based on how well they perform with the radiation they can use.

As previously reported (Yoon and Garboushian, 1994), the electricity production temperature dependence of concentrating hybrids is different from that in a normal photovoltaic module. For this hybrid, the electrical efficiency decrease as a function of temperature (K_T) is approximately -0.3%/°C whereas the typical value for a standard cell without concentration is -0.4%/°C (Wenham, 2007). There are two different reasons for this. The electrical efficiency curve presented in Figure 3.14 was calculated based on the temperature of the water and not that of the cells. Due to heat transfer resistance between these two elements, the water temperature will be somewhat lower than the cell temperature. This temperature difference is inversely proportional to the amount of heat transferred between them and it will decrease with increasing water temperature at constant solar intensity. This implies a lower efficiency temperature dependence of the hybrid, making the slope of the line slightly smoother (Figure 3.14). On the other hand, the temperature difference will increase with increasing radiation intensities at constant working temperature. This effect has a very low impact using the suggested test method since measurements were carried out only for high irradiation values according to the steady-state test method (Fisher et al., 2004). Possibly, in a future improved model, the cell efficiency should be modelled to increase with decreased irradiance intensities. The other effect is that a higher open-circuit voltage due to higher concentration actually reduces the temperature sensitivity of the cell (Yoon and Garboushian, 1994; Wenham et al., 2007). Previous experimental results have shown that the temperature influence in concentrating systems is lower, with 0.25%/°C drop in efficiency for high concentration levels at around 25°C (Yoon and Garboushian, 1994). Hence, concentrators have an advantage when used at high temperature operation compared with a non concentrating photovoltaic module.

The tracking system analysis shows that a one-axis tracking system should rotate around an axis aligned in the north-south direction, independently of its geographical location. If tilted towards the equator, the performance is further improved. Furthermore, a tracking concentrating system receives less usable radiation than a standard flat fixed collector. Consequently, the measured low hybrid efficiencies together with low usable irradiation generate low annual outputs. Additionally, the area covered by a conventional side-by-side system is comparable to the one used by the hybrid producing the same outputs. As a result, it is difficult for a concentrating hybrid to compete with conventional alternatives.

The optical efficiency is one of the factors that directly influence the final electric efficiency. The ideal thermal optical efficiency of the hybrid

can be theoretically estimated taking into account several loss factors. These are: glass transmission, reflectance factor and the absorptance and efficiency of the PV cells. In the same way, it is also possible to theoretically calculate the ideal electrical efficiency of the hybrid at 25°C. This is exemplified by equation 3.13 and equation 3.14, respectively:

$$(\tau\alpha)_{n\_ideal} = \tau \cdot r \cdot \left(1 - \eta_{cells\_ideal} - (1-\alpha)\right) \cdot \frac{A_{active\_thermal}}{A_{Hybrid}} =$$

$$= 0.90 \cdot 0.90 \cdot \left(1 - 0.16 - (1-0.93)\right) \cdot \frac{3.7}{4.6} = 0.50$$

Equation 3.13

$$\eta_{elect.\_ideal}(25°C) = \tau \cdot r \cdot \eta_{cells\_ideal} \cdot \frac{A_{active\_elect.}}{A_{Hybrid}} =$$

$$= 0.90 \cdot 0.90 \cdot 0.16 \cdot \frac{3.5}{4.6} = 0.10$$

Equation 3.14

The transmittance τ of the glass was measured to be 0.90 (Bernardo et al., 2007), while the reflectance r is 0.90 (Alanod Solar, 2010) and the absorptance α of the solar cells was assumed to be 0.93 (Brogren et al., 2001). Dividing the active thermal area by the total glazed area makes it possible to compare the theoretical calculations with the measurements. This analysis helps to understand why concentrating hybrids have lower efficiencies than conventional thermal collectors and PV modules. Furthermore, the theoretical values point out a general limitation to the final efficiencies of concentrating hybrids. As shown, the difference between the measured and the theoretical efficiencies is not significant. In the thermal case, this difference can mainly be explained by the reflector shape inaccuracies and because F' was not taken into account. F' can be difficult to estimate theoretically since the thermal absorber does not feature a selective surface and its conductance is also not known. In the electric case, the difference is related to uneven distribution of solar irradiation on the cells and light scattering after reflection.

This is one of the challenges to overcome in this new technology. Having uniform radiation distribution over the PV module becomes especially critical for series connected cells since the one with the lowest output will limit the entire final production (Sick and Erge, 1998; Coventry et al., 2002; Nilsson, 2007). This concept is known as the "current matching problem" (Royne et al., 2005). In future models, local diodes should be installed over each cell in order to bypass the current over the poorest cells

and help minimize the impact of uneven radiation. Reflector imprecision was not the only factor causing the decrease in the final electric output. Local shading effects, tracking inaccuracies, and variation between cells were also some of the obstacles found in this and other previous studies, making it difficult to achieve the efficiencies obtained when individual cells are tested under ideal conditions (Chow, 2010; Franklin and Coventry, 2002). Similar efficiency values were reported in recent studies of concentrating hybrids. Kostić et al. (2010) measured a thermal optical efficiency of 37% and an average value of the daily electrical efficiency of 3.7% in a hybrid using low concentrating flat reflectors. Also, Tripanagnostopoulos and Souliotis (2004) measured a thermal optical efficiency between 50% and 64% in solar thermal collectors using low concentrating parabolic reflectors. However, these last values would be further reduced in a PV/T hybrid since part of the irradiation would be used to produce electricity.

The system design still has margin for improvement on most of its components for future developments. It is very important that cells under concentration have very high efficiency; the glass cover should have very high transmittance while optical errors in the reflector should be avoided and reflectance maximized. In future studies, an analysis of the aging of the cells and the efficiency decrease with time should be performed. Also, it is recommended that not only the hybrid outputs but also the performance of the whole system should be estimated. In this further investigation it is relevant to know, among other factors, what are the hybrid application, the yearly load, its daily and annual profile and the storage and auxiliary backup characteristics. Hence, it becomes possible to estimate the total system performance weighted with the investment and maintenance costs awarding different values to the electricity and thermal energy produced by the hybrid.

When it comes to possible applications for the hybrid, in view of the fact that the thermal output is much higher than the electrical output, it seems that the argument regarding the thermal output as just a benefit one can get by cooling down the cells does not make sense. It is more realistic to think that, at present, PV/T hybrids can only become viable when a suitable application for the produced thermal energy is also found. The challenge is that the thermal system often requires a high temperature which reduces the PV module efficiency. Therefore the optimum operating point should be defined by a cost analysis investigation. If the generated electricity can be directly connected to the grid, then the system area should be designed to cover the thermal load. When the analyzed hybrid is compared with a side-by-side system based on total glazed area the results show that, in terms of occupied space and global energy produced, there is no difference in having the hybrid working for domestic hot water production or pool heating. In this case, due to its lower $F'U_0$ value compared with

the standard flat plate collector, what is "lost" in electricity production at high temperatures is compensated for by thermal production at almost the same rate.

4 Testing of the CPC collector system

4.1 Background

One of the most important goals to be achieved by a solar thermal system is a high annual solar fraction (Mills and Morrison, 2003; Helgesson et al., 2002). Generally, in geographical regions further away from the equator, the solar contribution profile peaks during the summer months and decreases during the winter period. On the other hand, the domestic hot water load is fairly constant over the year. This means that the annual production and consumption profiles do not match. In addition, daily consumption profiles tend also not to match the solar daily production. In fact, the largest domestic hot water loads take place early in the morning and late in the afternoon or at night. During these periods the solar irradiation values are lower or inexistent. Consequently, the annual solar fraction of the system is reduced.

The main objective of the investigation was to evaluate the performance of the CPC collector system and compare it with that of a conventional flat plate collector system. To the best of our knowledge there exists no validated model of a solar thermal system using this asymmetric compound parabolic collector design.

4.2 Collector design

A solar collector design in which a relatively expensive selective absorber material is replaced by cheap reflectors was studied. A compound parabolic concentrator (CPC) collector with a geometrical concentration factor of 1.5 has been developed (Helgesson, 2004 and Adsten et al., 2004). The collector consists of a reflector, a bi-facial selective absorber and a support structure. The parabolic reflector has an optical axis normal to the collector glass which defines the irradiation acceptance interval of the reflector (Figure 4.1). Once the incident radiation is outside this interval,

the reflectors do not redirect the incoming beam radiation to the absorber, and the optical efficiency of the collector is reduced. Hence, the collector's optical efficiency changes throughout the year depending on the projected solar altitude. The tilt determines the amount of total annual irradiation kept within the acceptance interval. As a result, by varying the tilt, it is possible to increase the collector area without causing overproduction in the summer when the collector has lower optical efficiency. Related concepts to this collector have been reported by Kothdiwala et al. (1995), Tripanagnostopoulos et al. (2000), Chaves and Pereira (2000), Mills and Morrison (2003).

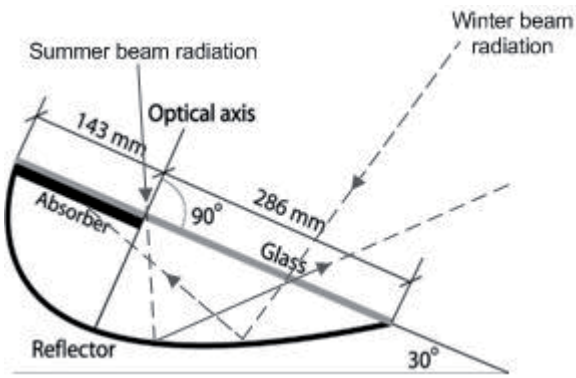

Figure 4.1 *Sketch of the compound parabolic concentrator collector profile (Helgesson, 2004).*

4.3 Evaluation method and model

Several measurements were carried out on the CPC collector in order to calculate the necessary parameters for the annual performance simulations. A simplified dynamic test method for determination of non-linear optical and thermal characteristics with multiple linear regressions was used (Perers, 1993; Perers, 1997). These parameters were then fed into a validated model in TRNSYS (Klein S., 2006) estimating the CPC collector system performance and comparing it with a flat plate collector system.

In order to accurately determine the collector incidence angle modifiers, a special measurement procedure was performed. The biaxial method described by Nilsson et al. (2006) to model the incidence angle modifiers in the transversal and longitudinal plan was used. Firstly, the influence of the glazing was measured in the longitudinal direction when the transversal incident angle was kept constant. Secondly, the dependence of the

reflector was measured on the transversal plane when the longitudinal incidence angle was also constant (Figure 4.2). In this study, the measured incidence angle modifier curves were included in the model using high grade polynomial equations. Hence, interpolations were avoided and the accuracy of the model increased. A TRSNSYS model describing the whole solar collector system was created. The system main components are shown in Figure4.3.

The domestic hot water load profile was built based on that described by Widén et al., (2009) but scaled to the latest data on Swedish total hot water consumption (Stengård 2009). Seven different water draw-offs were performed during the day (Figure 4.4). Furthermore, the annual hot water consumption variation effect was also introduced and it is shown in Figure 4.5 (Swedish Energy Agency, 2009c). The total annual consumption corresponds to 2050 kWh/year. The annual limit for the deterioration factor was set to 5000 °Ch/year. This number represents a reasonable value for the maximum overproduction (100 hours of stagnation with 150°C collector temperature, for example). Finally, by simulation iterations, the maximum collector area that corresponds to the maximum solar fraction but limts the overproduction to 5000 °Ch/year was determined.

Figure 4.2 *Compound parabolic concentrator collector turned 90° during the autumn equinox*

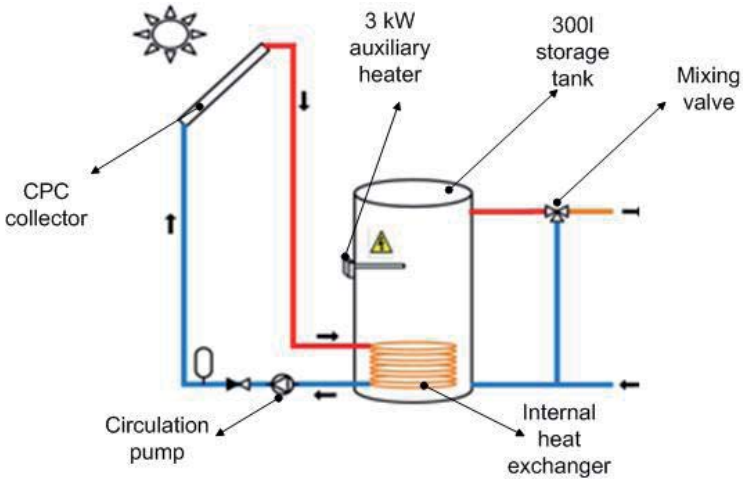

Figure 4.3 *Main components of the solar collector system model.*

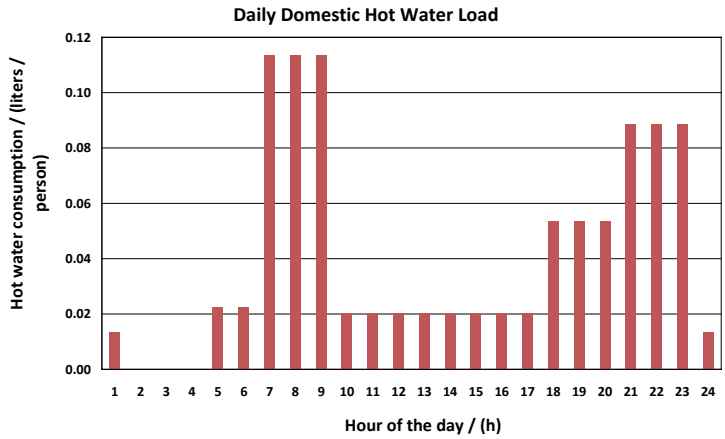

Figure 4.4 *Daily domestic hot water profile.*

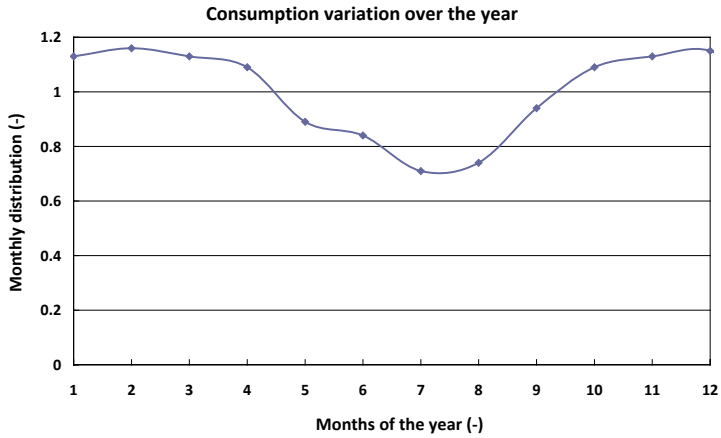

Figure 4.5 Yearly domestic hot water profile.

4.4 Measurement results and collector characterisation

The CPC collector parameters, estimated using multi linear regression on the measured data, and the parameters assumed to be typical for conventional flat plate collectors, are presented in Table 4.1.

Table 4.1 Measured CPC collector parameters and presumed typical flat plate collector parameters.

Parameters and units	CPC collector (measured)	Flat plate collector (presumed)
$F'(\tau\alpha)_n$ (-)	0.64	0.8
$F'(\tau\alpha)_n$ K_d(-)	0.31	0.72
$F'U_0$ / (W/m^2,°C)	2.8	3.6
$F'U_1$ /(W/m^2,°C^2)	0.035	0.014
$b_{o\_thermal}$ (-)	-	0.2
$(mC)_e$ /(J/m^2 °C)	1923	8000

Figure 4.6 shows the longitudinal and transversal beam incidence angle modifiers describing the influence of glazing and reflector, respectively. In order to obtain a symmetric curve for the longitudinal incidence angle modifier, the Fresnel and Snell's laws were used. The shown transversal incidence angle modifier was measured.

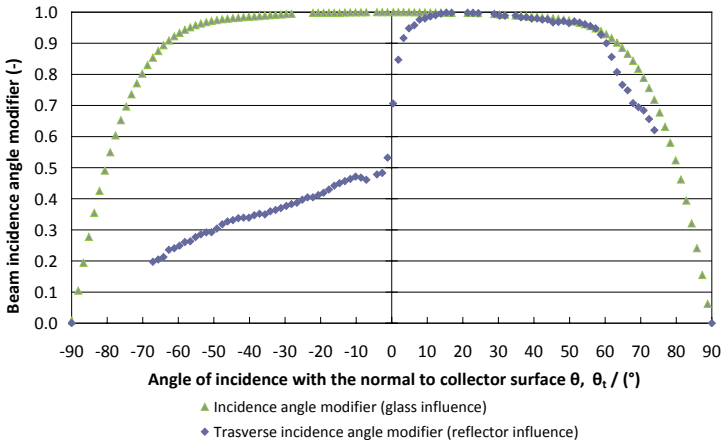

Figure 4.6 *Reflector and glazing incidence angle modifiers during autumn equinox*

4.5 Model validation

To validate the CPC collector model, the measured and modelled power outputs were compared during the test period (Figure 4.7). From the analysis of Figure 4.7, one can conclude that good agreement was found between the model and the measurements. In Figure 4.8 the modelled and measured power output are compared during a variable irradiation day. It was assumed that the CPC collector model is the only component that requires validation. The other components are standard and have been used with great reliability in the scientific community.

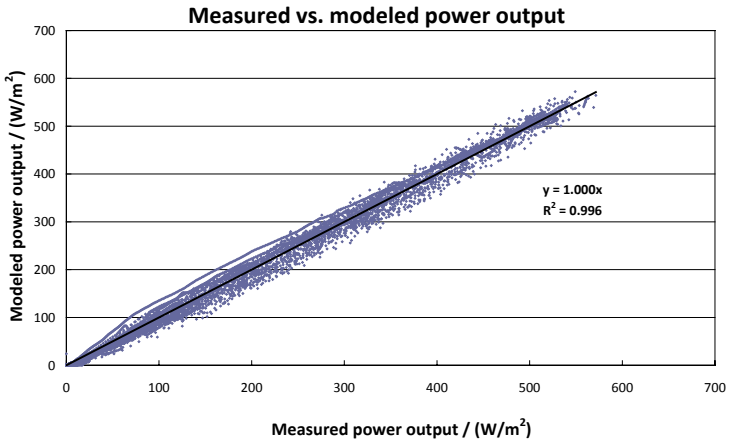

Figure 4.7 *Modelled and measured power output data during the testing period.*

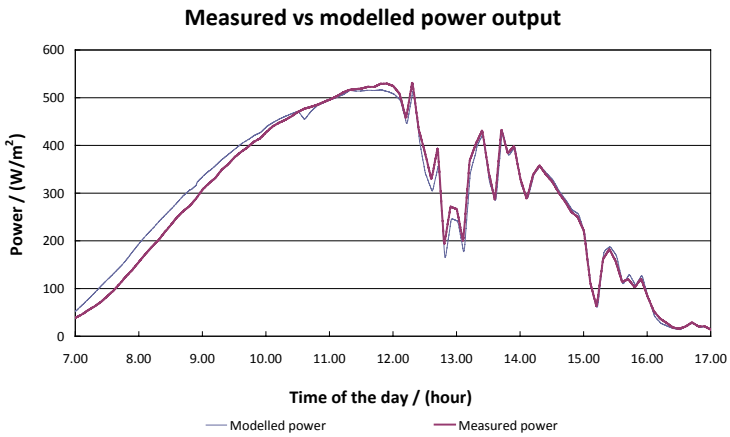

Figure 4.8 *Modelled and measured power output on the 20th September 2009.*

4.6 Performance analysis and discussion

The maximum solar fraction achieved by both systems, for several different tilts, is presented in the left axis in Figure 4.9. The corresponding maximum collector area that limits the annual overproduction under 5000°Ch/year is shown in the right axis of the same figure. These values correspond to the simulation results based on the validated model of the CPC collector.

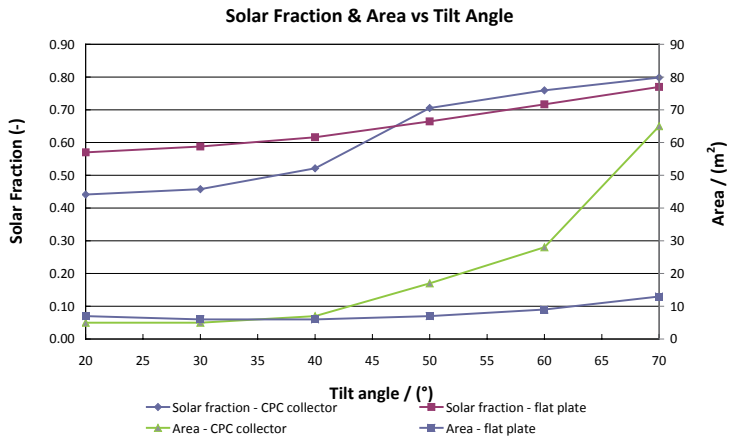

Figure 4.9 *Annual solar fraction and corresponding collector areas for both systems.*

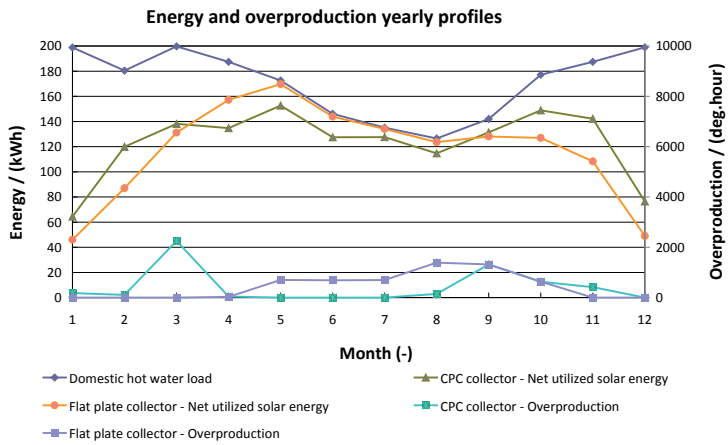

Figure 4.10 *Energy and overproduction profiles during the year for 50° tilt and 17m² of collector area.*

Analysing the simulation results, it can be concluded that, at 50° tilt, the load adapted system achieves a solar fraction of 71% using 17 m^2 of collector area compared to 66% and 7 m^2 of a flat plate collector system. In Figure 4.10, the annual production profile of the two solar systems is presented for 50° tilt. One can notice the suppressed solar production during the summer in the CPC collector and the overproduction moved to the spring and autumn periods. When the CPC collector system achieves higher solar fractions than the flat plate collector system, it requires, at least, 2.4 times more collector area. Taking into account that the selective absorber surface of the CPC collector is 1/3 of its total glazed area (Figure 4.1), one can conclude that the concentrating collector makes use of less absorber area. Obviously, this performance comparison is sensitive to the parameters assumed for the conventional flat plate collector. Nevertheless, there is an exaggerated optical efficiency decrease to less than half causing underproduction during the summer. If the reflector is improved, the CPC collector will achieve higher performances for the same collector area and become a more competitive solution when produced in a cheap way.

5 Simulations of the retrofitted solar thermal systems

5.1 Background

Since the solar tank is one of the most expensive components in a solar thermal system, retrofitting existing domestic hot water tank heaters when a new system is installed can reduce its total investment cost. Hence, the main boundary of this investigation was to use the most common type of existing heater in single family houses in Sweden. This information is very important for the system design but also very hard to attain. To the best of our knowledge, there is no official data concerning the most common tank size in such houses. According to the Swedish domestic hot water heater manufacturers, installers, plumbers and researchers in the field, the most common tank size in Swedish single family houses is 200 litres to 300 litres, depending on the family size. In any case, the tank volume tends to be proportional to the family size. Thus, the trend is that higher loads also correspond to higher available storage volumes and the system design strategy does not change. On the other hand, the average domestic hot water load in single family houses is documented. Preliminary results showed that retrofitting a 300 litre tank for such a domestic hot water load would achieve a higher annual solar fraction than using a 200 litre tank. Hence, to work on the safe side, it was decided to retrofit a 200 litre tank. If such a system achieves satisfactory performances the same should happen if a 300 litre tank is retrofitted instead.

Because of higher transfer rates due to a pump consuming very little energy, forced circulation systems can generally achieve higher performances than natural convection driven systems (Liu and Davidson, 1995). Hence, a forced circulation flow system was used when connecting solar collectors to conventional domestic hot water tank heaters. Since forced circulation is used, almost any kind of storage tank can be retrofitted when new solar thermal system is installed. This was carried out by means of

two pumps, one in the tank loop and the other in the solar collector loop. Four different system configurations were simulated in TRNSYS (Klein et al., 2006). Their annual performance was estimated and compared with that of a standard solar thermal system.

5.2 System configurations

Four different simulation models of the retrofitted system were created in TRNSYS software. Also, a conventional solar thermal system was analysed. Some of the systems details are not revealed due to patent pending. Each system model is made up of a solar collector array, storage tank/s, auxiliary heater, heat exchanger between the collector and the tank loops, circulation pump/s, and radiation processor. According to the statistics and as described previously in the chapter "Testing of the CPC collector system" the total annual domestic hot water consumption was 2050 kWh/year (Swedish Energy Agency, 2009b). The criterion used to design the collector array was to maximise the annual solar fraction but limit the overproduction under a certain point. Hence, by means of simulation, the maximum collector area that ensures the maximum solar fraction under the overproduction limit was determined for each system configuration.

The different configurations of all the analysed systems are shown in Figure 5.1 to Figure 5.5. The retrofitted systems were organized in increasing steps of complexity which also correspond to higher energy performances.

The first system sketch (Figure 5.1) represents a model of a standard solar thermal system. The tank has an internal heat exchanger and auxiliary heater. The reservoir volume was set to 255 litres to match the volume of the retrofitted system with the best performance (retrofitted system 4, Figure 5.5). Hence, since the collector array is also the same in both systems, the difference in their performances expresses only the different tank models and system configurations.

Retrofitted system 1 consists of assembling new solar collectors to an existing tank heater in a very simple way. An external heat exchanger makes the connection between the collector and the tank loops. These two loops are separated to avoid mixing between the freezing protection fluid running in the collector absorber and the domestic hot water inside the tank. One of the main challenges building the retrofitted system was to deal with a reduced number of pipe connections on the existing heaters. As shown in Figure 5.2, a conventional solar storage tank has four connections. Two correspond to the collector charging circuit and two others correspond to the domestic hot water consumption circuit. As exemplified in the same

figure, the retrofitted tank heaters have only two connections corresponding to the load. In order to overcome this technical challenge, the working period of the pump placed on the tank loop must be controlled with the domestic hot water draw-offs so they do not occur at the same time. This was performed in such a way that when no hot water was required, the pump was able to charge the tank. At the time of draw-offs, the pump was turned off and the incoming cold water was pressed in the bottom of the tank, replacing the outgoing domestic hot water at the top.

The next increase in complexity on the retrofitted system is shown in Figure 5.3. In retrofitted system 2, the auxiliary heater was moved to the side arm aiming to achieve stratification in the tank. The heater and the pump on the tank loop were turned on when charging of the tank was necessary.

In retrofitted system 3, a small 55 litre auxiliary heater storage was added to the system in parallel with the retrofitted tank (Figure 5.4). Consequently, the retrofitted storage was exclusively used for solar hot water and, as long as there is available hot water above the domestic hot water load temperature, the water inside the auxiliary heater tank will not be used.

Finally, the last retrofitted system, retrofitted system 4, consists of connecting the small heater storage to the existing heater in series instead (Figure 5.5). Thus, when hot water is drawn off by the user, the water at the top of the solar storage is pushed to the bottom of the small heater.

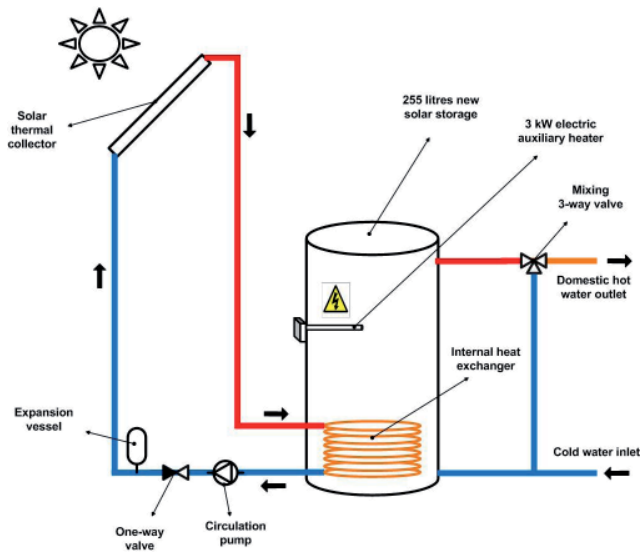

Figure 5.1. *Sketch of the standard solar thermal system for domestic hot water production.*

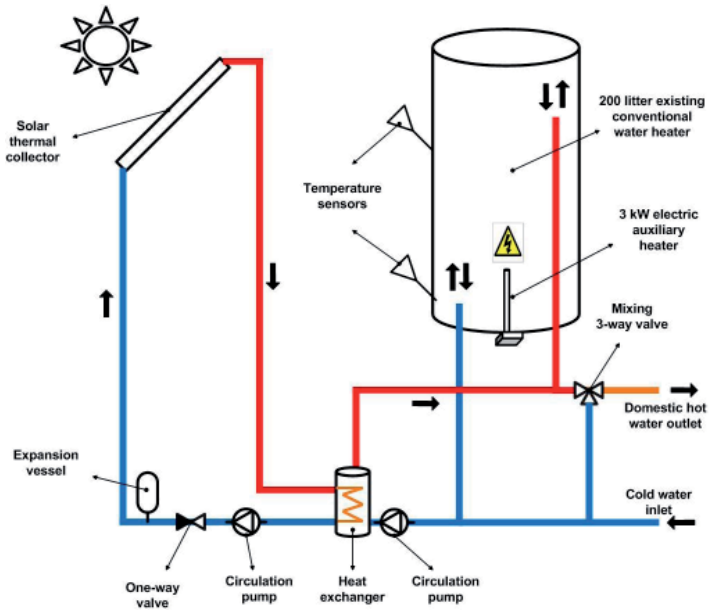

Figure 5.2. *Retrofitted system 1 - simple retrofitting of existing hot water heaters for domestic hot water production.*

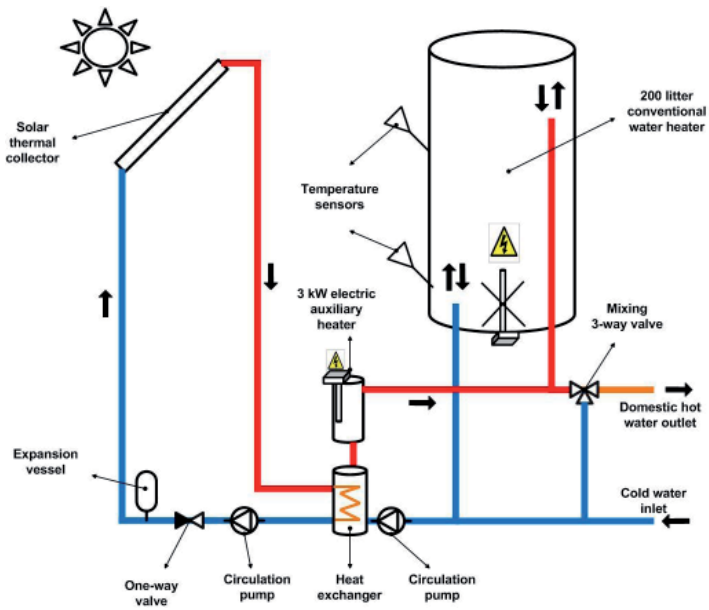

Figure 5.3. *Retrofitted system 2 - retrofitted system with auxiliary heater on the side-arm for domestic hot water production.*

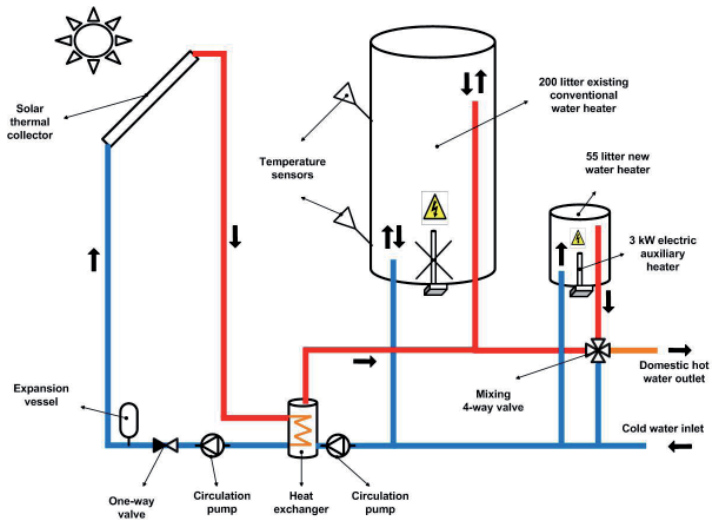

Figure 5.4. *Retrofitted system 3 - retrofitted system with an additional tank heater connected in parallel for domestic hot water production.*

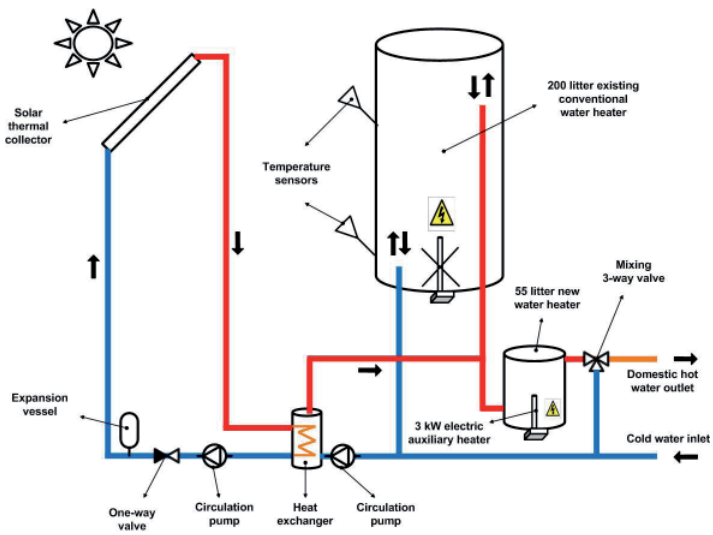

Figure 5.5. *Retrofitted system 4 - retrofitted system with an additional tank heater connected in series for domestic hot water production.*

5.3 Simulation results and discussion

The simulation results of the annual solar fraction for every system are presented in Table 5.1.

Table 5.1 Annual solar fraction of the various retrofitted systems and the standard solar thermal system.

System name	Annual solar fraction (%)
Standard system	52
Retrofitted system 1	6
Retrofitted system 2	15
Retrofitted system 3	42
Retrofitted system 4	53

The standard solar thermal system achieves a common value of annual solar fraction for the given load and climate in southern Sweden. When it comes to the retrofitted system 1 the estimated value for the solar fraction was 6%. The main reason for such low performance is the placing of the auxiliary heater at the tank bottom. This makes it impossible to establish any tank stratification. Also, incoming cold water at the bottom is continuously demanding auxiliary energy every time a draw-off takes place.

The results show that the annual solar fraction of retrofitted system 2 increases only to 15%. For such configuration, the upper volume of the tank is heated to 60°C while the bottom receives cold water almost continuously due to the daily draw-off schedule (see Figure 4.4). Due to the position of the tank inlets, the cold water at the tank bottom is heated by the collectors and placed at the very top of the tank. Since during long periods of the year the collector does not manage to heat up the water over 60°C, the tank top temperature decreases and stratification is destroyed. Consequently, the auxiliary heater is turned on during many hours of the year decreasing the annual solar fraction.

The estimated solar fraction of retrofitted system 3 was 42%. Since it was difficult to achieve stratification inside the retrofitted tank due to the position of its inlets, the auxiliary heater was placed in another tank. Hence, the retrofitted tank will work at lower temperatures increasing the collector working hours and efficiency. In addition, a new well insulated hot temperature tank provides the extra energy when solar energy is not available. One can say that the system “stratification” is achieved by two tanks with low stratification but working at different average temperatures.

For this particular configuration, the thermostat set-point temperature of the small tank does not significantly influence the annual performance. This is because the water in both tanks does not mix and the heat losses of the auxiliary tank are small.

Finally, the estimated annual solar fraction for retrofitted system 4 is 53%. The reason why the solar fraction of the series connected system is higher than the parallel connection is not obvious. The main reason is that, during the summer period when solar hot water is available over 60°C, the total storage volume of the series connected system is increased to 255 litres, since both tanks are connected in series and no auxiliary energy is needed.

Contrary on what happens with retrofitted system 3, the preset temperature of the heater in retrofitted system 4 influences significantly the annual performance. In fact, if the small heater connected in series is set to 80°C, the solar fraction decreases from 53% to 32% while the parallel connected system decreases only from 42% to 38%. This means that the system performing best depends on the auxiliary storage setup temperature (Figure 5.6). Simulation shows that if the auxiliary heater temperature is set to 70°C, retrofitted system 3 and 4 have approximate performances. These results are better understood by taking particular examples for different situations. If the temperature inside the retrofitted tank is 70°C and the tank heater temperature set to 60°C (Figure 5.7a and Figure 5.7b), there is no need to use auxiliary energy in both systems during a draw-off that requires 50°C. However, the series connected system has the advantage of saving energy since 70°C water enters the small tank and turns off the heater set to 60°C. Also, the total storage volume for solar hot water is increased to 255 litres since both tanks are connected in series. On the other hand, if one studies the case of having 70°C in the retrofitted tank but 80°C in the tank heater (Figure 5.7c and Figure 5.7d), the result is different. In the parallel connected system (Figure 5.7c), all the water is drawn from the retrofitted tank with no use of auxiliary energy. In the series connected system (Figure 5.7d), 70°C water is pushed in the small tank which uses auxiliary energy to heat it up to 80°C. Generalising the previous example one concludes the following:

- Temperature inside the retrofitted tank lower than the load (T_{solar}<50°C): calculation shows that the parallel connection presents a slightly better performance. The solar hot water is used for preheating and saves energy to the auxiliary heater in both systems.
- Temperature inside the retrofitted tank higher than the load but lower than the set point temperature of the auxiliary heater (50°C>T_{solar}<$T_{auxiliar}$): the parallel connected system performs better

since no auxiliary energy is required, contrary to the series connected system.

- Temperature inside the retrofitted tank higher than the set point temperature of the auxiliary heater ($T_{solar} > T_{auxiliar}$): the series connected system performs better since it saves energy to the auxiliary heater and increases the total solar hot water volume to both storages.

Hence, the period when the parallel connection is clearly advantageous over the series connection is during intervals where the temperature inside the retrofitted tank is higher than the load requested temperature but lower than the preset temperature in the tank heater. This period becomes short if the thermostat temperature is set to 60°C and thus the series connected system achieves the highest performance over the year.

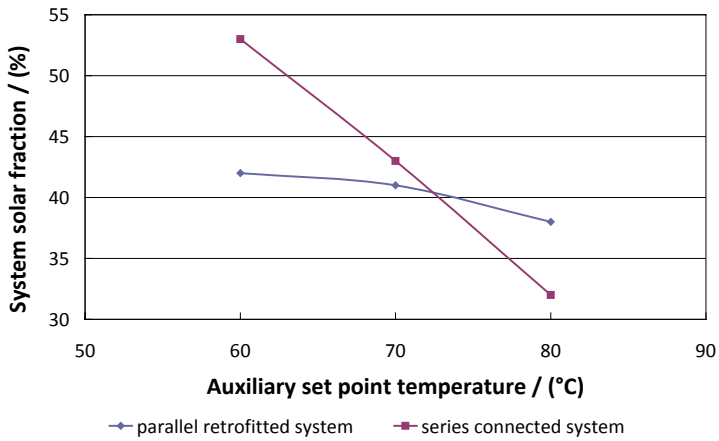

Figure 5.6. *Solar fraction temperature dependence of the parallel and series connected systems.*

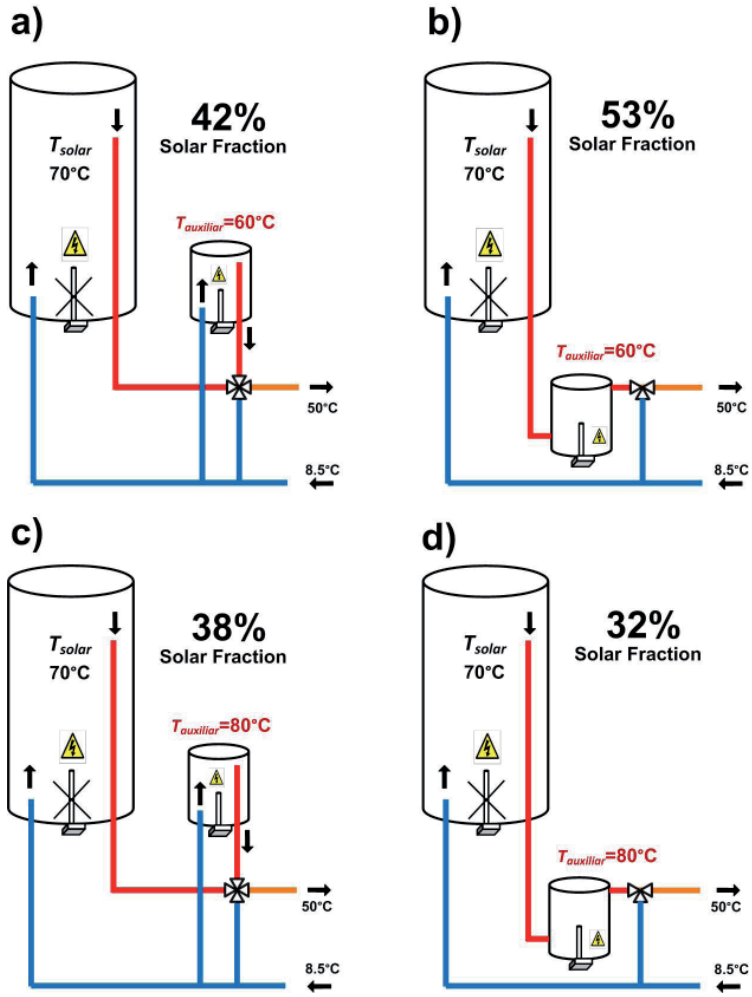

Figure 5.7 *Solar fraction results of: a) parallel connected system and 60°C thermostat temperature b) series connected system and 60°C thermostat temperature c) parallel connected system and 80°C thermostat temperature d) series connected system and 80°C thermostat temperature*

6 Discussion and conclusions

An advanced solar thermal system for domestic hot water production for electrically heated houses has been developed. The system consists of retrofitting existing domestic water heaters when solar collectors are installed. Two different collectors were tested outdoors: a low concentrating PV/T hybrid and a CPC-thermal collector. The concentrating hybrid was chosen since it aims to produce both hot water and electricity at a lower cost than a flat plate collector and a PV module working side-by-side. The CPC-collector aims to adapt the solar production to the domestic hot water load profile in order to achieve a higher annual solar fraction than a conventional flat plate collector. Both collectors were modelled in TRNSYS software and validated against measured data. Finally, a prototype of the retrofitted system was built for testing in the laboratory. Its design was built according to the simulation results which indicated the configuration with the best performance.

Previously, results were presented concerning the analysis of a concentrating PV/T hybrid, a CPC collector and different configurations of retrofitting existing tank heaters for solar thermal collectors. In the next subsections, the implication of these results on how to reduce the electricity consumption in single family electrically heated houses is discussed.

6.1 PV/T concentrating hybrid

The working temperature of a concentrating PV/T hybrid directly influences the production of heat and electricity. It is very important that the outlet temperature matches the load requirements. There are mainly two different strategies: either set the collector outlet at low temperatures to decrease the cell temperature and increase the electricity production or set the outlet temperature to high temperatures in order to collect heat at "usable" temperatures with lower electrical efficiencies. Either way, since

concentrating reflectors are used, relatively cold water must be available the whole year to prevent overheating damage to the cells. This is not possible for most domestic hot water applications in single family houses. For such applications the available cold water is dependent on the load profile and the available volume is limited by the existing tank size (usually 200 l-300 l). Hence, collectors in domestic hot water systems should be prepared to deal with stagnation. This becomes a problem for a concentrating hybrid since stagnation implies a temperature rise that would damage the cells. If a PV driven pump was used the flow speed would be proportional to the incident solar irradiation. Even in this case, the problem of having cold water temperatures to cool down the module every time solar irradiation is available would still remain.

Concentrating hybrids are probably more suitable in other kinds of systems. Such an example is residences with a pool that can work as a heat sink. Other possible applications are hotels or multifamily buildings with a high domestic hot water demand capable of continuously providing water at relatively low temperatures. For these applications, whether to set the collector outlet to high or low temperatures depends on how the electricity production decreases with temperature and the value attributed to the produced heat and electricity. For high temperature applications which prioritise heat production at higher temperatures, the hybrid size should be designed to match the heat load while the generated electricity is sent to the electric grid. Another option would be to use the temperature available in the ground or in the air to continuously cool down the receiver. This would remove heat from the solar cells and discharge it to the ground or the air. Taking into account that the main energy output from a concentrating hybrid is heat, it seems difficult that such a system is profitable.

The question is whether there is any PV/T hybrid collector suitable for single family domestic hot water applications. If a non concentrating flat PV/T hybrid were used, the cells would not be under dangerous light concentration. Moreover, the stagnation temperature of such a hybrid would be reduced if low back insulation were used. In fact, cooling would not be vital for these cells since without it they would not be damaged. Only the electric efficiency would be affected. Such a hybrid would be more convenient for a domestic hot water system where cold water is not always available during the year. Cold water available at the tank bottom is used to decrease the cell temperature and to store heat. If the tank is full of hot water, no water runs in the absorber and the PV/T hybrid behaves like a PV module with a lower efficiency.

Also, for a flat PV/T hybrid the working temperature directly influences the hybrid outputs. To better understand the impact on the generated heat and electricity for different working temperatures, simple simulations were

carried out for a flat PV/T hybrid. These results are used to roughly estimate the impact of different flow controls and should only be taken as a reference. The flat PV/T annual outputs were compared with a conventional system made of a flat plate collector and a PV module working together side-by-side. Both analysed systems are represented in Figure 6.1. The PV/T system glazed area is 1 m^2 while the side-by-side system is made of 1 m^2 of a flat plate collector and 1 m^2 of a PV module. Winsun, a TRNSYS based software for collector components, was used (Winsun Villa Software, 2009). The simulations were performed at a component level which means that only the outputs from the collectors were accounted for. High collector outlet temperatures were assumed to correspond to domestic hot water production (DHW) while low temperatures to preheating. Since no system is taken into account for such preliminary analysis, the collector outlet temperatures were set to be constant over the year. The thermal collector data for system 1 and system 2 is presented in Table 6.1. The average collector temperatures for each application are also shown. In Table 6.2 the PV module data for both systems is presented. It was assumed that both systems use the same type of solar cells and that these are series connected. Hence, the temperature conditioning the electrical output is the highest temperature in each PV module (Table 6.2). Finally, the annual output ratio between both systems is shown in Table 6.3.

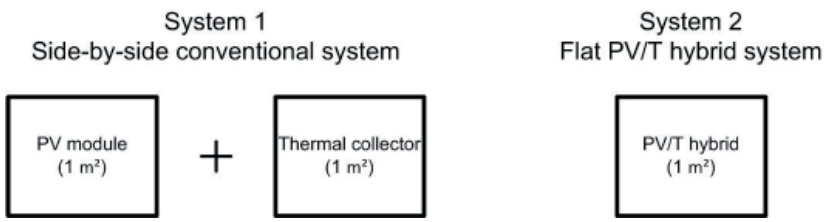

Figure 6.1 *Side-by-side and hybrid system sketches.*

Table 6.1 Thermal collector data for system 1 and system 2.

	System 1 thermal	System 2 thermal
$F'(\tau\alpha)_n$ (-)	0.8	0.65
$F'U_0$ (W/(m^2°C))	3.6	6
$F'U_1$ (W/(m^2°C^2))	0.014	0.014
T_m (preheating) (°C)	15	15
T_m (DHW) (°C)	40	40

Table 6.2 PV module data for system 1 and system 2.

	PV module
$\eta_{\_electrical}$ (25°C) (-)	0.15
K_T (%/°C)	0.40
System 1 highest temperature (°C)	30
System 2 highest temperature (DHW) (°C)	70
System 2 highest temperature (preheating) (°C)	20

Table 6.3 Annual energy output ratio System2/System1.

	System2/System1 (DHW)	System2/System1 (preheating)
Heat	0.51	0.78
Electricity	0.84	1.04

Results show that, for low temperature applications, the heat and electricity production of the hybrid system are not significantly affected when compared with a conventional side-by-side system. Actually, the cells in the hybrid system are cooled down and increase their production compared with a conventional PV module. Despite the high heat loss factor of the hybrid, the collector efficiency is not significantly reduced since it works close to ambient temperatures. Furthermore, the flat PV/T hybrid produces almost the same outputs as the side-by-side system but uses only half the space. When it comes to higher outlet temperatures, the hybrid heat production is halved while the electricity production decreases by 16% when compared with a conventional system. In any of the cases, the flat hybrid produces more energy per glazed area than a conventional side-by-side system.

The conclusion whether to use a concentrating or a flat PV/T hybrid can only be answered by a detailed cost analysis. Such investigation should assign different weights to the produced electricity and heat depending on the application. However, as described in the chapter "Testing of the PV/T concentrating hybrid", the use of concentrators implies lower usable annual irradiation levels together with lower efficiencies. A concentrating collector tracking around an axis aligned in the north-south direction receives 20% to 40% less usable irradiation than a static flat surface. In the particular case

study, the measured zero-loss efficiency of the concentrating hybrid was 45%, the $F'U_0$-value 1.9 W/m²°C and electric efficiency 6.4% (at 25°C). This combination of low efficiency together with low usable irradiation makes it difficult for concentrating hybrids to compete with a flat plate collector and a PV module working side-by-side. Also they require very specific system applications to be viable. Hence, it is logical to conclude that only a concentrating hybrid of very good cost-effectiveness and highly efficient cells could compete with conventional systems. Such cost effectiveness is easier to achieve when higher concentrations are used to make use of the cheaper reflector material compared to that of solar cells.

For all the previously mentioned reasons, the concentrating hybrid was found not to be a suitable solution on retrofitting tank heaters in practice. The use of thermal collectors for high solar fraction thermal systems was further investigated. Hence, the performance of a conventional flat plate collector system was compared to a CPC load adapted collector system for domestic hot water production in single family houses.

6.2 CPC collector system

Simulation results using the validated model of the CPC collector showed that the CPC collector system achieves a higher annual solar fraction than a conventional flat plate collector system. The measured zero-loss efficiency of the CPC collector was 64% while the heat loss factors $F'U_0$ and $F'U_1$ were 2.8 W/m²,°C and 0.035 W/m²,°C^2, respectively. The efficiency values assumed to be representative of a conventional flat plate collector were an optical efficiency of 80% and heat loss factor of 3.6 W/m²,°C and 0.014 W/m²,°C^2. From the simulation results one concludes that, at 50° tilt in Lund, the CPC-collector system achieves a solar fraction of 71% using 17 m² of collector area compared with 66% and 7 m² of a flat plate collector for the same design guidelines. This means that the CPC-collector uses 2.4 more collector area than a flat plate collector. However, the CPC-collector glass area is 3 times larger than the absorber area meaning that the CPC collector uses a smaller absorber. Hence, the higher performance and smaller absorber surface must compensate for the costs on having extra material such as reflectors, glass area, frames and possible difficulties in producing a parabolic reflector.

Both systems were designed to maximise their annual solar fraction but to limit the annual overproduction under a certain point. The aim was to introduce in the solar system design a deterioration factor that limits dangerous overproduction levels capable of permanently damaging the system components. This was carried out by considering not only

the number of stagnation hours but also how much the collector outlet temperature rose over 100 °C during stagnation periods. The annual limit for the deterioration factor was set to 5000 °Ch/year. This corresponds to a reasonable maximum overproduction level (100 hours of stagnation with 150°C collector temperature, for example). Further work is needed to understand how to account for overproduction in the system design in a more precise way. The assumed design guideline should be seen as a first iteration step in that direction. In a future analysis that takes into account the cost of every component, the system will be designed in order to improve its cost effectiveness. Another aspect of interest in the simulation results were the relatively high solar fraction values. These are mainly explained by the tank model used in the simulations. In such a tank model, the incoming water is placed at a height in the tank that has the closest matching temperature. Hence, very high stratification and consequently high solar performances were achieved. This simple tank model allowed time saving both in building the system model and the running period of the simulations.

For this analysis the important investigation to be performed is to conclude which solar thermal collector system performs best. For this reason, the significant result is the comparison between the performance of the two systems rather than the absolute values of their annual solar fraction. Since both system models are designed in the same way, the inaccuracies of one model are also present in the other one, making the comparison results valid. As the comparison results show, the collector achieving the highest annual performance was the CPC load adapted collector. This collector was then further used in the retrofitting system models.

6.3 Retrofitted system

Several retrofitting simulation models were created in order to estimate their annual performances and understand what the best configuration is. A comparison with a conventional flat plate system was also performed. In total four retrofitted system models were built ranging from simple connections to more advanced configurations. However, the complexity was never raised up to a level that would be technically difficult to build such a system in practice. Also, it was avoided to design configurations that would predictably cause such a rise on the investment cost that would be hardly paid back by the increase in energy savings. Simulation results show that it is difficult to achieve stratification when solar collectors are directly connected to conventional tank heaters. This is valid even if the auxiliary heater at the bottom of the tank is not used. This is due to their

inlet/outlet connection configuration. The best retrofitted configuration consists of connecting the existing water heater to a new small tank in series. Hence, the retrofitted tank will work together with the collectors at lower temperatures while the small additional tank works as a well insulated auxiliary heater. Consequently, during long periods of the year the collectors will work at low temperature conditions increasing the annual working hours and efficiency. The water heated by the collectors is then stored in the retrofitted tank and used for preheating the auxiliary heater. Since the tanks are series connected, when solar hot water is available the auxiliary heater is turned off and the whole storage volume is increased. One can say that the "system stratification" is achieved by means of two separate tanks featuring low stratification levels working at different temperatures. Preliminary simulation results show that the best retrofitted system achieves a performance comparable with that of a standard solar thermal system. This corresponds to an annual solar fraction of approximately 50%. Future work on the validation of these models will bring more accuracy to the results. Nevertheless, this comparative analysis is the proper investigation to be performed at this stage. If the studied system proves to be cost effective, this can be a very attractive solution not only due to its flexibility on retrofitting almost any kind of existing storage tank but also to its combination with new conventional tank heaters which industry is well developed and covers a world-wide market. Thus, a prototype of the best retrofitting configuration was built at the laboratory under continuous and detailed monitoring.

With the suggested solar thermal system installation, energy is saved directly on the consumer side where electricity cost is highest. On the contrary, if solar was used for large scale production, every saved energy unit would correspond to a saving cost of the electricity production before all the taxes and profits are added. This corresponds roughly to only 30% of the final electricity price (Figure 1.8 in the "Introduction" chapter). When installed on the end-user, every saved energy unit corresponds to the cost that accounts not only for electricity production but also the network company profits and all the taxes (electricity grid tax, energy tax and value added tax).

Also, if an air-to-air heat pump is installed, there is no "competition" between the energy produced by solar and the heat pump. On the other hand, when a solar thermal system is combined with an air-water heat pump, the situation is different. Every energy unit produced by the solar thermal system will only save a third or a quarter of the same quantity of electricity to the heat pump depending on its coefficient of operation. With an air-air heat pump, solar provides savings to the domestic hot water production while the heat pump provides savings to space heating.

This explains why this is probably one of the best applications for solar energy in Sweden.

At this point of the research work it is roughly estimated that, after the proposed energy renovation measures, the electricity consumption in electrically heated single family houses will be almost halved (Figure 6.2). For this calculation the approximate average loads corresponding to space heating, domestic hot water and domestic electricity were 9000 kWh/year (Swedish Energy Agency, 2009b), 2100 kWh/year (Stengård, 2009) and 6000 kWh/year (Swedish Energy Agency, 2009b), respectively. To estimate the decreases in energy use it was assumed that an air-to-air heat pump with coefficient of operation of 3 to 4 together with extra insulation and new windows would reduce the space heating load to one third. Also, the domestic hot water load was reduced to half since the retrofitted system calculations estimated an annual solar fraction of 50%. At this point no measures are planned to reduce the domestic electricity consumption. This means a total energy decrease estimated at 40%.

Theoretically, if all the existing half a million electrically heated single family houses carried out these energy renovation measures, the potential for electricity savings would be around 3.5 TWh/year. Since Sweden is an electricity exporter, this saving can be seen as a potential increase for export to other countries such as Germany and Poland which use coal-fired power plants. These energy renovation measures and their impact on the energy savings will be further investigated during our future work.

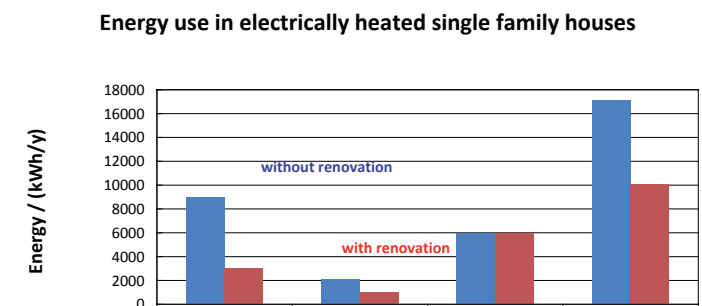

	space heating	DHW	domestic electricity	TOTAL
without renovation	9000	2100	6000	17100
with renovation	3000	1050	6000	10050

Figure 6.2 *Approximate estimations of the annual energy use in electrically heated single family houses with and without the proposed renovation measures.*

7 Future work

The remaining work to be carried out during the final period of our research is listed below.

7.1 Validation of the solar thermal systems models

One of the first assignments to be carried out during the continuation of our research work is to describe in detail the three monitored solar thermal systems built in the laboratory. After this, the collected measured data from the experimental setup will be analysed. With this information the previously described simulation models for the retrofitting will be adjusted to match the measurement results. At that point it will be important to accurately estimate the absolute value of the annual energy savings of the retrofitted system. Such savings will then be converted into costs savings on auxiliary energy and used in the economical assessment calculations.

7.2 Economical assessment of the retrofitted system

Having a validated result of the retrofitted thermal systems performance makes it possible to carry out an economical assessment. In such an evaluation the life cycle cost of three different alternatives will be estimated. These are: keep the old domestic hot water system as it is and do not invest in a new solar thermal system; scrap the existing water heater and install a new conventional solar thermal system; retrofit the existing water heater while installing the solar thermal system using the studied configuration.

7.3 Sketch of the retrofitting component prototype

Following the economical assessment it is then time to draw a general diagram of the prototype component that makes it possible to connect new solar collectors to existing conventional domestic hot water heaters. Such a component is the key not only for the retrofitting but also for using new water heaters. This will be the very practical base for a possible continuation of the project on the implementation of the product in real applications and in the market.

7.4 Model of an electrically heated conventional single family house and the impact of each renovation measure on its annual energy performance

The last step in the research work is to integrate the model of the developed retrofitted system into an accurate model of a typical electrically heated single family house in Sweden. Also, the impact on house energy performance will be estimated for every energy renovation measure. These include the installation of an air-air heat pump, new energy efficient windows and extra insulation in the most appropriate locations.

References

Absolicon Solar Concentrator AB (2008). Accessed 2008-08 from http://www.absolicon.com

Adsten, M., Helgesson, A. & Karlsson, B. (2004). Evaluation of CPC-collector designs for stand-alone, roof- or wall installation. *Solar Energy*, 79(6), 638-647.

Affolter, P., Eisenmann, W., Fechner, H., Rommel, M., Schaap, A., Sorensen, H., Tripanagnostopoulos, Y. & Zondag, H. (2004). *PVT road map, A European guide for the development and market introduction of PV-Thermal technology.* Energy Research Centre of the Netherlands, Netherlands. Accessed 2008-01 from http://www.pvtforum.org

Alanod Solar (2010). *Technical information concerning the reflector.* Accessed 2009-02 from http://www.alanod-solar.com

Aleklett, K. & Campbell, C. J. (2003). The peak and decline of world oil and gas production. *Minerals and Energy,* 18, 5-20. Download available at http://www.peakoil.net/files/OilpeakMineralsEnergy.pdf

Arvind, C. & Tiwari, G.N. (2010). Stand-alone photovoltaic (PV) integrated with earth to air heat exchanger (EAHE) for space heating/cooling of adobe house in New Delhi (India). *Energy Conversion and Management*, 51(3), 393-409.

Arvind, C., Tiwari G.N. & Avinash, C. (2009). Simplified method of sizing and life cycle cost assessment of building integrated photovoltaic system. *Energy and Buildings*, 41(11), 1172-1180.

Bernardo, L. R., Davidsson, H. & Karlsson, B. (2010). Performance Evaluation of a High Solar Fraction CPC-Collector System. Submitted to *Renewable Energy* in 2010-11.

Bernardo, L. R., Perers, B., Håkansson, H. & Karlsson, B. (2008). Evaluation of a Parabolic Concentrating PVT system. In proceedings of *Eurosun 2008*, Portugal.

Brogren, M., Nostell, P. & Karlsson, B. (2001). Optical efficiency of a PV–thermal hybrid CPC module for high latitudes. *Solar Energy,* 69(6), 173-185.

Chaves, J. & Pereira, M. C. (2000). Ultra flat ideal concentrators of high concentration. *Solar Energy,* 69(4), 269-281.

Chow, T. T. (2003). Performance analysis of photovoltaic-thermal collector by explicit dynamic model. *Solar Energy,* 75(2), 143-152.

Chow, T.T. (2010). A review on photovoltaic/thermal hybrid solar technology. *Applied Energy,* 87(2), 365-379.

Coventry, J.S., Franklin, E.T. & Blakers, A. (2002). Thermal and electric performance of a concentrating PV/Thermal collector: results from the ANU CHAPS collector. In proceedings of *Australian and New Zealand Solar Energy Society Conference 2002*. Download available at http://hdl.handle.net/1885/40837.

Cruickshank, C. & Harrison, S. (2004). Analysis of a Modular Thermal Storage for Solar Heating Systems. In proceedings of *Canadian Solar Buildings Conference 2004*. Download available at http://www.solar-buildings.ca/c/sbn/file_db/Analysis%20of%20a%20Modular%20Thermal%20Storage%20for%20Solar.pdf

Duffie, J.A. & Beckman, W. A. (2006). *Solar Engineering of Thermal Process*. John Wiley and sons, inc., Interscience, New York.

European commission (2006). *Photovoltaic geographical information system*. Accessed 2010-09 from http://re.jrc.ec.europa.eu/pvgis/

European Renewable Energy Council (2010). *RE-thinking 2050 – a 100% renewable energy vision for the European Union*. Accessed 2010-09 from http://www.erec.org/

European Union (2007). *The European Union climate and energy package*. Accessed in 2010/09 from http://ec.europa.eu/environment/climat/climate_action.htm

Fahrenbruch, A. & Bube, R. (1983). *Fundamentals of solar cells – Photovoltaic solar energy conversion.* Department of Materials Science and Engineering, Stanford University, Stanford, California. Academic Press Inc., New York. ISBN 0-12-247680-8.

Federal Institute for Geosciences and Natural Resources (2009). *Reserves, resources and availability of energy resources - BGR 2009*. Accessed 2010-10 from http://www.tsl.uu.se/uhdsg/Data/BGR/BGR2009.pdf

Fisher, S., Heidemann, W., Müller-Steinhagen, Perers, B., Berquist, P. & Hellström, B. (2004). Collector test method under quasi-dynamic conditions according to the European Standard EN 12975-2. *Solar Energy,* 76(1-3), 117-123.

Franklin, E.T. & Coventry, J.S. (2002). Effects of highly non-uniform illumination distribution on electrical performance of solar cells. In proceedings of *Australian and New Zealand Solar Energy Society Conference 2002*. Download available at http://hdl.handle.net/1885/40832

Government Bill (2008). *En sammanhållen klimat – och energipolitik – Energi (2008/9: 163)*. Accessed 2009-09 from http://www.sweden.gov.se/content/1/c6/12/27/85/65e0c6f1.pdf

Green, M. A. (1998). *Solar Cells - Operating Principles, Technology and System Apllications*. University of New South Wales, Australia.

Hausner, R. & Fink, C. (2000). *Stagnation behaviour of thermal solar systems.* Download available at www.aee-intec.at/0uploads/dateien119.pdf.

Hausner, R. & Fink, C. (2002). *Stagnation behaviour of solar thermal systems*. IEA SHC, task 26.

Helgesson, A. (2004). *Optical Characterization of Solar Collectors from Outdoor Measurements*. Licentiate thesis, ISBN 91-85147-07-9, pp 293-294.

Helgesson, A., Karlsson, B. & Nordlander, S. (2002). Evaluation of a Spring/Fall-MaReCo. In proceedings of *Eurosun 2002,* Bologna.

International Energy Agency statistics (2009). *Electricity information 2009*. Accessed 2010-09 from http://www.iea.org/

IPCC – Intergovernmental Panel for Climate Change (2007). *Assessment Report 4*. Accessed 2010-10 from http://www.ipcc.ch/pdf/assessment-report/ar4/syr/ar4_syr.pdf

IPCC – Intergovernmental Panel for Climate Change – Working Group 1 (2010). *Latest Findings to be assessed by WGI in AR5.* Accessed 2010-10 from http://www.ipcc.ch/pdf/presentations/COP15-presentations/stocker09unfcccCopenhagen_delegate_new.pdf

Klein, S.A., Beckman, W.A., Mitchell, J.W., Duffie, J.A., Daffie, N.A. & Freeman, T.L. (2006). *TRNSYS, a Transient System Simulation Program*. Solar Energy Laboratory, University of Wisconsin, Madison.

Kostić, Lj. T., Pavlović, T. M. & Pavlović, Z. T. (2010). Optimal design of orientation of PV/T collectors with reflectors. *Applied Energy,* 87, 3023-3029.

Kothdiwala, A., Norton, B. & Eames, P. (1995). The effect of variation of angle of inclination on the performance of low-concentration-ratio compound parabolic concentrating solar collectors. *Solar Energy*, 55(4), 301-309.

Lin, Q. (1998). *Analysis, Modelling and Optimum Design of Solar Domestic Hot Water Systems*. Ph.D. thesis, ISBN 87-7877-023-8.

Liu, W. & Davidson, J. (1995). Comparison of Natural Convention Heat Exchangers for Solar Water Heating Systems. In proceedings of *American Solar Energy Society Conference 1995*. Download available at http://www.p2pays.org/ref/20/19434.pdf

Menova Energy (2010). Accessed 2010-11 from http://www.mbssales.com/menova.html

Meteonorm 5.0 (2010). *Global meteorological data base for solar energy and applied meteorology*. Accessed 2010-08 from http://www.meteonorm.com/pages/en/meteonorm.php

Mills, D. & Morrison, G. (2003). Optimisation of minimum backup solar water heating system. *Solar Energy,* 74(6), 505-511.

Nilsson, J., Håkansson, H. & Karlsson, B. (2007). Electrical and thermal characterization of a PV-CPC hybrid. *Solar Energy,* 81(7), 917-928.

Perers, B. (1993). Dynamic method for solar collector array testing and evaluation with standard database and simulation programs. *Solar Energy,* 50(6), 517-526.

Perers, B. (1997). An improved dynamic solar collector test method for determination of non-linear optical and thermal characteristics with multiple regression. *Solar Energy,* 59, 163-178.

Perers B. & Bales C. (2002). *A Solar Collector Model for TRNSYS Simulation and System Testing.* A Report of IEA SHC - Task 26 Solar Combisystems. Download available at http://www.les.ufpb.br/portal/index2.php?option=com_docman&task=doc_view&gid=190&Itemid=30

Persson, T. (2006). *Combined solar and pellet heating systems for single-family houses*. Doctoral thesis ISBN 91-7178-538-8.

Royne A., Dey C.J. & Mills D.R. (2005). Cooling of photovoltaic cells under concentrated illumination: a critical view. *Solar Energy Materials and Solar Cells,* 85(4), 451-83.

Sick, F. & Erge, T. (1998). *Photovoltaic in buildings: a design handbook for architects and engineers.* IEA task 16. ISBN 1 873936 59 1, pp 27-28.

Solar Collector, LTH. Software developed by Bengt Hellström and Hasse Kvist at the Energy and Building Design Division, Lund Technical University, Sweden.

Stengård, L. (2009). *Mätning av kall- och varmevattenanvändning i 44 hushåll*. Acessed 2009-10 from http://webbshop.cm.se/System/ViewResource.aspx?p=Energimyndigheten&rl=default:/Resources/Permanent/Static/b9a064ece4d747868b5c20d1a03ab0a2/2124W.pdf

Swedish Energy Agency (2009a). *Energy in Sweden 2008*. Accessed 2010-06 from http://webbshop.cm.se/System/ViewResource.aspx?p=Energimyndigheten&rl=default:/Resources/Permanent/Static/ab6822c96d86401c8d2a5e362bdfa0d7/ET2009_30.pdf

Swedish Energy Agency (2009b). *Energy statistics for one- and two- dwelling buildings in 2008*. Accessed 2010-02 from http://webbshop.cm.se/System/ViewResource.aspx?p=Energimyndigheten&rl=default:/Resources/Permanent/Static/60373ee0cdc743898284fec420067527/2128W.pdf

Swedish Energy Agency (2009c). *FEBY – Krav Specifikation för Minienergihus.* Accessed 2010-01 from http://www.energieffektivabyggnader.se/download/18.712fb31f12497ed09a58000141/Kravspecifikation_Minienergihus_version_2009_oktober.pdf

Tripanagnostopoulos, Y. & Souliotis, M. (2004). Integrated collector storage solar systems with asymmetric CPC reflectors. *Renewable Energy*, 29, 223-248.

Tripanagnostopoulos, Y., Yianoulis, P., Papaefthimiou, S. & Zafeiratos, S. (2000). CPC solar collectors with flat bifacial absorbers. *Solar Energy*, 69, 191-203.

TRNSYS, 2010. TRNSYS official website accessed 2010-09 from http://sel.me.wisc.edu/trnsys/

Wenham, S. R., Green, M. A., Watt, M. E. & Corkish, R. (2007). *Applied Photovoltaics.* University of New South Wales School of Photovoltaic and Renewable Energy Engineering, Australia.

Widén, J., Lundh, M., Vassileva, I., Dahlquist, E., Ellegård, K. &Wäckelgård, E. (2009). Constructing load profiles for household electricity and hot water from time-use data—Modelling approach and validation. *Energy and Buildings*, 41(7), 753-768.

Winston, R., Miñano, J. & Benítez, P. (2005). *Nonimaging Optics*. ISBN 0-12-759751-4.

Winsun Villa Educational Software (2009). Perers, B., SERC Högskolan Dalarna, Sweden. http://www.serc.se

World Energy Council (2007). *Survey of Energy Resources 2007*. Accessed 2010-01 from http://www.tsl.uu.se/uhdsg/Data/WEC2007.pdf

Yoon, S. & Garboushian, V. (1994). Reduced temperature dependence of high-concentration photovoltaic solar cell open circuit voltage (V_{OC}) at high concentration levels. In proceedings of the first *WCPEC* in Hawaii, 5-9 December.

Article I

EUROSUN 2008
1st International Congress on Heating, Cooling, and Buildings
7th to 10th October, Lisbon - Portugal

321 – Evaluation of a Parabolic Concentrating PVT System

Luís Ricardo Bernardo*, Bengt Perers, Håkan Håkansson and Björn Karlsson

Energy and Building Design Division, Lund Technical University, Box118 SE-221 00 Lund, Sweden

* Corresponding Author, Ricardo.Bernardo@ebd.lth.se

Abstract

The purpose of this study was testing and performance simulation of an innovative tracking hybrid solar system being developed by the Swedish Company *Arontis*. The *Solar8* collector produces both electrical and thermal energy in one system. Its performance was compared with conventional photovoltaic panels and solar thermal collectors working side-by-side which are already on the market. The *solar8* sample tested in Lund is a prototype designed for small demonstration projects and further development is ongoing.

The evaluation shows that the thermal collector has an overall heat loss coefficient of 3.1 W/(m^2.ºC), an optical efficiency of 65% and an electrical efficiency at 25ºC of 8% per active glazed area. If we account the total glazed area instead, the thermal collector has an overall heat loss coefficient of 2.5 W/(m^2.ºC), an optical efficiency of 52% and an electric efficiency at 25ºC of 6%. The electric efficiency of the bare cells is 16%. Annual performance simulations were carried out for the Swedish (Stockholm), Portuguese (Lisbon) and Zambian (Lusaka) climate. From the simulations one can conclude that: Solar8 can be replaced by a traditional PV-thermal collector side-by-side system using less space and producing the same electric and thermal outputs; tracking around one axis placed in North-South direction is considerably better then tracking around an axis set on East-West direction; the global irradiation on a static surface is always higher when compared with the beam irradiation towards a tracking concentrating surface; the ratio between electric and thermal output decreases when *Solar8* is moved to the equator.

Keywords: Solar8, Solar Hybrids, Photovoltaic Thermal Concentrators, PVT

1. Introduction

The overall problem with the use of PV-systems is the high cost of the solar cells. This makes it appealing to concentrate irradiation on the PV module in order to minimise the required PV-area for the same output. With increased light concentration, there will be a demand of increased cooling on the PV cells in order to lower the working temperature preventing damages and maintaining cell efficiency. Solar8 is a photovoltaic/thermal parabolic concentrating system that tracks and concentrates light into a water cooled photovoltaic module working as a thermal absorber. By using the heat generated in the absorber, the photovoltaic/thermal device (PVT) generates not only electrical, but also thermal energy (Fig. 1). The photovoltaic module is formed by two sections, each one with 32 cells. These sections can be connected both in series and parallel. Generally, a concentrating system with a large number of series connected cells like Solar8 is highly sensitive of local defects in the optical system and on the solar cells, supposed to receive an equal amount of irradiation. The total electric

EUROSUN 2008
1st International Congress on Heating, Cooling, and Buildings
7th to 10th October, Lisbon - Portugal

output is limited by the output coming from the poorest cell since all the cells are series connected. This is one of the challenges to overcome in this new technology. Local diodes installed in each cell can be able to bypass the current over the poorest cells and help reducing the problem with uneven radiation.

Fig. 1. Solar8 trough in Energy and Building Design Laboratory, Lund Technical University (LTH).

It is important to notice that the production of both heat and electricity is favoured by lowering the operating temperature. However a minimum water temperature is generally required by the given application involving higher working temperature on the cells. Due to lower insulation, the hybrid system thermal losses are higher when compared to a normal solar collector. Hence, it is expected that a flat plate hybrid system will deliver approximately 10% less electricity and 10% less heat compared to a thermal collector beside a PV module with the same cells amount [1]. It is also important to have in mind that when an electric load is connected to the PV cells, the thermal efficiency is further decreased since part of the radiation is converted into electricity.

3. Measurement results and system design

3.1. Electrical performance

During this study it was not possible to measure the cells temperature directly since the trough structure is closed. Hence, the average water temperature running inside the thermal absorber at the moment of the electrical efficiency measurement is presented instead. Using the maximum electric power extracted by *Solar8* together with the incident beam irradiation it was possible to estimate the electrical efficiency behaviour of the system depending on its working temperature (Fig. 2).

From the linear representations of the electrical performance it is possible to estimate that the electrical efficiency is 8.3% per active glazed area and 6.3% per total glazed area at 25ºC average water temperature running inside the thermal absorber. The slope of the electrical performance trend lines fits fairly close the classical 0.4% drop in efficiency per ºC in cells temperature increase. For this study, active area was defined as the maximum glazed area the system can make use of.

EUROSUN 2008
1st International Congress on Heating, Cooling, and Buildings
7th to 10th October, Lisbon - Portugal

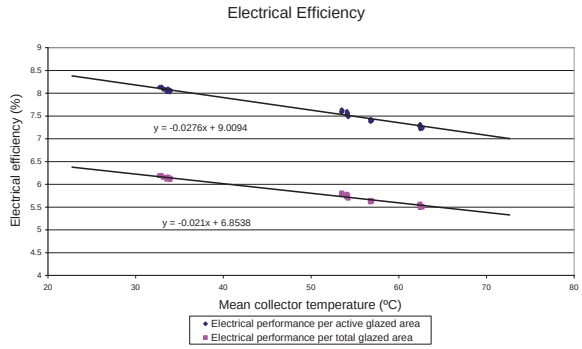

Fig. 2. Electrical efficiency calculated per active glazed area and total glazed area for different working temperatures. Linear adjustments representative of the electrical performance of the trough. ($A_{active\ elect.}$= 3.5m^2 A_{total}=4.6m^2).

3.2. Thermal performance

Using linear adjustments, the hybrid optical efficiency η_0(-) and the thermal losses coefficient U(W/m^{2}ºC) were calculated. The thermal losses coefficient is the slope of the thermal efficiency estimated linear behaviour while the optical efficiency is the interception of that line with the yy axis (Fig. 3 and Table 1). The optical efficiency represents the thermal efficiency when there are no thermal losses since the ambient temperature is the same as the average temperature in the thermal receiver.

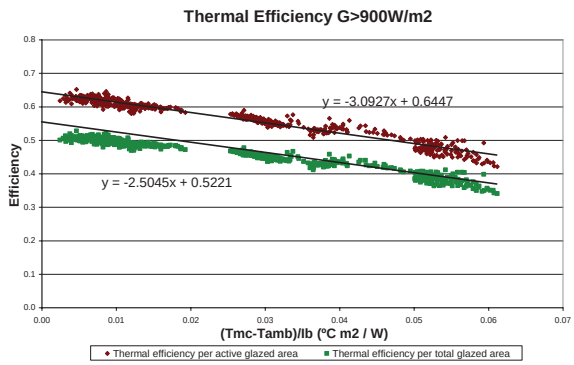

Fig. 3. Assumed linear thermal behaviour based on thermal efficiency measurements calculated per active glazed area and total glazed area. The efficiency was estimated based on measurements for global irradiation values higher than 900W/m^2. ($A_{active\ thermal}$=3.7m^2 A_{total}=4.6m^2)

EUROSUN 2008
1st International Congress on Heating, Cooling, and Buildings
7th to 10th October, Lisbon - Portugal

Table 1. Measured optical efficiency η_0(-) and thermal losses coefficient U(W/m_2ºC).

Thermal parameters	Per active glazed area ($A_{active\ thermal}$=3.7m^2)	Per total glazed area (A_{total}=4.6m^2)
η_0(-)	0.64	0.52
U(W/m^2ºC)	3.1	2.5

3.3. Electric and thermal output interaction

In Fig. 4, it is possible to comprehend the performance of a PVT hybrid system when it comes to thermal and electrical outputs interaction. As it is represented, when an electric load is connected to the electric circuit, electric power can be extracted. This means that part of the incoming irradiation is transformed into electricity by the PV cells instead of being absorbed by the thermal receiver. Hence, the thermal output decreases as much as the electrical output is extracted.

3.4. Reflector optical accuracy and design

Given that the measured system electrical efficiency (8.3% at 25ºC) is significantly lower when compared with the bare cells efficiency (16% at 25ºC), experiments were carried out in several components accuracy in order to estimate their influence in the final electric and thermal output breakdown. One of the most significant inaccuracies relates to the reflector. Ideally, every light beam perpendicularly incident to the glazed cover of the trough should be reflected to the PV module. Laser beam tests were carried out during the night and the glazed areas where the light was not focused on the PV cells were marked and are illustrated in Fig. 5. I-V curves were measured with and without the covers and the electrical output was roughly the same. The glazed marked area is approximately 15% of the total glazed area and can represent an optical efficiency margin of improvement on the reflector accuracy for future models. The system design still has a relevant margin of improvement on most of its components accuracy which makes it possible to achieve higher efficiencies in the future.

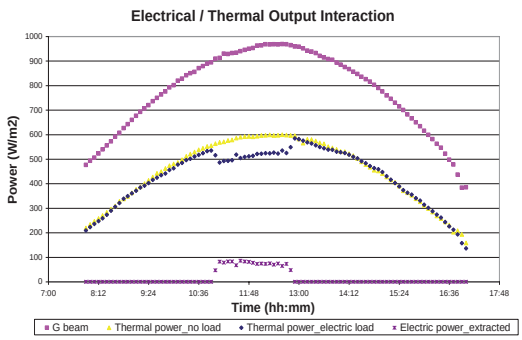

Fig. 4. *Solar8* electric and thermal outputs interaction per active glazed area measured along two clear days with and without electric load. ($A_{active\ thermal}$=3.7m^2 $A_{active\ elect.}$= 3.5m^2)

Fig. 5. Areas covered with paper where the incident light is not focused on the PV cells.

EUROSUN 2008
1st International Congress on Heating, Cooling, and Buildings
7th to 10th October, Lisbon - Portugal

4. Simulation and calculation

4.1. Model and parameters

The model of the power outputs calculated in the performed simulations is described by the following equations and parameters [2].

$$P = \eta_{ob}K_{ta}G_b + \eta_{od}G_d - a_1((T_{out}+T_{in})/2-T_{amb}) - a_2((T_{out}+T_{in})/2-T_{amb})^2 \quad (1)$$

where $K_{ta} = 1-b_o(1/\cos\theta-1)$ (2)

$\eta_{od}=K_{diffuse}*\eta_{ob}$ (3)

Monitored parameters:

P	Power from collector (W/m^2)
G_b	Beam Irradiance (W/m^2)
G_d	Diffuse Irradiance (W/m^2)
T_{in}	Inlet temperature
T_{out}	Outlet temperature
T_{amb}	Ambient temperature

Glazed areas:

$A_{active\ elect.}$= 3.5m^2	*Solar8* electric active glazed area
$A_{active\ thermal}$= 3.7m^2	*Solar8* thermal active glazed area
$A_{Solar8.}$= 4.6m^2	*Solar8* total glazed area

Parameters in the collector model:

η_{ob}	Beam efficiency
a_1	Heat loss factor [W/m^2 K]
a_2	Temperature dependence of heat loss factor [W/m^2 K^2]
$a=a_1+a_2*\Delta T$	(4)
K_{ta}	Angle of incidence modifier for beam irradiance
b_o	Angular coefficient
$K_{diffuse}$	Diffuse incident angle modifier
θ [º]	Angle of incidence onto the collector

Simulation Parameters:

Table 2. Systems parameters introduced in the performed simulations with *Winsun* software.

Solar system	η_{0b} (-)	$K_{diffuse}$ (-)	a_1 (W/m^2 ºC)	a_2 (W/m^2 ºC^2)	b_0 (-)
Thermal *Solar8* per active glazed area	0.64	0.1	3.09	0	0.1
Electrical *Solar8* per active glazed area (50 ºC)	0.076	0.1	0	0	0.1
Flat plate collector (50 ºC)	0.8	0.9	3.5	0	0.1
PV module (25 ºC)	0.16	0.9	0	0	0.1

4.2. Sun tracking orientation

The *Solar8* system is mounted on our laboratorial facilities with its tracking axis oriented in the East-West position. It is possible to simulate the received irradiation by a tracking surface both with the axis in East-West and North-South direction for several climates at different latitudes. The results are given in Table 3.

By the analysis of the results, one can conclude that it is always better to track the sun around an axis with North-South direction. This effect is even more relevant when the system is moved closer to the equator where the sun reaches higher altitudes and moves around the sky from East to West direction, mostly.

Table 3. Incoming beam and global irradiation onto a tracking surface with axis in East-West and North-South direction for Stockholm, Lisbon and Lusaka.

Sun tracking orientation of the surface	Stockholm (lat=59.2ºN)		Lisbon (lat=38.7ºN)		Lusaka (lat=15.4ºS)	
	G (kWh/m^2,yr)	G_b (kWh/m^2,yr)	G (kWh/m^2,yr)	G_b (kWh/m^2,yr)	G (kWh/m^2,yr)	G_b (kWh/m^2,yr)
Tracking surface around North-South axis	1343.0	787.3	2187.0	1445.0	2594.0	1754.0
Tracking surface around East-West axis	1262.0	717.6	1973.0	1263.0	2289.0	1474.0
Ratio N-S/E-W tracking	1.06	1.10	1.11	1.14	1.13	1.19

4.3. Static surface vs. tracking concentrating surface

Another issue to take into account is that concentrating solar systems, with concentration ratio C=10, can make use only of the beam irradiation plus 10% of the diffuse one, roughly. On the contrary, non-concentrating systems make use of the global irradiation coming from the sun. Thus, the received global irradiation by a non-concentrating static surface was compared with the beam irradiation plus 10% of the diffuse onto a tracking concentrating surface (Table 4).

Table 4. Incident irradiation on a static non-concentrating surface and on a tracking concentrated surface. Static surface inclination from horizontal is 40º in Stockholm, 30º in Lisbon and 20º in Lusaka.

Static surface vs. tracking concentrating surface	Stockholm (lat=59.2ºN)	Lisbon (lat=38.7ºN)	Lusaka (lat=15.4ºS)
Static non-concentrating surface G (kWh/m^2,yr)	1170.0	1865.0	2164.0
North-South tracking concentrating surface Gb + 10%*G_{diff} (kWh/m^2,yr)	842.1	1518.2	1836.9
Ratio Static/Tracking concentrating surfaces output	1.39	1.23	1.18

The global irradiation incident on a static surface is higher when compared with the beam irradiation plus 10% of the diffuse towards a tracking concentrating surface. This means that a non-concentrating fixed collector receives more usable irradiation than a tracking concentrating one like *Solar8*. Closer to the equator, the beam irrradiation values are higher and this result becomes less accentuated.

4.3. Electric/Thermal power ratio in Solar8

Knowing that the beam fraction of the global irradiation increases when we move closer to the equator, conclusions can be taken on *Solar8* electrical/thermal output ratio depending on its location (Table 5).

Table 5. *Solar8* electric and thermal annual outputs per square meter of total glazed area, on a N-S tracking axis and 50ºC average working temperature. The total glazed are on *Solar8* is 4.6m^2.

Solar8 annual outputs per glazed area (A_{Solar8}= 4.6 m^2)	Stockholm (lat=59.2ºN)	Lisbon (lat=38.7ºN)	Lusaka (lat=15.4ºS)
Solar8 electric annual output per glazed area (kWh/m^2,yr)	47.7	86.8	105.7
Solar8 thermal annual output per glazed area (kWh/m^2,yr)	159.7	434.9	605.3
Ratio Electric/Thermal	0.30	0.20	0.17

The ratio between electric and thermal outputs decreases when *Solar8* is moved closer to the equator where the beam irradiation values are higher. The electric output is proportional to the irradiation thus, a PV module as constant efficiency for the same working temperature. A solar collector as higher efficiencies for higher irradiances since the thermal output increases more than proportional when the irradiation increases.

4.4. *Solar8* vs. traditional side-by-side system based on glazed area

There are many ways and factors to take in account when comparing the performance of a concentrating hybrid with a traditional side-by-side system composed by a PV module and a solar collector working separately. The following tables feature *Solar8* comparison with the traditional side-by-side system based on their power outputs and total glazed area (Table 6 to Table 8).

Table 6. *Solar8* electric and thermal outputs with a N-S tracking axis at 50ºC average working temperature.

Solar8 annual outputs (A_{Solar8}= 4.6 m^2)	Stockholm (lat=59.2ºN)	Lisbon (lat=38.7ºN)	Lusaka (lat=15.4ºS)
Solar8 total electric annual output (kWh,yr)	219.2	399.0	486.1
Solar8 total thermal annual output (kWh,yr)	733.9	1998.9	2782.1

Table 7. Traditional side-by-side-system electric and thermal outputs per square meter of glazed area. The PV module η_{0b}=16% at 25ºC. The flat plate collector η_{0b}=80%, a_1=3.5 W/m^{2}ºC and operates at 50ºC average working temperature.

Traditional side-by-side system	Stockholm (lat=59.2ºN) Fixed tilt=40º	Lisbon (lat=38.7ºN) Fixed tilt=30º	Lusaka (lat=15.4ºS) Fixed tilt=20º
PV module output per glazed area (kWh/m^2,yr)	173.2	278.7	324.5
Flat plate collector output per glazed area (kWh/m^2,yr)	478.7	999.7	1266.0
PV area needed to equal Solar8 electric annual output (m^2)	1.3	1.4	1.5
Collector area needed to equal Solar8 thermal annual output (m^2)	1.5	2.0	2.2

Table 8. Traditional side-by-side-system and *Solar8* comparison based on total glazed area.

Side-by-side system vs. Solar8 (A_{Solar8}=4.6m^2)	Stockholm (lat=59.2ºN) Fixed tilt=40º	Lisbon (lat=38.7ºN) Fixed tilt=30º	Lusaka (lat=15.4ºS) Fixed tilt=20º
PV module area / Solar8 total glazed area (%)	27.5	31.1	32.6
Thermal collector area / Solar8 total glazed area (%)	33.4	43.5	47.8
Side-by-side system area / Solar8 total glazed area (%)	60.9	74.6	80.4

The traditional side-by-side system uses less area than *Solar8* for the same electric and thermal outputs. This difference decreases when the systems are moved closer to the equator since *Solar8* is exposed to higher beam irradiation values. In Lisbon, for instance, *Solar8* can be replaced by 1.4m^2 of PV module and 2m^2 of thermal collector for the same outputs. Hence, it would use 74% of *Solar8* total glazed area (4.6m^2). Practically, two components require more space than one component.

4.5. *Solar8* vs. traditional PV module based on cells area

One of the most common arguments in favour of PVT concentrating systems is the higher electrical efficiency per cells area when compared with a regular PV module with the same cells area. In this situation and based only on the PV cells point of view, *Solar8* has a considerable higher efficiency per cell area when compared with the PV module (Table 9). This result can be explained by the higher irradiation the cells receive due to the reflector concentration factor and the tracking system. The thermal output can be seen just as an additional output one can get by cooling down the cells.

Table 9. *Solar8* and traditional PV module electric output comparison based on cells area. PV module inclination is 40º in Stockholm, 30º in Lisbon and 20º in Lusaka. A_{ceels}=0.33m^2.

Electric annual output per cells area (kWh/m^2)	Stockholm (lat=59.2ºN)	Lisbon (lat=38.7ºN)	Lusaka (lat=15.4ºS)
Solar8 tracking N-S (50ºC)	661.8	1204.7	1467.6
Traditional static PV module (25ºC)	192.4	309.7	360.6
Ratio Solar8/PV module	3.4	3.9	4.1

For this simulation it was considered that the PV module has16% efficiency at 25ºC, the same cells area as *Solar8* and that they cover 90% of its glazed area.
It is important to notice that the thermal and electric outputs shown previously don't take into account system distribution losses, array shading effects and load distribution.

5. Conclusions

With this study several conclusions can be taken not only for *Solar8* but also perhaps to the general photovoltaic/thermal concentrating hybrids being developed:

1. *Solar8* can be replaced by a traditional side-by-side system using less space and producing the same electric and thermal output.
2. Local diodes installed in each cell can be able to bypass the current over the poorest cells and help reducing the problem with uneven radiation.
3. One axis tracking around North-South direction is considerably better than tracking around an axis placed on East-West direction.
4. The global irradiation on a static surface is higher when compared with the beam irradiation towards a tracking concentrating surface.
5. The ratio between electric and thermal output decreases when *Solar8* is moved to the equator where the beam irradiation values are higher.
6. This PV/T combination still present lower outputs when compared with the traditional side-by-side system for the same glazed area. It is possible to say that there is chain efficiency around the most important components in *Solar8*. If every part of this chain works accurately and perfectly integrated in the system, higher efficiencies can be achieved in future models.

5. References

[1] Measurement report: Test of PVT module "PVtwin". IEA task 35. Danish Technological Institute.
[2] Duffie, J.A., & Beckman, W.A. (1980). Solar Engineering of Thermal Process. Wiley Interscience, New York.

6. Acknowledgement

This study was supported by *SolNet* - Advanced Solar Heating and Cooling for Buildings - the first coordinated international PhD education program on Solar Thermal Engineering.

Article II

Performance Evaluation of Low Concentrating Photovoltaic/Thermal Systems
A case study from Sweden

L. R. Bernardo*, B. Perers, H. Håkansson and B. Karlsson
Energy and Building Design Division, Lund Technical University, Box 118 SE-221 00 Lund, Sweden
* Corresponding Author, Ricardo.Bernardo@ebd.lth.se

Abstract

Some of the main bottlenecks for the development and commercialization of photovoltaic/thermal hybrids are the lack of an internationally recognized standard testing procedure as well as a method to compare different hybrids with each other and with conventional alternatives. A complete methodology to characterize, simulate and evaluate concentrating photovoltaic/thermal hybrids has been proposed and exemplified in a particular case study. By using the suggested testing method, the hybrid parameters were experimentally determined. These were used in a validated simulation model that estimates the hybrid outputs in different geographic locations. Furthermore, the method includes a comparison of the hybrid performance with conventional collectors and photovoltaic modules working side-by-side. The measurements show that the hybrid electrical efficiency is 6.4% while the optical efficiency is 0.45 and the U-value 1.9 W/m²ºC. These values are poor when compared with the parameters of standard PV modules and flat plate collectors. Also, the beam irradiation incident on a north-south axis tracking surface is 20 to 40% lower than the global irradiation incident on a fixed surface at optimal tilt. There is margin of improvement for the studied hybrid but this combination makes it difficult for concentrating hybrids to compete with conventional PV modules and flat plate collectors.

Keywords: Evaluate Solar Hybrids, Photovoltaic Thermal Concentrators, PVT

Nomenclature

Monitored parameters:

$P_{thermal}$	Hybrid thermal power (W/m²)
$P_{electric}$	Hybrid electric power (W/m²)
G_b	Beam Irradiance (W/m²)
G_d	Diffuse Irradiance (W/m²)
T_{in}	Inlet temperature (°C)

T_{out}	Outlet temperature (°C)
T_{amb}	Ambient temperature (°C)
dV/dt	Flow (m^3/s)
C_p	Heat capacity (water) (J/kg°C)
ρ	Density (water) (kg/m^3)
A_{Hybrid}	Total glazed collector area (m^2)
$A_{active\ elect.}$	Electric active glazed area
$A_{active\ thermal}$	Thermal active glazed area
τ	Transmittance coefficient of the glass (-)
r	Reflectance coefficient of the reflector (-)
α	Absorptance coefficient of the solar cells(-)

Parameters in the collector model:

η_{od}	Diffuse efficiency (%)
$\eta_{ob\_thermal}$	Beam thermal optical efficiency (%)
$\eta_{ob\_electric}$	Beam electric optical efficiency (%)
a_1	Heat loss factor (W/m^2 °C)
a_2	Temperature dependence of heat loss factor (W/m^2 °C^2)
$K_{ta\_thermal}$	Thermal angle of incidence modifier for beam irradiance (-)
$K_{ta\_electric}$	Electric angle of incidence modifier for beam irradiance (-)
$b_{o\_thermal}$	Thermal angular coefficient (-)
$b_{o\_electric}$	Electric angular coefficient (-)
$K_{diffuse}$	Diffuse incident angle modifier (-)
K_T	Electric efficiency temperature dependence (%/°C)
θ	Angle of incidence onto the collector (°)

1. Introduction

The overall problem with the use of photovoltaic (PV) systems is the high cost of the solar cells. This makes it attractive to concentrate irradiation on the PV module in order to minimise the required cell area for the same output. With increased light concentration, there will be a demand for increased cooling of the PV cells in order to lower the working temperature, prevent damage and maintain cell efficiency (Nilsson et al., 2007). Usually, a photovoltaic/thermal (PVT) concentrating system tracks and concentrates light into a water/air-cooled photovoltaic module working as a thermal absorber. Hence, not only electricity is generated from the absorber but also heat. The production of both heat and electricity is favoured by lowering the operating temperature; however, a minimum water temperature, which raises the working temperature on the cells, is generally required by the given application (Affolter et al., 2004). At the end, a life cycle cost analysis is necessary to determine whether the concentrating system reduced the unit cost of produced electricity (Arvind and Tiwari, 2010; Arvind et al., 2009).

Concentrating hybrid design is an emerging technology and there are still constraints to its development and commercialization. One of the most important is the lack of an internationally accepted method to test these devices (Affolter et al., 2004). Traditionally, steady-state thermal models are used to predict the annual performance but recent studies have been introducing the use of dynamic models as well (Chow, 2003). However, there is not an established method of comparing different hybrids with each other or with a traditional side-by-side system made of standard flat plate collectors and PV modules. Furthermore, there exist very few evaluations on the electric and thermal efficiency of tracking concentrating hybrids. Since there are a small number of commercialized systems, there is also a need for experimental data exchange so it is possible to draw general conclusions about concentrating hybrid performance.

For a better understanding of the conducted work in a particular case study and its contributions to the field, the main objectives of the paper are summarised below:

- To propose a testing method to characterize concentrating photovoltaic/thermal hybrids.
- To suggest a series of simulations and performance analysis for different latitudes based on the results from the testing method.
- To compare the hybrid performance with conventional PV modules and solar collectors.

Thus, several conclusions can be drawn concerning the performance of the tested concentrating hybrids, their possible applications and viability in different climates and locations.

2. Method

2.1. Experimental setup and hybrid design

This photovoltaic/thermal parabolic concentrating system tracks and concentrates light into a water-cooled photovoltaic module working as a thermal absorber. By using the heat generated in the absorber, the photovoltaic/thermal device generates not only electrical, but also thermal energy (Figure 1). The PVT system consists of a photovoltaic module, thermal absorber, parabolic reflector, tracking system, glazed protection and supporting structure (Figure 2). Two sections form the photovoltaic module, each one with 32 series connected cells laminated on both sides of the V-shaped thermal absorber. These sections can be interconnected both in series and parallel. The photovoltaic cells, which are specially designed for concentrated light, are made of monocrystalline silicon and have a nominal efficiency of 16% at 25°C (Absolicon Solar Concentrator AB, 2008). The total surface area of the cells is 0.33 m². Water runs inside the aluminium thermal absorber where the cells are laminated. The parabolic reflector is made of a silver coated plastic film laminated on a steel sheet with a reflectance factor of 90% (Alanod Solar, 2010). The geometrical concentration ratio of the reflector is C=7.8. It is important to notice that the reflector is 40cm longer than the absorber at the edges to also make use of the irradiation in the morning and afternoon. The tracking is carried out by rotating the structure around an axis oriented in the east-west direction. The

adjustment of the tilt angle is carried out periodically according to the calculated position of the sun. The parabolic trough is covered by a 4.6 m² glass pane with a measured transmission coefficient of 90% (Bernardo, 2007).

In this study, two hybrid areas were defined: total glazed area and active glazed area. For this particular hybrid the total glazed area (A_{Hybrid}) equals 4.6 m². Active glazed area was defined as the maximum glazed area that the system can make use of. This excludes surface areas where it is impossible for the irradiation to reach the absorber such as frames and gaps between solar cells and reflector edges which are longer than the absorber (Figure 1). The electric and thermal active glazed areas are different since the thermal absorber is wider than cells. The electric active glazed area ($A_{active\ elect.}$) is 3.5 m² while the thermal active glazed area ($A_{active\ thermal}$) equals 3.7 m².

The relative uncertainties of the measuring instruments stated by the manufacturers are estimated for ideal measurement and installation conditions. In practice, somewhat higher relative uncertainties were assumed in order to take into account a safety margin that includes inaccuracies related to the installation and operation of those instruments at our laboratory. The pyranometer relative uncertainty was assumed to be +-2%, the flow meter +-1% and the Pt100 temperature measurement +-2%. The temperature dependence of the heat capacity and specific mass of the water was taken into account in the calculations. Hence, using the standard method of the square root of the quadratic sum for the uncertainty propagation, the global uncertainty of the efficiency measurements was estimated to be 3%.

Figure 1 - PVT concentrator trough and photovoltaic cells laminated on one side of the thermal absorber.

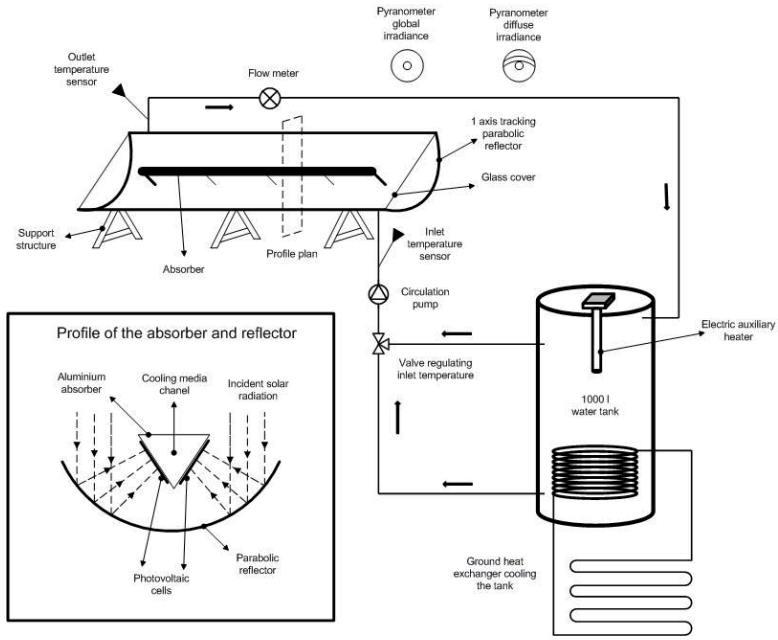

Figure 2 – Schematic diagram of the experimental setup system and its monitoring points.

2.2. Procedure

2.2.1. Testing and characterization method

The testing and characterization method can be seen as a modified solar collector testing method described in the following steps:

a) Simultaneous monitoring of heat and power where the photovoltaic module operates continuously at maximum power point;

b) Characterization of the thermal collector according to the steady-state test method (Fisher et al., 2004);

c) Characterization of the photovoltaic module at high irradiances and variable working temperatures;

d) Description of the thermal and electrical incidence angle modifier during one day with stable high solar intensity;

e) Using the previous tested parameters to generate a mathematical steady-state model capable of accurately describing the thermal and electrical outputs;

f) Validation of the model by comparison between measurements and model outputs during days with varying weather conditions.

Both the electrical and thermal outputs were measured every six minutes for different temperature conditions in the collector. The maximum electric power output extracted by the hybrid was calculated based on periodical I-V curve measurements. Using this value together with the incident beam irradiation, the system electrical efficiency as a function of its working temperature was determined. In reality, it is expected that an electric load is permanently connected to the PV cells and electric power is continuously extracted at maximum power point. However, measuring I-V curves instantaneously simplifies the whole test procedure, making it cheaper, less time consuming while still achieving an accurate result. If an electric load was continuously connected, the absorber would be colder since part of the incoming radiation would be converted to electricity. In this case, the outlet water temperature would be slightly lower than the one measured. This difference is very small and has little impact on the results. In this specific case, since the structure is closed, it was not possible to measure the cell temperature directly. Instead, the temperature of the outlet water, running inside the thermal absorber at the moment of the electrical efficiency measurement, is presented. This is the temperature limiting the whole electric output since the cells are series connected.

Since there is no electric load continuously connected to the hybrid, all the incoming irradiation is used to produce heat. This output was calculated by equation (1) (Duffie and Beckman, 2006) where the monitored parameters are described in the nomenclature section at the beginning of the paper.

$$P=(\rho\, dV/dt \cdot C_p \cdot (T_{out}-T_{in})/A_c)\ (W/m^2) \quad (1)$$

The thermal power was then obtained by subtracting the measured electric power from this heat output. The incidence angle modifier (K_{ta}) for the thermal and electric efficiency was calculated with equation (2) (Duffie and Beckman, 2006).

$$K_{ta}(\theta) = \frac{\eta_{0b}(\theta)}{\eta_{0b}(\theta \approx 0)} \quad \textbf{(2)}$$

The function generally used to fit the incidence angle modifier data between 0° and 60° is given by equation (3) (Duffie and Beckman, 2006). The parameter b_0 shapes the curvature of the function, setting higher or lower incidence angle modifier values for the same incidence angle.

$$K_{ta}(\theta) = 1 - b_0 * \left(\frac{1}{\cos(\theta)} - 1 \right) \quad (3)$$

The hybrid was continuously tested at the Energy and Building Design laboratory of Lund Technical University in Sweden (latitude 55°44'N, longitude 13°12'E) during the period 1/06/2008 – 13/09/2008.

2.2.2.Simulation model

By analyzing the measured data, one can determine the hybrid parameters and develop simple mathematical models capable of describing its behaviour and estimate its outputs for any geographic location. The monitored parameters and the model equations are presented in equations (4) to (9) (Duffie and Beckman, 2006).

$$P_{thermal}=\eta_{ob\_thermal}\cdot K_{ta\_thermal}\cdot G_b+\eta_{od}\cdot G_d-a_1\cdot((T_{out}+T_{in})/2-T_{amb})-a_2\cdot((T_{out}+T_{in})/2-T_{amb})^2 \quad (4)$$

where $K_{ta\_thermal}=1-b_{o\_thermal}\cdot(1/\cos\theta-1)$ (5)

$$\eta_{od}=K_{diffuse}\cdot\eta_{ob\_thermal} \quad (6)$$

$$P_{electric}=(\eta_{ob\_electrical\ (25°C)}\cdot K_{ta\_electric}\cdot G_b+\eta_{od}\cdot G_d)-(K_T\,\eta_{ob\_electrical\ (25°C)}\cdot G_b\,(T_{out}-25)) \quad (7)$$

where $K_{ta\_electric}=1-b_{o\_electric}\cdot(1/\cos\theta-1)$ (8)

$$\eta_{od}=K_{diffuse}\cdot\eta_{ob\_electric} \quad (9)$$

The hybrid parameters were then fed into *Winsun* (Winsun Villa Software, 2009), a TRNSYS based simulation software developed by Bengt Perers which estimates the annual thermal and electrical outputs using the described model. It is important to notice that all calculations represent collector outputs not taking into account the whole electric and thermal system. Hence, system distribution, storage losses, array shading effects and load distribution are not taken into account either. Only the energy produced by the collectors was estimated.

2.2.3.Comparison with conventional PV modules and thermal collectors

In order to compare the hybrid performance with standard thermal collectors and photovoltaic modules, simulations were also carried out for these standard components. It was assumed that the produced hot water should be used for domestic hot water applications since this can represent 90% of the potential market for these hybrids (Affolter et al., 2004). Therefore, the output temperature from the collectors should be around 65-70°C which was assumed to imply 40°C of mean absorber temperature depending on the flow and irradiation levels. Consequently, the hybrid solar cells, but not the individual PV module, would work at 65-70°C. As the PV module is independent from the flat plate collector it was assumed that it could work at around 25°C. In order to understand how the hybrid performance would change if it was used for low temperature applications, simulations were also carried out for pool heating. For this application it was assumed that the required outlet temperature would be around 30°C which was estimated to imply 20°C average water temperature in the hybrid since the cold water inlet is around 10°C. The diffuse incidence angle modifier ($K_{diffuse}$) was calculated as being the inverse of the geometrical concentration ratio (1/C where C=7.8) (Winston et al., 2005). All the parameters for the side-by-side system were assumed to be common values for standard components.

3. Measurement results

3.1. Electrical and thermal output interaction

One of the most important aspects to take into account when studying photovoltaic/thermal hybrids is the interaction between electrical and thermal outputs (Affolter et al., 2004). When an electric load is connected to the electric circuit, electric and thermal power is extracted. This means that part of the incoming irradiation is transformed into electricity by the PV cells instead of being absorbed by the thermal receiver. Hence, the thermal output decreases as much as the extracted electrical energy. During this experiment, an electric load was connected to the PV modules during a part of the day extracting the maximum possible power from the cells. By analysing Figure 3, one can understand the interaction between the thermal and electrical outputs of a PVT hybrid system. The outputs were calculated for total glazed area.

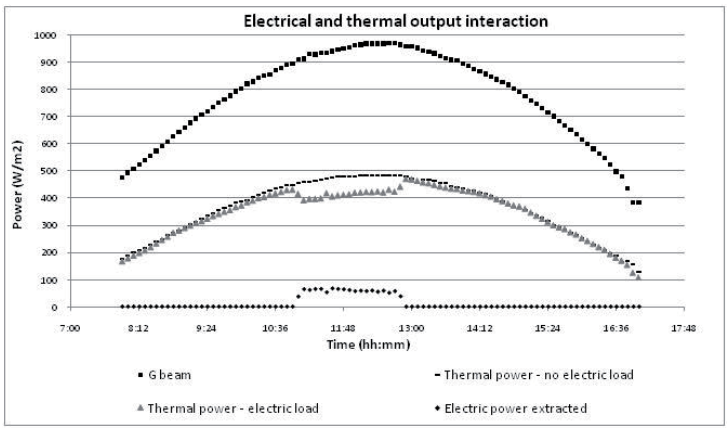

Figure 3 - Electric and thermal outputs interaction measured on two clear days with and without electric load. Power outputs per total glazed area (A_{Hybrid}=4.6 m²).

3.2. Electrical performance

In Figure 4 the system electrical beam efficiency as a function of the water outlet temperature is presented. Based on this data, several collector parameters were calculated and presented in Table 1. The measured electrical efficiency is 6.4% at 25°C water outlet temperature while the electric efficiency temperature dependence equals 0.3%/°C. The measured total peak power was 61 W/m² of total glazed area at 28°C inlet and 39°C outlet water temperature and 997 W/m² incident beam radiation.

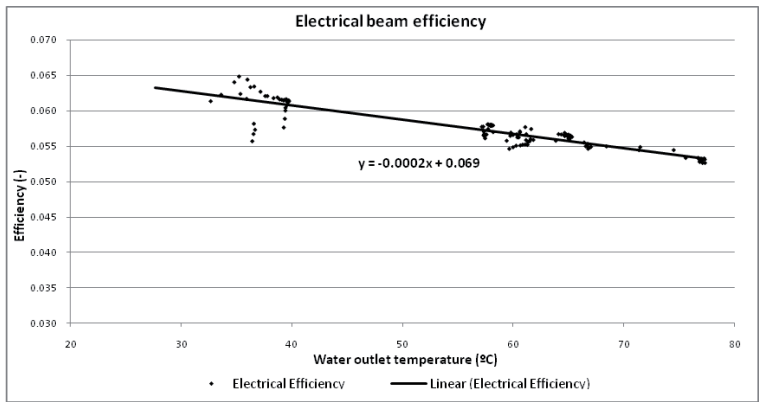

Figure 4 - Electrical beam efficiency calculated per total glazed area for different working temperatures and beam irradiation higher than 900 W/m².

Table 1 - Measured electrical efficiency $\eta_{electric}$, loss coefficient K_T(%/ºC) and electrical peak power per total and active glazed area.

Electrical parameters	Expressed by total glazed area (A_{Hybrid}=4.6 m²)	Expressed by active glazed area ($A_{active\ elect}$=3.5 m²)
$\eta_{b\_electric}$ at 25°C (%)	6.4 %	8.4 %
K_T (%/ºC)	0.3 %/ºC	0.3 %/ºC
Peak Power (W/m²)	61 W/m²	81 W/m²

3.3. Thermal performance

The measured thermal beam efficiency as a function of the working temperature and incident radiation is presented in Figure 5. Using linear approximation, the hybrid beam optical efficiency (η_{0b}) and the heat

loss coefficient (U) were determined and are shown in Table 2. They equal 0.45 and 1.9W/ºC m² of total glazed area. The measured thermal peak power was 435 W/m² of total glazed area at the same conditions described above.

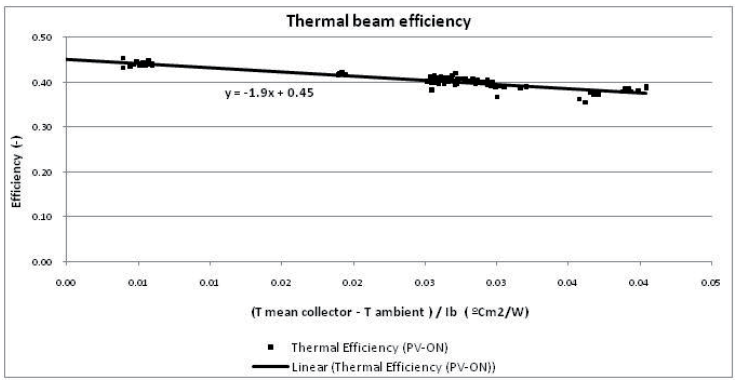

Figure 5 - Thermal beam efficiency calculated per total glazed area for different working temperatures and beam irradiation higher than 900 W/m².

Table 2 - Measured beam optical efficiency η_{0b}(-), heat loss coefficient U(W/m²ºC) and thermal peak power per total and active glazed area.

Thermal parameters (PV–ON)	Expressed by total glazed area (A_{Hybrid}=4.6 m²)	Expressed by active glazed area ($A_{active\ thermal}$=3.7 m²)
η_{0b}(-)	0.45	0.56
U(W/m²ºC)	1.9 W/m²ºC	2.3 W/m²°C
Peak Power (W/m²)	435 W/m²	541 W/m²

3.4. Incidence angle modifier

During the morning and afternoon, the reflection losses at the glass cover and absorber increase due to high angles of incidence. This effect causes a thermal and electrical output drop in the system. The measured sensitiveness of the thermal and electrical efficiency to the increase in the angle of incidence is presented in Figure 6. The measured b_0 fitting the thermal and electric data was 0.14 and 0.28 respectively showing that higher angles of incidence have a greater impact on the electrical performance. This is mainly due to two effects. Firstly, at high angles of incidence in the morning and afternoon, the reflector edges will not redirect the incoming light to the whole length of the absorber. Hence, from the moment that the first cell in the absorber edge is not fully illuminated, the whole electrical output is affected.

These are known as edge and shadow effects. Secondly, optical imprecision and tracking inaccuracies become more relevant at high angles of incidence. This effect is not as sensitive to heat as it is for electricity production since the cells are series connected and the thermal absorber is also wider.

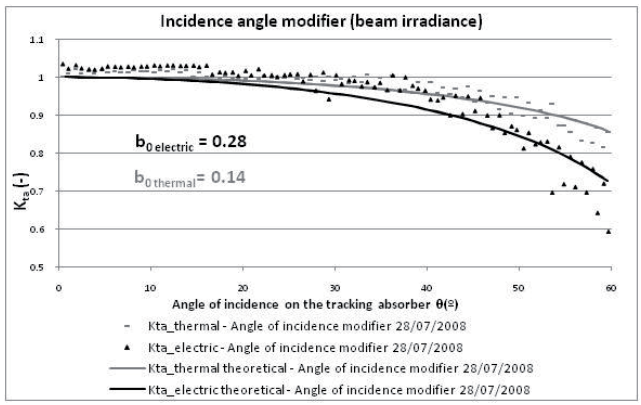

Figure 6 - Thermal and electrical incidence angle modifier for beam radiation during one clear day and θ<60º.

3.5. Model validation

The hybrid measured parameters are summarized in Table 3 and Table 4. The corresponding generated thermal and electric power outputs illustrated in Figure 7 and Figure 8 show that good agreement between model and measurements has been achieved even during unstable days, validating the models.

Table 3 - Parameters for electricity production used in the simulations, expressed by total glazed area.

Model electrical parameters	η_{0b} (-)	$K_{diffuse}$ (-)	K_T (%/°C)	$b_{0\_electric}$ (-)
Hybrid Electric (25°C)	0.064	0.13	0.3 %/°C	0.28
PV module (25°C)	0.16	0.9	0.4 %/°C	0.10

Table 4 - Parameters for hot water production used in the simulations, expressed by total glazed area.

Model thermal parameters	η_{0b} (-)	$K_{diffuse}$ (-)	a_1 (W/m²°C)	a_2 (W/m²°C²)	$b_{0\_thermal}$ (-)
Hybrid Thermal (PV-ON)	0.45	0.13	1.9 W/m²°C	0 W/m²°C²	0.14
Flat plate collector	0.8	0.9	3.6 W/m²°C	0.014 W/m²°C²	0.15

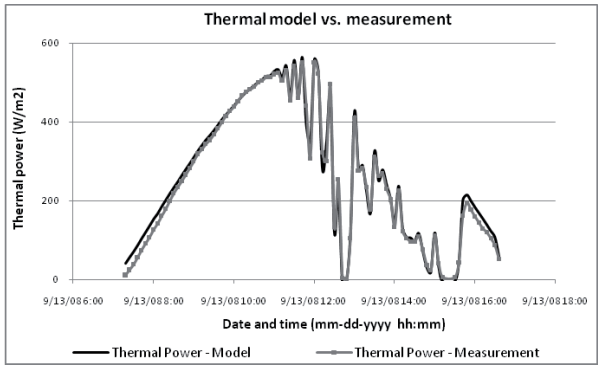

Figure 7 - Thermal model and measurements during unstable irradiation day.

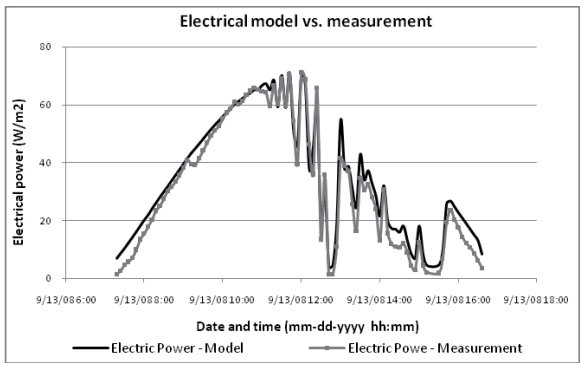

Figure 8 - Electrical model and measurements during unstable irradiation day.

4. Performance analysis

Following the measurement test method described previously, a performance analysis procedure is proposed in this section: simulation of the annual performance for different latitudes and performance comparison with separate standard photovoltaic modules and thermal collectors.

4.1. Tracking system

The tested hybrid system is thought to work with its tracking axis oriented in the east-west direction. Simulations were carried out to estimate the received irradiation by a tracking surface with the axis horizontally oriented in both the east-west and north-south directions for several climates at different latitudes. The results are given in Table 5. Analysing the results, one can conclude that it is always better to track the sun around an axis in the north-south direction, independently on the geographical position. (10-20% better) This effect is even more relevant when the system is moved closer to the equator where the sun reaches higher altitudes. All the following simulations take into account this result, estimating the annual outputs as the hybrid would be tracking the sun in a more productive way with its axis in the north-south direction.

As it is known, concentrating solar systems can only make use of a fraction of the diffuse light. In contrast, non-concentrating systems like standard PV modules and flat plate collectors use the global irradiation. The concentrator can make use of the beam irradiation plus (1/C) of the diffuse irradiation (G_b+G_d/C) (Winston et al., 2005). This comparison is presented in Table 5. The global irradiation incident on a static surface is higher than the beam irradiation on a one-axis tracking concentrating surface. This means that, independently of its location, a non-concentrating fixed collector receives more usable irradiation than a tracking concentrating one like the studied hybrid (roughly 20% to 40% in this case). Closer to the equator, the beam irradiation values are higher and this result becomes less accentuated. This is even clearer as the concentration ratio increases.

Table 5 – Annual output ratio between a north-south and a east-west oriented tracking axis; annual output ratio between the usable irradiation (G_b+G_d/C) incident on a static and north-south tracking concentrating surface. Optimal static surface inclination from horizontal corresponds to 40º in Stockholm, 30º in Lisbon and 20º in Lusaka.

Annual output ratio	Stockholm (lat=59.2°N)	Lisbon (lat=38.7°N)	Lusaka (lat=15.4°S)
Output ratio N-S/E-W tracking axis	1.10	1.14	1.19
Output ratio static/tracking concentrating surfaces	1.41	1.24	1.18

4.2. Annual performance results

Based on the system parameters previously presented in Table 3 and Table 4, the total annual performance for the hybrid and the traditional side-by-side system were calculated for the three different climates. These results are presented in Table 6. For Stockholm, the hybrid electric and thermal annual output is 45.1 kWh/m^2,yr and 187.6 kWh/m^2,yr, respectively. The PV module produces 164.5 kWh/m^2,yr while the thermal collector generates 401.6 kWh/m^2,yr.

Table 6 – Hybrid and traditional side-by-side-system electric and thermal outputs per square metre of total glazed area for domestic hot water application.

Annual outputs per total glazed area	Stockholm (lat=59.2°N)	Lisbon (lat=38.7°N)	Lusaka (lat=15.4°S)
Hybrid electric annual output (kWh/m^2,yr)	45.1	83.3	102.5
Hybrid thermal annual output (kWh/m^2,yr)	187.6	456.7	612.6
PV module annual output (kWh/m^2,yr)	164.5	264.8	308.3
Thermal collector annual output (kWh/m^2,yr)	401.6	887.7	1143.8

4.3. Hybrid concentrator vs. standard PV module based on cell area

One of the most common arguments in favour of PVT concentrating systems is its higher electric output when compared with a regular PV module with the same cell area. According to this point of view, the expensive cell area can be reduced and the thermal application can be considered just a tool to cool down the cells. Hence, if the thermal output is neglected, the hybrid can even work at a high flow rate, making the cells colder and more efficient. The production per cell area of the hybrid and the traditional PV module is presented in Table 7 and the ratio between the two annual electric outputs is shown in Figure 9. The results show that the concentrating hybrid cells produce 3.6 to 4.4 times more electricity than a PV module with the same cells area. This kind of analysis provides very useful information concerning the real extra electricity production one gets with the use of the reflector in different climates. For this simulation it was considered that the standard PV module cells have 16% efficiency at 25°C.

Table 7 - PVT north-south concentrating hybrid and traditional PV module electric output comparison based on cell area. PV module inclination from the horizontal is set to optimum values of 40º in Stockholm, 30º in Lisbon and 20º in Lusaka. $A_{cells\ hybrid}$=0.33m^2.

Electric annual output per cells area (kWh/m^2,yr)	Stockholm (lat=59.2°N)	Lisbon (lat=38.7°N)	Lusaka (lat=15.4°S)
Hybrid tracking N-S (65°C)	626.5	1156.1	1422.2
Traditional static PV module (25°C)	173.2	278.7	324.5

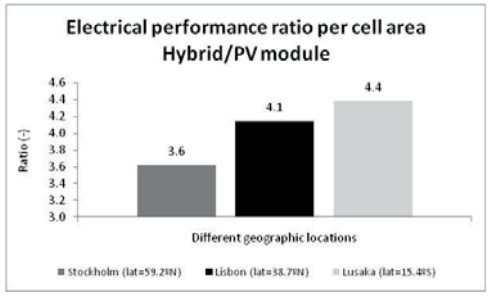

Figure 9 - Ratio between the hybrid and standard PV module annual electric production per cell area.

4.4. Hybrid concentrator vs. standard side-by-side system based on glazed area

In another point of view, since heat is the largest energy fraction produced by the hybrid, it should be considered as a valuable output taken into account when the concentrating hybrid is compared with a conventional system. Hence, the hybrid outputs were compared with an individual PV module and a solar thermal collector working separately for both domestic hot water production and pool heating. The parameters used in the simulation are presented in Table 3 and Table 4. The hybrid comparison with the traditional side-by-side system based on their power outputs per total glazed area is presented in Figure 10. This is particularly useful for areas where the available space is a strong limitation. As it is generally accepted, probably the most expensive part of these two systems is the solar cells. Hence, it makes sense to compare them taking into account that the hybrid and the PV module in the traditional system have the same cell area. This is not the only way to compare the systems but it seems to be the more reasonable one. The results show that, regardless of whether the produced hot water is used for domestic hot water application or for pool heating, the occupied ground area by the traditional side-by-side system, which generates the same electrical and thermal outputs as the hybrid, is almost the same. This result is not obvious and is further considered in the discussion section.

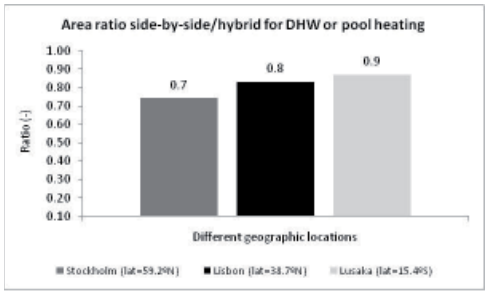

Figure 10 - Ratio between side-by-side system and hybrid total glazed areas producing the same electrical and thermal annual outputs for DHW or pool heating.

5. Discussion

In this chapter the implication of the results concerning the measured hybrid parameters, the annual performance and the comparison with conventional systems are discussed.

Using the efficiency per total glazed area one can estimate how much space one needs to reach the energy demand. It is then possible to determine, between several different hybrids, which one has the best performance for the space it uses and which hybrid is a reasonable choice for the available space. The efficiency per active glazed area may be said to be a more scientific indicator that allows a technical comparison between hybrids based on how well they perform with the radiation they can use.

As previously reported (Yoon and Garboushian, 1994), the dependence of electricity production with temperature of concentrating hybrids is different from that in a normal photovoltaic module. For this hybrid, the electrical efficiency decrease with temperature (K_T) is approximately -0.3%/°C whereas the typical value for a standard cell without concentration is -0.4%/°C (Wenham, 2007). There are two different reasons for this. The electrical efficiency curve presented in Figure 4 was calculated based on the temperature of the water and not that of the cells. Due to heat transfer resistance between these two elements, the water temperature will be somewhat lower than the cell temperature. This temperature difference is inversely proportional to the amount of heat transferred between them and it will decrease with increasing water temperature at constant solar intensity. This implicates a lower efficiency temperature dependence of the hybrid, making the slope of the line slightly smoother (Figure 4). On the other hand, the temperature difference will increase with increasing radiation intensities at constant working temperature. This effect has a very low impact using the suggested test method since measurements were carried out only for high irradiation values according to the steady-state test method (Fisher et al., 2004). Possibly, in a future improved model, the cell efficiency should be modelled to increase with decreased irradiance intensities. The other effect is that a higher open-circuit voltage due to higher concentration actually reduces the temperature sensitivity of the cell (Yoon and Garboushian, 1994; Wenham et al., 2007). Previous experimental results have shown that the temperature influence in

concentrating systems is lower, with -0.25%/°C drop in efficiency for high concentration levels at around 25°C (Yoon and Garboushian, 1994). Hence, concentrators have an advantage when used at high temperature operation compared with a non concentrating photovoltaic module.

The tracking system analysis shows that a one-axis tracking system should rotate around an axis aligned in the north-south direction, independently on its geographical location. If tilted towards the equator, the performance is further improved. Furthermore, a tracking concentrating system receives less usable radiation than a standard flat fixed collector. Consequently, the measured low hybrid efficiencies together with low usable irradiation generate low annual outputs. Additionally, the area covered by a conventional side-by-side system is comparable to the one used by the hybrid producing the same outputs. As a result, it is difficult for a concentrating hybrid to compete with conventional alternatives.

The optical efficiency is one of the factors that directly influence the final electric efficiency. The ideal thermal optical efficiency of the hybrid can be theoretically estimated taking into account several loss factors. These are: glass transmission, reflectance factor and the PV cells absorptance and efficiency. In the same way, it is also possible to theoretically calculate the ideal electrical efficiency of the hybrid at 25°C. This is exemplified by equation (10) and (11), respectively:

$$\eta_{o\_thermal\_ideal}=\tau \cdot r \cdot \alpha \cdot (1-\eta_{cells\_ideal}) \cdot A_{active\_thermal}/A_{Hybrid}= \quad (10)$$
$$=0.90*0.90*0.93*(1-0.16)*3.7/4.6=0.51$$

$$\eta_{elect\_ideal}(25°C)=\tau \cdot r \cdot \alpha \cdot \eta_{cells\_ideal} \cdot A_{active\ elect.}/A_{Hybrid}= \quad (11)$$
$$=0.90*0.90*0.93*0.16*3.5/4.6=0.09$$

The transmittance of the glass τ was measured to be 0.90 (Bernardo, 2007), while the reflectance r is 0.90 (Alanod Solar, 2010) and the absorptance of the solar cells α was assumed to be 0.93 (Brogren et al., 2001). Dividing the active thermal area with the total glazed area makes it possible to compare the theoretical calculations with the measurements. This analysis helps to understand why the efficiencies of concentrating hybrids are lower than conventional thermal collectors and PV modules. Furthermore, the theoretical values point out a general limitation to the final efficiencies of concentrating hybrids. As shown, the difference between the measured and the theoretical efficiencies is not significant. In the thermal case, this difference can mainly be explained by the reflector shape inaccuracies. In the electric case, the difference is related to uneven distribution of solar irradiation on the cells and scattering after reflection. This is one of the challenges to overcome in this new technology. Having uniform radiation distribution over the PV module becomes especially critical for series connected cells since the one with the lowest output will limit the entire final production (Sick and Erge, 1998; Coventry et al., 2004; Nilsson, 2007). This concept is known as the "current matching problem" (Royne et al., 2005). In future models, local diodes should be installed over each cell in order to bypass the current over the poorest cells and help minimize the impact of uneven radiation. Reflector imprecision was not the only factor causing the decrease in the final electric output. Local shading effects, tracking inaccuracies, and variation between cells were also some of the obstacles found in this and other previous studies, making it difficult to achieve the efficiencies obtained when individual cells are tested under ideal conditions (Chow, 2010; Franklin and Coventry, 2004). Similar efficiency values were reported in recent studies of concentrating hybrids. Kostić et al. (2010) measured a thermal optical efficiency of 37% and an average value of the daily electrical efficiency of 3.7% in a hybrid using low concentrating flat reflectors. Also, Tripanagnostopoulos and Souliotis (2004) measured a thermal optical efficiency between 50% and 64% in solar thermal collectors using low concentrating parabolic reflectors. However, these last values would

be further reduced in a PV/T hybrid since part of the irradiation would be used to produce electricity. The system design still has margin for improvement on most of its components for future developments. It is very important that cells under concentration feature very high efficiency; the glass cover should have very high transmittance while optical errors in the reflector should be avoided and reflectance maximized. In future studies, an analysis of the aging of the cells and the efficiency decrease with time should be performed. Also, it is recommended that not only the hybrid outputs but also the performance of the whole system should be estimated. In this further investigation it is relevant to know, among other factors, what the hybrid application is, the yearly load, its daily and annual profile and the storage and auxiliary backup characteristics. Hence, it becomes possible to estimate the total system performance weighted with the investment and maintenance costs awarding different values to the electricity and thermal energy produced by the hybrid.

When it comes to possible applications for the hybrid and considering that the thermal output is much higher than the electrical output, it seems that the argument regarding the thermal output as just a benefit one can get by cooling down the cells does not make sense. It is more realistic to think that, at present, PVT hybrids can only become viable when a suitable application for the produced thermal energy is also found. The question is that the thermal system often requires a high temperature which decreases the PV module efficiency. Therefore it might be difficult to find the optimum operating point. If the generated electricity can be directly connected to the grid, then the system area should be design to cover the thermal load. When the analyzed hybrid is compared with a side-by-side system based on total glazed area the results show that, in terms of occupied space and global energy produced, there is no difference in having the hybrid working for domestic hot water production or pool heating. In this case, due to its lower U value compared with the standard flat plate collector, what is “lost” in electricity production at high temperatures is compensated for by thermal production at almost the same rate.

6. Conclusions

A complete methodology to characterize, simulate and evaluate the performance of a concentrating hybrid has been proposed and exemplified in a particular case study. The method includes a comparison with a traditional side-by-side system formed by conventional PV modules and flat plate collectors.

The evaluated hybrid of geometrical concentration 7.8 is constructed around PV cells of 16% efficiency. The evaluation results show that the optical efficiency is 0.45 and the U-value is 1.9 W/m²ºC. The electrical efficiency is 6.4%. These values are drastically lower than for standard solar collectors and PV modules. Furthermore, the annual global irradiation incident on a tilted flat module is 20%-40% higher than the beam irradiation incident on a concentrating system tracking the light around a horizontal axis aligned in the north-south direction. Hence, the low hybrid efficiencies in combination with low usable irradiation generate a low annual performance. Conventional PV modules and flat plate collectors, producing the same electric and thermal annual output as a concentrating hybrid, are comparable with the hybrid area. Even though there is a margin for improvement on the tested hybrid parameters, it is difficult for a concentrating hybrid to compete with conventional alternatives. It is very important that PV-cells under concentration have very high efficiency and that the glass cover and the reflector have very good

properties. Optical errors in the reflector must be avoided and the system should be tracking around an axis aligned in the north-south direction, tilted towards the equator.

Acknowledgement

This study was supported by a Marie Curie program, *SolNet* - Advanced Solar Heating and Cooling for Buildings - the first coordinated international PhD education program on Solar Thermal Engineering. Homepage: http://cms.uni-kassel.de/unicms/?id=2141

Johan Nilsson is acknowledged for valuable discussions and proof reading the article.

References

Absolicon Solar Concentrator AB, 2008. www.absolicon.com

Alanod Solar, 2010. Technical information concerning the reflector. www.alanod-solar.com

Affolter, P., Eisenmann, W., Fechner, H., Rommel, M., Schaap, A., Sorensen, H., Tripanagnostopoulos, Y., Zondag, H., 2004. *PVT road map, A European guide for the development and market introduction of PV-Thermal technology*, ed. Energy Research Centre of the Netherlands, Netherlands. Download at www.pvtforum.org.

Arvind, C. and Tiwari, G.N., 2010. *Stand-alone photovoltaic (PV) integrated with earth to air heat exchanger (EAHE) for space heating/cooling of adobe house in New Delhi (India).* Energy Conversion and Management 51(3), 393-409.

Arvind, C., Tiwari G.N. and Avinash, C., 2009. *Simplified method of sizing and life cycle cost assessment of building integrated photovoltaic system.* Energy and Buildings 41(11), 1172-1180.

Bernardo, L. R., 2007. *Evaluation of the concentrating system Solar8.* Master Thesis.

Chow, T.T., 2010. *A review on photovoltaic/thermal hybrid solar technology.* Applied Energy 87(2), 365-379.

Chow, T. T., 2003. *Performance analysis of photovoltaic-thermal collector by explicit dynamic model.* Solar Energy 75(2), 143-152.

Coventry, J.S., Franklin, E.T., Blakers, A., 2002. *Thermal and electric performance of a concentrating PV/Thermal collector: results from the ANU CHAPS collector*. In: proceedings of Australian and New Zealand Solar Energy Society Conference, 2002. Download available at http://hdl.handle.net/1885/40837.

Duffie, J.A., Beckman, W.A., 2006. *Solar Engineering of Thermal Process*. John Wiley & Sons.

Fisher, S., Heidemann, W., Müller-Steinhagen, Perers, B., Berquist, P., Hellström, B., 2004. *Collector test method under quasi-dynamic conditions according to the European Standard EN 12975-2.* Solar Energy 76, 117-123.

Franklin, E.T., Coventry, J.S., 2002. *Effects of highly non-uniform illumination distribution on electrical performance of solar cells.* In: proceedings of Australian and New Zealand Solar Energy Society Conference, 2002. Download available at http://hdl.handle.net/1885/40832.

Kostić, Lj. T., Pavlović, T. M., Pavlović, Z. T., 2010. *Optimal design of orientation of PV/T collectors with reflectors.* Applied Energy 87, 3023-3029.

Nilsson, J., 2007. *Optical Design for Stationary Solar Concentrators.* PhD thesis, ISBN 978-91-85147-21-2, pp 23-27.

Nilsson, J., Håkansson, H., Karlsson, B., 2007. *Electrical and thermal characterization of a PV-CPC hybrid.* Solar Energy 81(7), 917-928.

Royne A., Dey C.J., Mills D.R., 2005. *Cooling of photovoltaic cells under concentrated illumination: a critical view.* Solar Energy Materials and Solar Cells 85(4), 451-83.

Sick, F., Erge, T., 1998. *Photovoltaic in buildings: a design handbook for architects and engineers.* IEA task 16. ISBN 1 873936 59 1, pp 27-28.

Tripanagnostopoulos, Y., Souliotis, M., 2004. *Integrated collector storage solar systems with asymmetric CPC reflectors.* Renewable Energy 29, 223-248.

Wenham, S., Green, M., Watt, M., Corkish, R., 2007. *Applied Photovoltaics*, Earthscan second edition, London.

Winston R., Miñano J., Benítez P., 2005. *Nonimaging Optics*. ISBN 0-12-759751-4.

Winsun Villa Educational Software, 2009. Perers, B., SERC Högskolan Dalarna, Sweden. www.serc.se.

Yoon, S., Garboushian, V., 1994. *Reduced temperature dependence of high-concentration photovoltaic solar cell open circuit voltage (V_{OC}) at high concentration levels.* In: Procedings of the first WCPEC in Hawaii, 5-9 December.

Article III

Performance Evaluation of a High Solar Fraction CPC-Collector System

L. R. Bernardo*, H. Davidsson and B. Karlsson

Energy and Building Design Division, Lund Technical University, Box 118 SE-221 00 Lund, Sweden

* Corresponding Author, Ricardo.Bernardo@ebd.lth.se

Abstract

One of the most important goals on solar collector development is to increase the system's annual performance without increasing overproduction. The studied collector is formed by a compound parabolic reflector which decreases the collector optical efficiency during the summer period. Hence, it is possible to increase the collector area and thus, the annual solar fraction, without increasing the overproduction. Collector measurements were fed into a validated TRNSYS collector model which estimates the solar fraction of the concentrating system and also that of a traditional flat plate collector, both for domestic hot water production. The system design approach aims to maximise the collector area until an annual overproduction limit is reached. This is defined by a new deterioration factor that takes into account the hours and the collector temperature during stagnation periods. Then, the highest solar fraction achieved by both systems was determined. The results show that, at 50° tilt, the concentrating system achieves 71% solar fraction using 17 m^2 of collector area compared to 66% solar fraction and 7 m^2 of a flat plate collector system. Thus, it is possible to install 2.4 times more collector area and achieve a higher solar fraction using the load adapted collector. However, the summer optical efficiency reduction was proven to be too abrupt. If the reflector geometry is properly design, the load adapted collector can be a competitive solution in the market if produced in an economical way.

Keywords: Concentrating, Solar Thermal, Domestic Hot Water System, High Solar Fraction

Nomenclature

Monitored parameters:

Q	Collector thermal power (W/m²)
G_b	Beam Irradiance (W/m²)
G_d	Diffuse Irradiance (W/m²)
T_{in}	Collector inlet temperature (°C)
T_{out}	Collector outlet temperature (°C)
T_m	Fluid mean temperature (°C)
T_{amb}	Ambient temperature (°C)
dV/dt	Flow (m^3/s)
C_p	Heat capacity (water) (J/(kg°C))
ρ	Density (water) (kg/m^3)
A_c	Collector area (m²)

Parameters in the collector model:

$F'(\tau\alpha)_n K_d$	Diffuse zero-loss efficiency (-)
$F'(\tau\alpha)_n$	Beam zero-loss efficiency (-)
$F'U_0$	Heat loss factor (W/m^2 °C)
$F'U_1$	Temperature dependence of heat loss factor (W/m^2 °C^2)
$g(\theta)$	Beam incidence angle modifier for the glazing
$K_b(\theta)$	Incidence angle modifier for beam irradiance (-)
$K_{bl}(\theta_l,0)$	Longitudinal incidence angle modifier for beam irradiance (-)
$K_{bt}(0,\theta_t)$	Transversal incidence angle modifier for beam irradiance (-)
K_d	Incidence angle modifier for diffuse irradiance (-)
$(mC)_e$	Collector effective thermal capacitance (J/(m^2°C))
θ	Angle of incidence onto the collector normal (°)
$R_t(\theta_t)\cdot$	Beam incidence angle modifier for the reflector
t	Time (h)

1. Introduction

One of the most important goals to be achieved by a solar thermal system is a high annual solar fraction (Mills and Morrison, 2003; Helgesson et al., 2002). While solar thermal systems can generally achieve a high annual solar fraction in areas near the equator, in regions where the annual solar irradiation is lower it can be difficult. In most such regions, the solar contribution profile peaks during the summer months and decreases during the winter period. On the contrary, the domestic hot water load is fairly constant during the whole year which means that these two factors do not match all year round. Thus, the annual solar fraction is reduced.

It is common to design the system collector area in such way that the production over the summer period meets the thermal load (Helgesson, 2004 and Adsten et al., 2004). The aim of these systems is to achieve a solar fraction close to 100% during this period not taking into account overproduction at all. However, the solar production and consumption profiles are very different throughout the day as well. The solar production does not entirely take place at the same time as it is consumed by the users. Only a fraction of this extra energy can be stored in the solar tank. Hence, the system ends up with many hours where the collectors are in stagnation and other hours where auxiliary energy is needed. Furthermore, long stagnation periods influence long-term reliability and low maintenance operation of the collector system (Hausner and Fink, 2000). Common problems are overheating and permanent damage on system components, regular loss of fluid, condensation pressure chocks, deterioration of the fluid that ends up clogging the system, fluid circulation noise (Hausner and Fink, 2002). Hence, there is a need to define a deterioration factor taken into account when designing a new system. Using this criteria will limit the stagnation period along the year and, consequently, minimizes the risk of system malfunctions along its lifetime.

This paper describes a collector design approach that increases the solar fraction by maximizing the energy contribution of the thermal collector system but also limiting the overproduction. This is accomplished by using the collector's special reflector design at optimal tilt, collector area and flow. As a result of these optimizations, the system is able to reduce the difference between the solar production and the domestic hot water load throughout the year and still avoid overproduction under a user-determined value. Related concepts to this collector have been reported by Kothdiwala et al. (1995), Tripanagnostopoulos et al. (2000), Chaves and Pereira (2000), Mills and Morrison (2003). The collector parameters were determined based on a dynamic testing method and multi linear regression (Perers B., 1997). These parameters were then fed into a validated model in TRNSYS (Klein S., 1997) estimating the compound parabolic concentrator (CPC) system performance and comparing it with a flat plate collector system. There exists no validation model of a solar thermal system using this asymmetric CPC.

The main objective of the work was to evaluate the performance of the CPC collector system and compare it with a conventional flat plate collector system.

2. Method

2.1. Experimental setup and collector design

A solar collector design in which relatively expensive selective absorber material is replaced by cheap reflectors was studied. A compound parabolic concentrator (CPC) collector with a geometrical concentration factor of 1.5 has been developed (Adsten, 2004). The collector consists of a reflector, a bi-facial selective absorber and a support structure. The parabolic reflector has an optical axis normal to the collector glass which defines the irradiation acceptance interval of the reflector (Figure 1) (Helgesson, 2004). Once the incident radiation is outside this interval, the reflectors do not redirect the incoming beam radiation to the absorber, and the optical efficiency of the collector is reduced (Figure 1). Hence, the collector's optical efficiency changes throughout the year depending on the projected solar altitude. The tilt determines the amount of total annual irradiation kept within the acceptance interval. As a result, by varying the tilt, it is possible to increase the collector area without causing overproduction in the summer when the collector has lower optical efficiency. Since the absorber is parallel to the glass, in the upper part of the collector a pocket of hot air is created decreasing convection heat losses. The support structure is made of light wood with empty spaces in between in order to reduce its weight, wind obstruction and material costs.

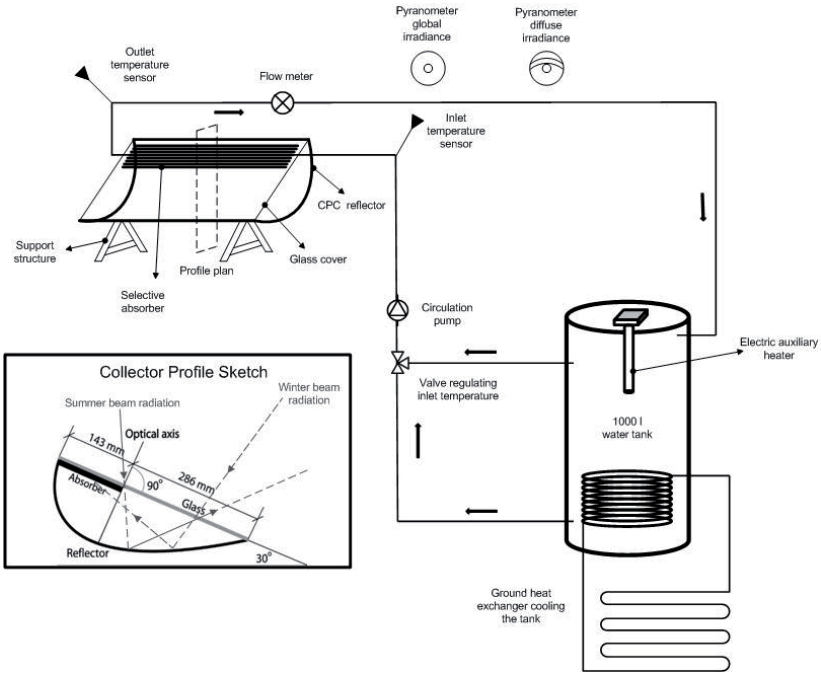

Figure 1. Experimental setup and CPC collector profile.

2.2. Testing and characterization method

Several measurements were carried out on the CPC collector in order to calculate the necessary parameters for the annual performance simulations. Measured average data was stored every 6 minutes between the 20th and the 29th of September, 2009. A simplified dynamic test method for determination of non-linear optical and thermal characteristics with multiple linear regression was used (Perers, 1993; Perers, 1997; Duffie and Beckman, 2006):

$$Q = F'(\tau\alpha)_n K_b(\theta) G_b + F'(\tau\alpha)_n K_d G_d - F'U_0(T_m - T_{amb}) - F'U_1(T_m - T_{amb})^2 - (mC)_e \frac{dT_m}{dt} \quad (\mathrm{W/m^2}) \qquad \textit{equation 1}$$

$$Q = \frac{\rho \frac{dV}{dt} C_p (T_{out} - T_{in})}{A_c} \quad (\mathrm{W/m^2}) \qquad \textit{equation 2}$$

McIntire (1982) presented a biaxial incidence angle modifier model described in the longitudinal and transverse directions:

$$K_b(\theta_l,\theta_t) \approx K_{bl}(\theta_l,0)\cdot K_{bt}(0,\theta_t) \quad (-) \qquad \textit{equation 3}$$

However, this model presents disadvantageous. Rönnelid et al. (1997) showed that the model underestimates the optical losses in the glass and that large errors can occur at high incidence angles. This effect is reduced since the optical losses in the glass are accounted twice.

In this study an incidence angle modifier model proposed by Nilsson et al. (2006) was used. The biaxial model uses the projected transverse incidence angle to determine the influence of the reflector and the real angle of incidence to determine the influence of the glazing in the following way:

$$K_b(\theta_l,\theta) \approx R_t(\theta_t)\cdot g(\theta) \quad (-) \qquad \textit{equation 4}$$

Firstly, the influence of the glazing was measured in the longitudinal direction when the transversal incident angle was kept constant. Secondly, the dependence of the reflector was measured on the transversal plane when the longitudinal incidence angle was also constant. This was carried out by testing two identical CPC collectors during the autumn equinox, both tilted 55° from horizontal (Lund's latitude) but placing one of them horizontally and the other vertically like shown in Figure 3. This procedure is described in detail in (Helgesson, 2004). Typically, the measured curves are included in the collector model using a matrix made of singular incidence angle modifiers. The rest of them are linearly interpolated. At incidence angles close to the collector acceptance angle, the incidence angle modifiers variation is abrupt. Hence, interpolating discrete values can cause large inaccuracies. In this study, the measured incidence angle modifiers were included in the model using high grade polynomial equations. Hence, interpolations were avoided and the accuracy of the model increased.

2.3. Simulation model

A TRSNSYS model describing the whole solar collector system was created. Its main components are shown in Figure 4 and listed below:

- Thermal collector – CPC collector type 832, created by Bengt Perers and further developed by Hellström, Fisher, Bales, Haller, Dalibard and Paavilainen (Perers and Bales, 2002). In this study, the biaxial incidence angle modifiers described by polynomial equations were added to the model;
- Radiation processor – type 109-TMY2, Lund weather data (latitude 55°44'N, longitude 13°12'E), Sweden;
- Circulation pump – type 3b, single speed. The collector flow was design to maximise the solar fraction for each collector area and tilt angle;
- Storage tank – type 4c, stratified storage with uniform losses and variable inlets. This storage model adjusts the inlets location continuously in order to place the incoming fluid at a level as

close to its temperature as possible. This improves greatly stratification in the tank and consequently the annual solar fraction. The total volume is 300 litres and 1.60m high. The 3kW auxiliary heater is placed at the top with a set-point temperature of 60˚C;

- Domestic hot water load profile – type 14 for the daily load profile and type 14h for the yearly variation.

The domestic hot water load profile was built based on the one described by Widén et al., (2009) but scaled to the latest data on Swedish total hot water consumption (Stengård, 2009). 7 different water draw-offs were performed during the day (Figure 2). Furthermore, the annual hot water consumption variation effect was also introduced and it is shown in Figure 2 (Swedish Energy Agency, 2009). The total annual consumption is 2050 kWh/year. The annual limit for the deterioration factor was set to 5000 ˚C.h/year. This value takes into account not only the number of stagnation hours but also how much the collector outlet temperature raised over 100 ˚C during that period in the following way:

$\Sigma (T_{out}-100)\ t$ *(°C.h)* (during stagnation periods) *equation 5*

Stagnation period was defined by the time period during which both the top of the storage tank and the outlet collector temperature was above 100˚C. During this period, the collector pump is stopped. Has shown in equation 5, it was assumed that stagnation time and collector outlet temperatures above 100˚C have a linear influence on the parameter. The figure 5000˚C.h/year represents a reasonable maximum overproduction (100 hours of stagnation with 150˚C collector temperature, for example). Finally, by simulation iterations, the maximum collector area that corresponds to the maximum solar fraction but limits the overproduction to 5000˚C.h /year was determined. This design criterion is further discussed in the discussion section.

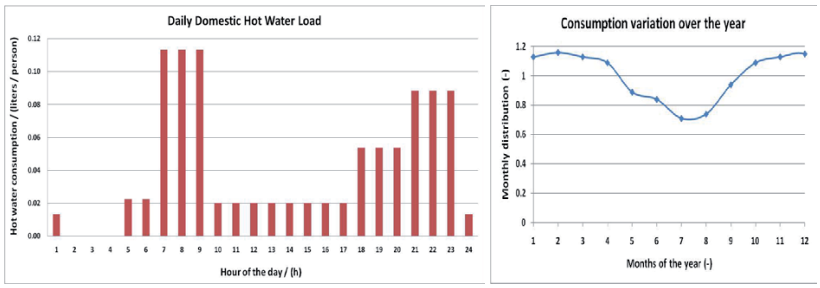

Figure 2 – Daily and yearly domestic hot water profile.

Figure 3 – CPC collector turned 90˚ during the autumn equinox.

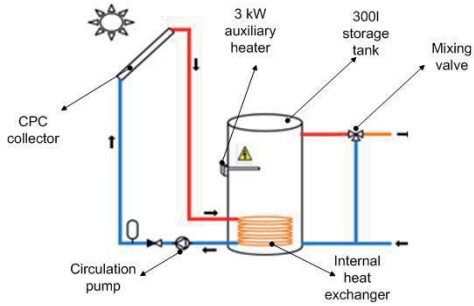

Figure 4 – Main components of the solar collector system model.

3. Measurement results

3.1. Thermal performance

Table 1 shows the CPC collector parameters, estimated using multi linear regression on the measured data, and the parameters assumed to be typical for conventional flat plate collectors.

Table 1. Measured CPC collector parameters and assumed typical flat plate collector parameters.

Parameters and units	CPC collector (measured)	Flat plate collector (presumed)
$F'(\tau\alpha)_n$ (-)	0.64	0.8
$F'(\tau\alpha)_n K_d$ (-)	0.31	0.72
$F'U_0$ / (W/m^2,°C)	2.8	3.6
$F'U_1$ /(W/m^2,°C^2)	0.035	0.014
$b_{o\_thermal}$ (-)	-	0.2
$(mC)_e$ /(J/m^2 °C)	1923	8000

3.2. Incidence angle modifiers

Figure 5 shows the longitudinal and transversal incidence angle modifiers describing the influence of glazing and reflector, respectively. The transversal incidence angle modifier was measured while the longitudinal incidence angle modifier was estimated by the Fresnel and Snell's laws.

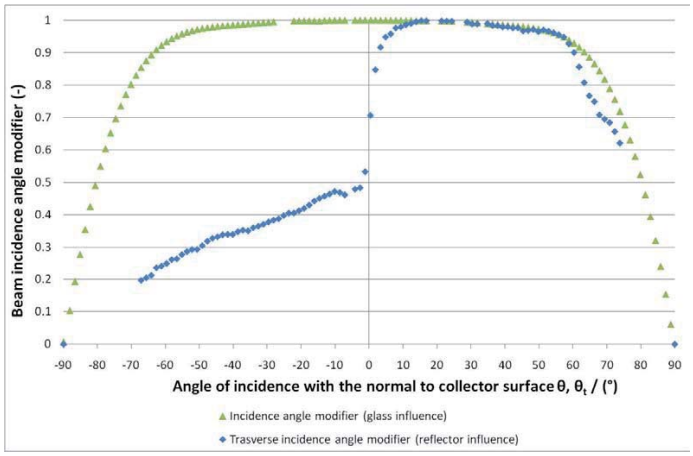

Figure 5 –Reflector and glazing beam incidence angle modifiers during autumn equinox.

3.3. Model validation

To validate the CPC collector model, the measured and modelled power outputs were compared during the test period (Figure 6). From the analysis of Figure 6, one can conclude that good agreement was found between the model and the measurements. In Figure 7 the modelled and measured power output are compared during a variable irradiation day. It was assumed that the CPC collector model is the only component that requires validation. The other component models are TRNSYS standard models and have been used with great reliability in the scientific community.

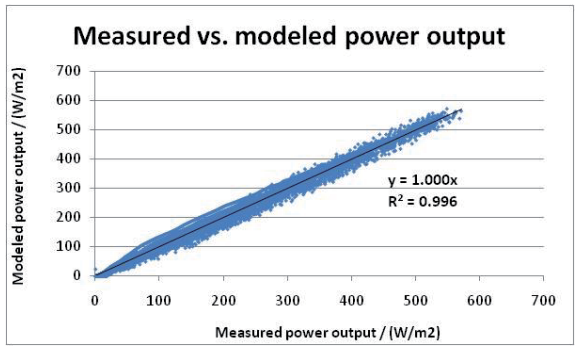

Figure 6 – Measured and modelled power output data during the testing period.

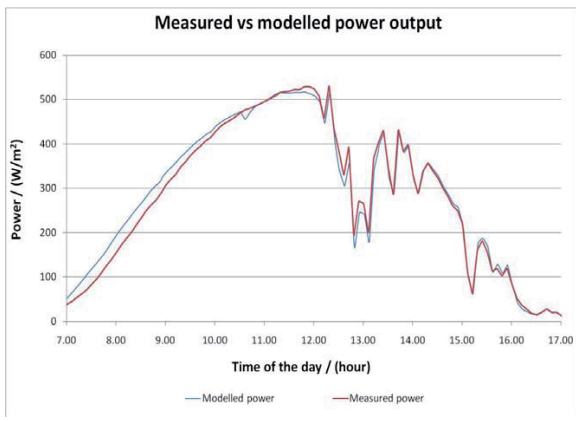

Figure 7 – Measured and modelled power output on the 20th September 2009.

4. Performance analysis and discussion

Using the collector measured parameters, TRNSYS simulations were carried out for the concentrating collector and a traditional flat plate solar thermal system situated in Lund, Sweden. The assumed design criterion limiting the collector area takes into account not only the number of stagnation hours but also the collector outlet temperature. This deterioration factor was set to 5000 °C.h/year. Obviously, this design criterion can be questioned, especially when it comes to the particular chosen number of 5000 ˚C.h/year.

Also, it is uncertain if temperature and time during stagnation periods should have equal weight on this factor. Further work is needed to understand how to account for overproduction in the system design in a more precise way and to account the weight of this factor on the system design. The assumed design guideline should be seen as a first iteration step in that direction. The intention is to consider a deterioration factor when designing a new solar thermal system. The important analysis at this stage is result comparison between these two different collector systems rather than conclude about the absolute value of the solar fraction results. As both systems were design in the same way, inaccuracies that occur in one system will occur in the same way in the other one. This makes it significantly more reliable to take conclusions about the systems performances. In a future analysis taking into account the costs for every kind of component, the system will be design in order to improve its cost-effectiveness.

The maximum solar fraction achieved by both systems, for several different tilts, is presented in the left axis in Figure 8. The corresponding maximum collector area that limits the annual overproduction under 5000˚C.h/year is shown in the right axis of the same figure. Analysing the results it can be concluded that when the concentrating collector is set to low tilts the optical efficiency is high during the whole year and it behaves like a flat plate collector with peak production in the summer. On the other hand, when it is set to higher tilts, the optical efficiency is reduced along the year and overproduction only occurs for large collector areas. The balance between these two situations for Lund is somewhere around 50˚ tilt where the optical efficiency is only reduced during the summer resulting in a high annual solar fraction and still not using extremely large collector areas. For that tilt, the load adapted system achieves a solar fraction of 71% using 17 m^2 of collector area compared to 66% and 7 m^2 of a flat plate collector system. Contributing to these high solar fraction values is the very high stratification and well insulated model of the tank. In such a tank model, the incoming water is placed at a height in the tank that has the closest matching temperature. Also, no losses were taken into account in piping. Hence, very high stratification and consequently high solar performances were achieved. This simple tank model allowed time saving both in building the system model and the running period of the simulations.

In Figure 9 it is shown the annual production profile of the two solar systems for 50˚ tilt. One can notice the suppressed solar production during the summer in the CPC collector and the overproduction moved to the spring and autumn periods. When the CPC collector system achieves higher solar fractions than the flat plate collector system, it requires, at least, 2.4 times more collector area. Taking into account that the selective absorber surface of the CPC collector is 1/3 of its total glazed area (Figure 1), one can say that the concentrating collector makes use of less absorber area. This decrease together with higher performance must compensate the extra material such as reflector and glass as well as the possible technical difficulties of manufacturing a parabolic shape. Nevertheless, there is an exaggerated optical efficiency decrease to less than half causing underproduction during the summer. If the reflector geometry is improved, the CPC collector will achieve higher performances for the same collector area and become a more competitive solution when produced in a cheap way.

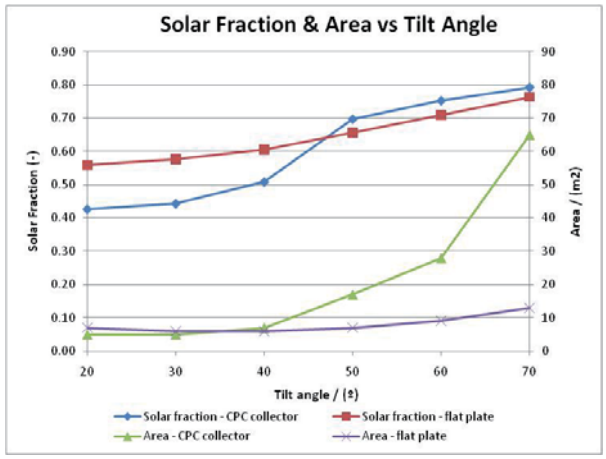

Figure 8 – Annual solar fraction and corresponding collector areas for both systems.

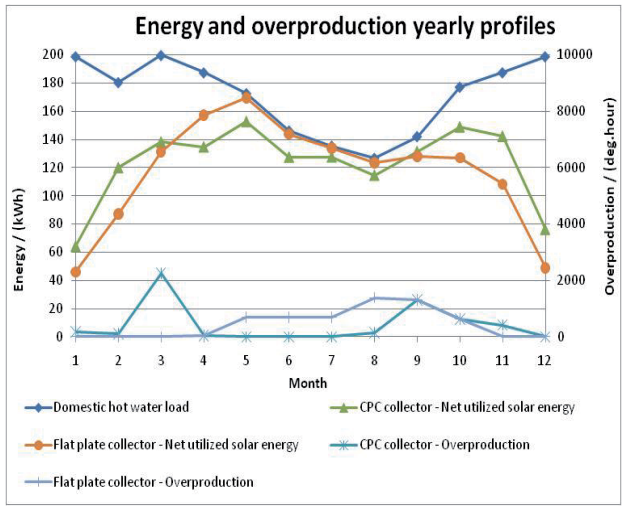

Figure 9 – Energy and overproduction profiles during the year for 50 ° tilt, 17m^2 of collector area and 0.12 l/min/m^2 of water flow.

5. Conclusions

An evaluation of a load adapted CPC collector system was presented. The collector design aims to increase the solar fraction by adapting the solar production to the load. The evaluation includes a new design approach for the collector system that estimates the collector area based on an annual overproduction limit. A comparison with a standard flat plate collector system is also included.

The results show that, at 50˚ tilt, it is possible to install larger collector areas of the concentrating system and achieve higher solar fractions without increasing overproduction. For this tilt, the concentrating system achieves 71% solar fraction using 17 m^2 of collector area compared to 66% solar fraction and 7 m^2 of a flat plate collector system. This means 2.4 times more collector area with a somewhat higher performance. For the same glazed area, the absorber surface of the flat plate collector is 3 times higher than that of the concentrating system. Thus, from the result analysis, one can conclude that the concentrating collector absorber area is smaller than the flat plate collector. This is one of the most expensive components of the collector. Hence, the absorber surface reduction together with the higher performance must compensate the cost increase on the other materials such as glass, parabolic reflector, frames so that the concentrating system can compete with standard flat plate collectors. Obviously, this performance comparison is sensitive to the parameters assumed for the conventional flat plate collector. Nevertheless, these values are valid for this particular collector design where the optical efficiency is reduced to less than half during the summer. This exaggerated effect causes underproduction during this period reducing the annual solar fraction. If the reflector geometry is improved, the collector can become an even more competitive solution in the market if produced in an inexpensive way.

Acknowledgement

This study was supported by a Marie Curie program, *SolNet* - Advanced Solar Heating and Cooling for Buildings - the first coordinated international PhD education program on Solar Thermal Engineering. Homepage: http://cms.uni-kassel.de/unicms/?id=2141

References

Adsten, M., Helgesson, A. and Karlsson, B., 2004. *Evaluation of CPC-collector designs for stand-alone, roof- or wall installation.* Solar Energy 79(6), 638-647.

Chaves, J. and Pereira, M. C., 2000. *Ultra flat ideal concentrators of high concentration.* Solar Energy 69(4), 269-281.

Duffie, J.A., Beckman, W.A., 2006. *Solar Engineering of Thermal Process.* John Wiley & Sons.

Hausner, R. and Fink, C., 2000. *Stagnation behaviour of thermal solar systems*. Download available at www.aee-intec.at/0uploads/dateien119.pdf.

Hausner, R. and Fink, C., 2002. *Stagnation behaviour of solar thermal systems*. IEA SHC, task 26.

Helgesson, A., Karlsson, B. and Nordlander, S., 2002. *Evaluation of a Spring/Fall-MaReCo*. In: proceedings of Eurosun Conference, Bologna.

Helgesson, A., 2004. *Optical Characterization of Solar Collectors from Outdoor Measurements.* Licentiate thesis, ISBN 91-85147-07-9, pp 293-294.

Klein, S. et al., 1997. TRNSYS, a Transient System Simulation. University of Wisconsin, Madison.

Kothdiwala, A., Norton, B., Eames, P., 1995. *The effect of variation of angle of inclination on the performance of low-concentration-ratio compound parabolic concentrating solar collectors.* Solar Energy 55(4), pp 301-309.

McIntire, W. R., 1982. Factored approximations for biaxial incidence angle modifiers . Solar Energy 29(4), 315-322.

Mills, D. and Morrison, G., 2003. *Optimisation of minimum backup solar water heating system.* Solar Energy 74(6), 505-511.

Nilsson, J., Brogren, M., Helgesson, A., Roos, A. and Karlsson, B., 2006. Biaxial model for the incidence angle dependence of the optical efficiency of photovoltaic systems with asymmetric reflectors. Solar Energy 80(9), pp 315-322.

Perers, B., 1993. *Dynamic method for solar collector array testing and evaluation with standard database and simulation programs*. Solar Energy 50(6), pp 517-526.

Perers, B., 1997. *An improved dynamic solar collector test method for determination of non-linear optical and thermal characteristics with multiple regression*. Solar Energy 59, 163-178.

Perers B. and Bales C., 2002. *A Solar Collector Model for TRNSYS Simulation and System Testing*. A Report of IEA SHC - Task 26 Solar Combisystems. Download available at http://www.les.ufpb.br/portal/index2.php?option=com_docman&task=doc_view&gid=190&Itemid=30

Rönnelid, M., Perers, B. and Karlsson, B., 1997. *On the factorisation of incidence angle modifiers for CPC collectors.* Solar Energy 59(4-6), pp 281-286.

Stengård, L., 2009. *Mätning av kall- och varmevattenanvändning i 44 hushåll*. Acessed in 2009/10 from http://webbshop.cm.se/System/ViewResource.aspx?p=Energimyndigheten&rl=default:/Resources/Permanent/Static/b9a064ece4d747868b5c20d1a03ab0a2/2124W.pdf

Swedish Energy Agency, 2009. *FEBY – Krav Specifikation för Minienergihus*. Download available at http://www.energieffektivabyggnader.se/download/18.712fb31f12497ed09a58000141/Kravspecifikation_Minienergihus_version_2009_oktober.pdf

Tripanagnostopoulos, Y., Yianoulis, P., Papaefthimiou, S. and Zafeiratos, S., 2000. *CPC solar collectors with flat bifacial absorbers.* Solar Energy 69, 191-203.

Widén, J., Lundh, M., Vassileva, I., Dahlquist, E., Ellegård, K. and Wäckelgård, E., 2009. *Constructing load profiles for household electricity and hot water from time-use data—Modelling approach and validation.* Energy and Buildings 41(7), pp 753-768.

Article IV

Retrofitting Domestic Hot Water Tanks for Solar Thermal Collectors
A theoretical analysis

L. R. Bernardo*, H. Davidsson and B. Karlsson

Energy and Building Design Division, Lund Technical University, Box 118 SE-221 00 Lund, Sweden

** Corresponding author. Tel: +46 462227606, Fax: +46 462224719, E-mail: Ricardo.Bernardo@ebd.lth.se*

Abstract

One of the most expensive components of a solar thermal system is the storage tank. Retrofitting conventional domestic hot water heaters when installing a new solar hot water system can decrease the total investment cost. In this study, retrofitting of existing water heaters using forced circulation flow was investigated. A comparison with a standard solar thermal system is also presented. Four simulation models of different system configurations were created and tested for the climate in Lund, Sweden. The results from the simulations indicate that the best configuration consists on connecting the collectors to the existing heater throughout an external heat exchanger and adding a small heater storage in series. For this retrofitted system, preliminary results show that an annual solar fraction of 53% is achieved. In addition, a conventional solar thermal system using a standard solar tank achieves a comparable performance for the same storage volume and collector area. Hence, it is worth to further investigate and test in practice this retrofitting. Furthermore, using the same system configuration, solar collectors can also be combined with new standard domestic hot water tanks at new installations, accessing a world-wide developed and spread industry.

Keywords: *Solar thermal, Storage tank, Water heater, Retrofit, Domestic hot water.*

Nomenclature

$T_{auxiliar}$	Preset temperature of the auxiliary heater (°C)
T_{out}	Collector outlet temperature (°C)
T_{solar}	Solar hot water temperature in the upper part of the retrofitted tank (°C)
t	Time during stagnation periods (h)

1. Introduction

Only in Sweden there exist more than half a million electrically heated single family houses that use conventional water heaters for domestic hot water production (Swedish Energy Agency, 2009a). Since the solar tank is one of the most expensive components in a solar thermal system, retrofitting existing domestic water heaters when installing a new system can decrease its total investment cost. Previous research approached similar retrofitting using natural convection systems (Cruickshank and Harrison, 2004). Thermosyphon systems became popular in several parts of the world such as Eastern Asia and Australia mainly due to its simplicity and reliability (Lin, 1998). The thermosyphon driving force depends on the pressure difference and frictional losses between the heat exchanger side-arm and the

tank. Hence, the generated flow will be complex function of the state of charge of the tank, the temperature profile along the heat exchanger and pipes, the height difference between the top of the heat exchanger and the top of the tank and the pressure drop in the heat exchanger, piping and connections (Fraser et al., 1995).

Such dependence on the heat exchanger pressure drop and tank characteristics limits how the retrofit is carried out and which storage tanks can be used. Moreover, Liu and Davidson (1995) showed that, when properly designed, forced circulation systems can generally achieve higher performances compared to natural convection driven systems. This is explained by the energy transfer rate increase at a low energy driving cost. For example, a 40 W pump can generate a driving force 45 times higher than the one achieved by thermosyphon (Liu and Davidson, 1995). In addition, there are now available low energy pumps at a low cost.

In this research forced circulation was used to connect solar collectors to conventional domestic water heaters. This was carried out by means of two pumps, one in the tank loop and the other in the solar collector loop. Four different system configurations were simulated in TRNSYS (Klein S., 1997). Since forced circulation is used, almost any kind of storage tank can be retrofitted when installing a new solar thermal system. For a better understanding of the research contribution to the field and to increase the paper readability, the main objectives of the study are stated bellow:

- To compare the performance of different alternatives on retrofitting conventional domestic water heaters when installing a solar thermal system;
- To compare the performance of the retrofitted system with the performance of a standard solar thermal system.

2. Methodology

Four different simulation models of the retrofitted system were created in TRNSYS software (Klein S., 1997) in order to estimate the configuration achieving the highest performance. A comparison with a conventional flat plate system was also performed. The retrofitted system models range from simple connections to more advanced configurations. However, the complexity was never raised up to a level that would be technically difficult to build such a system in practice. Also, it was avoided to design configurations that would predictably cause such a rise on the investment cost that would be hardly paid back by the increase in energy savings. Some of the systems' details are not revealed due to patent pending. Each system model is made up of a solar collector array, storage tank/s, auxiliary heater, heat exchanger between the collector and the tank loops, circulation pump/s, and radiation processor:

- Thermal collector – CPC collector type 832, created by Bengt Perers and further developed by Hellström, Fisher, Bales, Haller, Dalibard and Paavilainen (Perers and Bales, 2002). In Bernardo (2010) the biaxial incidence angle modifiers described by polynomial equations were added and the model validated. This collector makes it possible to achieve higher solar fractions when compared to a flat plate collector (Helgesson et al., 2002 and Bernardo et al., 2010);
- Standard storage tank – type 534. The total volume is set to 255 litres and 1.60m high. The coil heat exchanger is distributed in the lower third of the tank. The 3 kW auxiliary heater is

set horizontally at approximately 0.5m from the top with a set-point temperature of 60˚C (Figure 2);

- Retrofitted storage tank – type 534. The total volume is set to 200 litres and 1.60m high. The connections are placed at the top and bottom of the tank. Only system 2 uses the auxiliary heater placed at the bottom (Figure 3). In all the other systems this heater is disabled;
- Small heater storage tank – type 534. The total volume is set to 55 litres and 0.60m high. The connections are placed at the top and bottom of the tank. The 3 kW auxiliary heater is placed at the bottom with a set-point temperature of 60˚C (Figure 5);
- External heat exchanger – type 5b, counter flow (Figure 3);
- Circulation pumps – type 3b, single speed. The collector and tank flow are the same and were optimized by iterations to maximise the solar fraction;
- Radiation processor – type 109-TMY2, Lund weather data (latitude 55°44'N, longitude 13°12'E), Sweden;
- Domestic hot water load profile – type 14 for the daily load profile (Figure 1);

The main boundary of this investigation was to use the most common type of existing heater in single family houses in Sweden. This information is very important for the system design but also very hard to attain. To the best of our knowledge, there is no official data concerning the most common tank size in such houses. According to the Swedish domestic water heater manufacturers, installers and researchers in the field, the most common Swedish single family house tank size is 200-300 litres, depending on the family size. In any case, the tank volume tends to be proportional to the family size. Thus, the trend is that higher loads also correspond to higher available storage volumes and the system design strategy does not change. On the other hand, the average domestic hot water load in single family houses is documented. Preliminary results showed that retrofitting a 300 litre tank for such a domestic hot water load would achieve a higher annual solar fraction than using a 200 litre tank. Hence, to work on the safe side, it was decided to retrofit a 200 litre tank. If such a system achieves satisfactory performances the same should happen if a 300 litre tank is retrofitted instead.

An auxiliary heater power of 3 kW was used in all models since this is also the most common. The auxiliary heater keeps the top volume of the storage at 60˚C. This is a recommendation of the Swedish building regulations to avoid legionella problems (Swedish Building Regulation, 2008). The same document legislate that it is mandatory that the hot water temperature available at the tap is not less than 50°C. As a design guideline it is recommended that the domestic hot water system can be able to deliver two times 140 litres of 40°C water in one hour (Swedish Building Regulation, 2008). If the temperature setting is increased, all the different simulated systems reach approximately this peak on consumption. In practice, the thermostat is set to 60°C which ensures that ordinary loads are fulfilled. In case of extraordinary large draw-offs, the user has the possibility to steer the set point temperature. This is also normally the case for stand-alone conventional heaters.

The domestic hot water load profile consists on seven different draw-offs during the day. It is a simplification of the hourly profile described by Widén et al., 2009 but scaled down to the latest data on the Swedish average hot water consumption of 42 litres/person/day (Stengård 2009). Simulation results show that using a detailed hour profile would have a minimum impact on the results and would only increase the simulation total time. The measured average cold water temperature in the taps was 8.5°C. The consumption variation during the year was also introduced (Swedish Energy Agency, 2009b). The daily and yearly domestic hot water profiles used in the models are shown in Figure 1. The average number of inhabitants in Swedish single-family houses is three (Statistics Sweden, 2006).

Hence, the domestic hot water annual consumption in these houses was estimated to be 2050 kWh/year.

Since long stagnation periods affect the system's long-term reliability and can cause serious permanent damages on its components (Hausner and Fink, 2000 and 2002), the criteria used to design the collector array was based on the maximum solar fraction possible to be achieve under a certain overproduction limit. This deterioration factor was set to 5000 °C.h/year and integrates the number of hours which the collector was under stagnation and how much the collector outlet temperature raised over 100 °C during that period. This was calculated in the following way:

$\Sigma (T_{out}-100)\ t$ *(°C.h)* (during stagnation periods) *equation 1*

Stagnation period was defined by the time period during which both the top of the storage tank and the outlet collector temperature was above 100°C. During this period the pump on the collector loop is stopped. Has shown in equation 1, it was assumed that stagnation time and collector outlet temperatures above 100°C have a linear influence on this parameter. 5000°C.h/year was considered to represent a reasonable practical maximum overproduction. This corresponds to, for example, 100 hours at stagnation where the collector outlet temperature was 150°C. Hence, by means of simulation, the maximum collector area that ensures maximum solar fraction under the overproduction limit was determined for each system configuration at a 50° collector tilt from horizontal. This design criteria is further discussed in the "Results and Discussion" chapter.

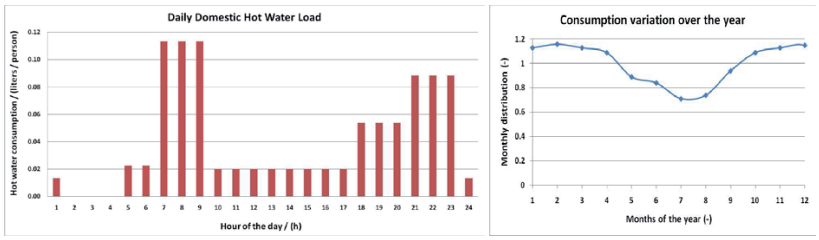

Figure 1 – Daily and yearly domestic hot water profile.

2.1. Standard system

A model of a standard solar thermal system was created and is described by the sketch in Figure 2. The figure illustrates a solar tank with and internal heat exchanger and auxiliary heater. The storage volume is 255 litres in order to match the volume of the retrofitted system that has the best performance (retrofitted system 4, Figure 6). There are three temperature sensors that control the pump, two placed on the tank's surface and the other at the collector outlet.

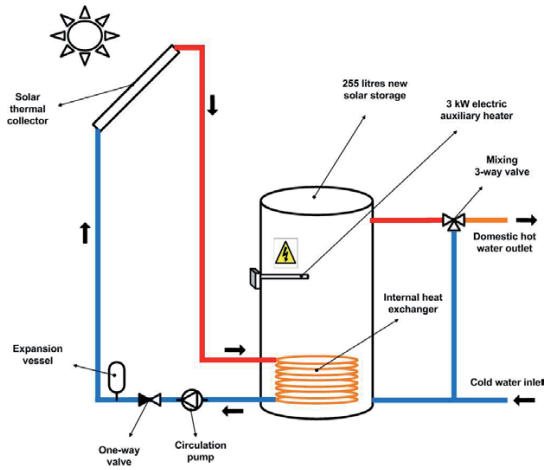

Figure 2. Sketch of the standard solar thermal system.

2.2. Retrofitted system 1

Figure 3 describes one of the most simple and direct ways of assembling solar collectors to existing tank heaters. The connection is carried out by means of an external side-arm heat exchanger between the collector and the tank loops. Also, two temperature sensors are placed on the tank's surface in order to control both the collector and the tank pumps. As exemplified in Figure 2, solar storages are specially designed for solar thermal applications with, at least, two connections for the domestic hot water and two others for the solar collector loop. On the other hand, conventional tank heaters have only the two connections for domestic hot water (see Figure 3). In order to overcome this technical challenge, the working period of the pump placed on the tank loop must be controlled with the domestic hot water draw-offs so they do not coincide. When no hot water is required, the pump is able to charge the tank. When draw-offs take place, the pump is turned off and the incoming cold water is pressed in the bottom of the tank replacing the outgoing domestic hot water at the top.

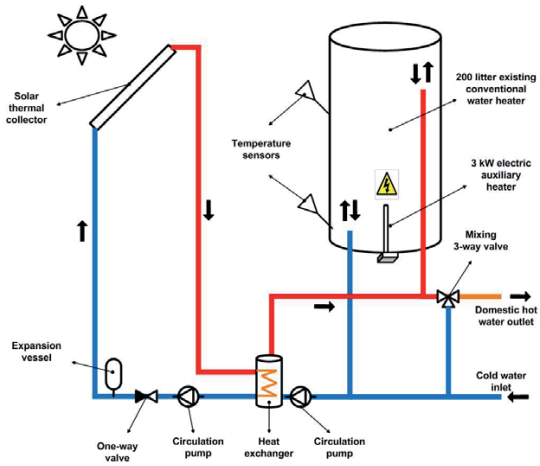

Figure 3. Retrofitted system 1 - simple retrofitting of existing hot water heaters.

2.3. Retrofitted system 2

In this system, a new 3 kW auxiliary water heater is added to the side-arm heat exchanger (Figure 4). Alternatively, if possible, the old auxiliary heater at the bottom of the existing tank can be used. The aim is to achieve stratification in the tank. The heater and the pump on the tank loop are turned on when the temperature in the sensor placed on the top of tank falls below the set point temperature minus the dead band. Consequently, the cold water in the tank bottom flows through the heat exchanger and is heated up in the side-arm heater before entering the top of the tank. The heater is turned off when the temperature on the upper sensor is higher than the set point temperature plus the dead band.

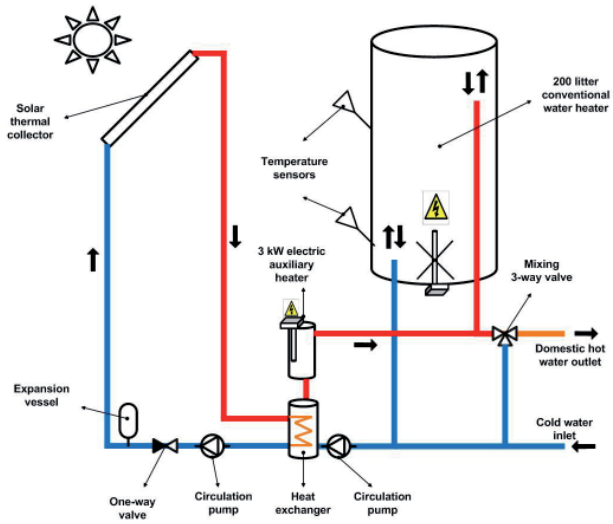

Figure 4. Retrofitted system 2 - retrofitted system with auxiliary heater on the side-arm.

2.4. Retrofitted system 3

In retrofitted system 3, a small 55 litre auxiliary heater storage was added to the system (Figure 5). This means that the retrofitted storage is exclusively used for solar hot water. The volume of 55 litres was chosen based on design guideline for the domestic hot water load. The 4-way valve was modelled in TRNSYS using type 221 (Nordlander and Bales, 2007). The valve has three inlets, two from hot sources and one from a cold source. It is programmed in order to use as much water volume as possible from the colder hot source which, in this case, corresponds to the solar storage. Hence, as long as there is available solar hot water in the retrofitted storage at the same temperature or above the domestic hot water load temperature, the water inside the auxiliary heater tank will not be used.

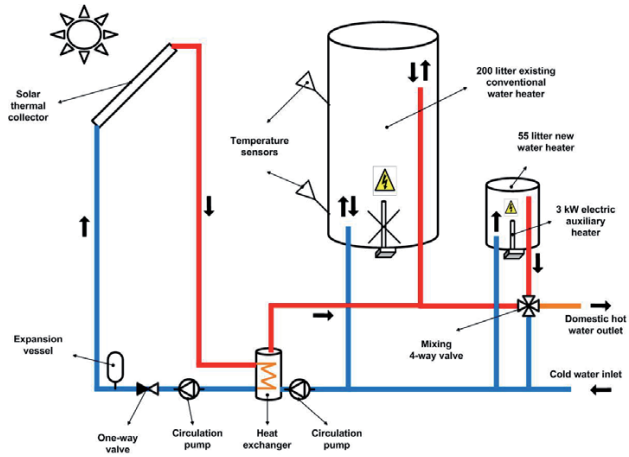

Figure 5. Retrofitted system 3 - retrofitted system with an additional tank heater connected in parallel.

2.5. Retrofitted system 4

The last retrofitted system consists of connecting the small heater storage to the existing heater in series instead (Figure 6). Thus, when hot water is drawn off by the user, the water at the top of the solar storage is pushed to the bottom of the small heater.

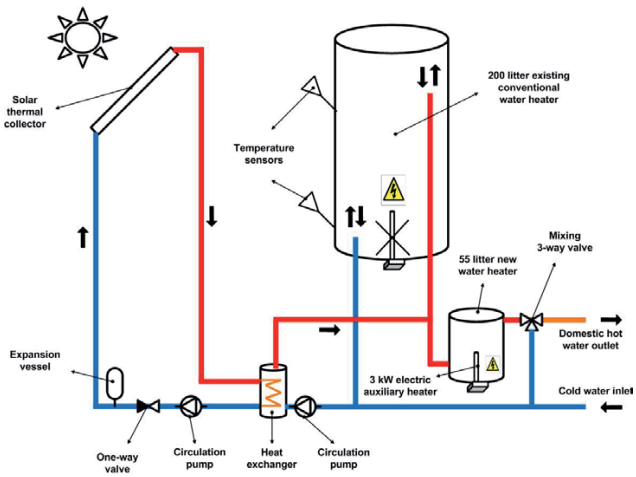

Figure 6. Retrofitted system 4 - retrofitted system with an additional tank heater connected in series.

3. Results and Discussion

The assumed design criterion limiting the collector area takes into account not only the number of stagnation hours but also the collector outlet temperature. This deterioration factor was set to 5000 °C.h/year. Obviously, this design criterion can be questioned, especially when it comes to the particular chosen number of 5000 °C.h/year. Also, it is uncertain if temperature and time during stagnation periods should have equal weight on this factor. Hence, further research is needed to understand how to quantify this factor and what should be its weight on the system design. However, the intention is to take into account a deterioration factor when designing a new solar thermal system. The assumed design guideline should be seen as a first iteration step in that direction. The important analysis at this stage is result comparison between these two different collector systems rather than conclude about the absolute value of the solar fraction results. As both systems were designed in the same way, inaccuracies that occur in one system will occur in the same way in the other one. This makes it significantly more reliable to take conclusions about the systems performances. In a future analysis the system should be design to minimize the costs per produced energy unit.

The simulation results of the annual solar fraction for every system are presented in Table 1.

Table 1. Annual solar fraction of the various retrofitted systems and the standard solar system.

System name	Annual solar fraction (%)
Standard system	52%
Retrofitted system 1	6%
Retrofitted system 2	15%
Retrofitted system 3	42%
Retrofitted system 4	53%

Retrofitted system 1 shows a very low annual solar fraction of 6%. This can be explained by the auxiliary heater placing at the bottom of tank which makes it impossible to establish any tank stratification. In addition, the cold water pushed in the bottom of the tank is directly heated to the set point temperature of 60°C demanding constantly auxiliary energy every time a draw-off takes place. Also, the inlet collector temperature is 60°C practically all year long which decreases the working hours and its efficiency.

In retrofitted system 2 the auxiliary heater is moved to the tank side-arm aiming to increase stratification. The results show that the annual solar fraction increases only to 15%. This is mainly explained by two factors: the small stratification increase and the losses increase in the side-arm. In this configuration, the upper volume of the tank is always at least at 60°C while the bottom is fairly cold most of the time. This is because hot water is extracted during the whole day and replaced by cold water at the bottom. Hence, the collector pump works many hours when the collector outlet temperature is higher than the tank bottom but lower than 60°C. Due to the inlets geometry of the retrofitted tank, water heated by the collector is placed at the very top of the tank. Consequently, the tank top temperature will decrease and destroy stratification making the auxiliary heater run during most of the year. Also, since the heater is placed at the side arm, hot water is continuously transported through these pipes to the tank. This increase the heat losses and the energy provided to drive the pump.

Simulation results of retrofitted system 3 show that the solar fraction increases to 42%. Since it is difficult to achieve stratification with the connections of the retrofitted tank it is more advantageous to place the heater in another tank. This prevents the heater to be turned on almost continuously when the collector is working at temperatures under 60°C. Hence, the retrofitted tank will work at lower temperatures increasing the collector working hours and efficiency. In addition, a new well insulated hot temperature tank provides the extra energy when solar energy is not available. Having the larger tank working at lower temperatures and the smaller tank at higher temperatures, decrease significantly the heat losses. One can say that the system "stratification" is achieved by two tanks with low stratification but working at different average temperatures. For this particular configuration, the thermostat temperature of the small tank does not influence significantly the annual performance since the tank heat losses are small.

The estimated annual solar fraction for retrofitted system 4 is 53%. The reason why the solar fraction of the series connected system is higher than the parallel connection is not obvious. The main reason is that, during the summer period when solar hot water is available over 60°C, the total solar storage volume of the series connected system is increased to 255 litres, since both tanks are connected in series and no auxiliary energy is needed.

In contrast to what happens with retrofitted system 3, the preset temperature of the heater in retrofitted system 4 significantly influences the annual performance. In fact, if the small heater connected in series is set to 80°C, the solar fraction decreases from 53% to 32% while the parallel connected system decreases only from 42% to 38%. This means that the system performing best depends on the auxiliary storage setup temperature (Figure 7). Simulation shows that if the auxiliary heater temperature is set to 70°C, retrofitted system 3 and 4 have approximate performances. These results are better understood by taking particular examples for different situations. If the temperature inside the retrofitted tank is 70°C and the tank heater temperature set to 60°C (Figure 8a and Figure 8b), there is no need to use auxiliary energy in both systems during a draw-off that requires 50°C. However, the series connected system has the advantage of saving energy since 70°C water enters the small tank and turns off the heater set to 60°C. Also, the total solar storage volume is increased to 255 litres since both tanks are connected in series. On the other hand, if one studies the case of having 70°C in the retrofitted tank but 80°C in the tank heater (Figure 8c and Figure 8d), the result is different. In the parallel connected system (Figure 8c), all the water is drawn from the retrofitted tank with no use of auxiliary energy. In the series connected system (Figure 8d), 70°C water is pushed in the small tank which uses auxiliary energy to heat it up to 80°C.

Generalising the previous example one concludes the following:

- Temperature inside the retrofitted tank lower than the load (T_{solar}<50°C): calculation shows that the parallel connection presents a slightly better performance. The solar hot water is used for preheating and saves energy to the auxiliary heater in both systems.

- Temperature inside the retrofitted tank higher than the load but lower than the set point temperature of the auxiliary heater (50°C>T_{solar}<$T_{auxiliar}$): the parallel connected system performs better since no auxiliary energy is required, contrary to the series connected system.

- Temperature inside the retrofitted tank higher than the set point temperature of the auxiliary heater (T_{solar}>$T_{auxiliar}$): the series connected system performs better since it saves energy to the auxiliary heater and increases the total solar hot water volume to both storages.

Hence, the period when the parallel connection is clearly advantageous over the series connection is during intervals where the temperature inside the retrofitted tank is higher than the load requested temperature but lower than the preset temperature in the tank heater. This period becomes short if the thermostat temperature is set to 60°C and thus the series connected system achieves the highest performance over the year.

At this stage, the important analysis is to compare the performance results of each system rather than focus on their absolute value. This investigation is useful to understand which system performs best and should be built in practice for further analysis. Since the series connected retrofitted system achieves a comparable performance to a new standard solar system, it is worth to further investigate this solution. In the future, model validation and an economical viability study are needed. If the studied system proves to be cost effective, this can be a very attractive solution not only due to its flexibility on retrofitting almost any kind of existing storage tank but also to be combined with new conventional tank heaters which industry is well developed and covers a world-wide market.

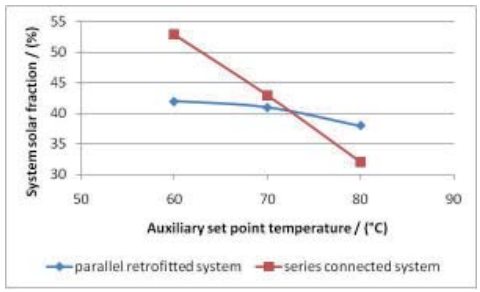

Figure 7. Solar fraction temperature dependence of the parallel and series connected systems.

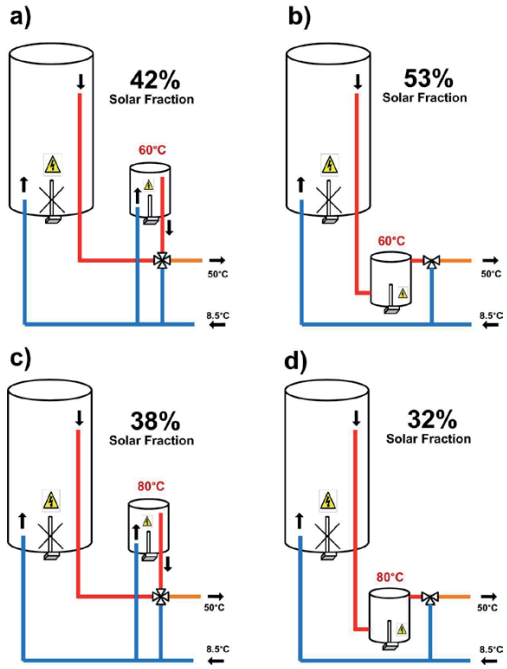

Figure 8. Solar fraction results of:
a) parallel connected system and 60°C thermostat temperature
b) series connected system and 60°C thermostat temperature
c) parallel connected system and 80°C thermostat temperature
d) series connected system and 80°C thermostat temperature

4. Conclusions

Four different system configurations on how to retrofit existing domestic hot water heaters were theoretically analysed. The simulation results show that the best configuration for the retrofitting consists on using the existing tank for solar hot water storage and connect it in series with a small auxiliary heater tank. The system annual performance was compared with that of a conventional solar thermal system. Preliminary results show that its annual solar fraction is 53% compared to 52% of a standard solar thermal system with the same storage volume. This means that both system performances are comparable. Hence, it is worth to further investigate and develop this retrofitting in practice. In the future, the model validation and an economical assessment will be performed. If it proves to be cost-effective, this solution can be very interesting since it can be applied not only in retrofitting existing tank heaters but also in combination with new heaters accessing a world-wide industry.

Acknowledgement

This study was supported by a Marie Curie program, SolNet - Advanced Solar Heating and Cooling for Buildings - the first coordinated international PhD education program on Solar Thermal Engineering. Homepage: http://cms.uni-kassel.de/unicms/?id=2141

References

Klein, S. et al., 1999. TRNSYS, a Transient System Simulation. University of Wisconsin, Madison.
Bernardo, L. R., Davidsson, H. and Karlsson, B., 2010. *Performance Evaluation of a High Solar Fraction CPC-Collector System.* Submitted to Renewable Energy, November 2010.

Cruickshank, C. and Harrison, S., 2004. *Analysis of a Modular Thermal Storage for Solar Heating Systems*. In: proceedings of Canadian Solar Buildings Conference, 2004. Download available at http://www.solarbuildings.ca/c/sbn/file_db/Analysis%20of%20a%20Modular%20Thermal%20Storage%20for%20Solar.pdf

Fraser, K. F., Hollands, K. G. T. And Brunger, A. P., 1995. *An Empirical Model for Natural Convection Heat Exchangers in SDHW Systems*. Solar Energy 55(2), 75-84.

Hausner, R. and Fink, C., 2000. *Stagnation behaviour of thermal solar systems*. Download available at www.aee-intec.at/0uploads/dateien119.pdf

Hausner, R. and Fink, C., 2002. *Stagnation behaviour of solar thermal systems*. IEA SHC, task 26.
Helgesson, A., Karlsson, B. and Nordlander, S., 2002. *Evaluation of a Spring/Fall-MaReCo*. In: proceedings of Eurosun Conference, Bologna.

Klein, S. et al., 1999. TRNSYS, a Transient System Simulation Program. University of Wisconsin, Madison.

Liu, W. and Davidson, J., 1995. *Comparison of Natural Convention Heat Exchangers for Solar Water Heating Systems*. In: proceedings of American Solar Energy Society Conference, 1995. Download available at http://www.p2pays.org/ref/20/19434.pdf

Lin, Q., 1998. *Analysis, Modelling and Optimum Design of Solar Domestic Hot Water Systems*. Ph.D. thesis, ISBN 87-7877-023-8.

Nordlander S. and Bales C., 2007. TRNSYS type 221, distributed by the Solar Energy Research Centre, Sweden.

Perers B. and Bales C., 2002. *A Solar Collector Model for TRNSYS Simulation and System Testing*. A Report of IEA SHC - Task 26 Solar Combisystems. Download available at http://www.les.ufpb.br/portal/index2.php?option=com_docman&task=doc_view&gid=190&Itemid=30

Statistics Sweden, 2006. *Boende och boendeutgifter 2006, BO 23 SM 0801*. Download available at http://www.scb.se/statistik/HE/HE0103/2006A03/HE0103_2006A03_SM_BO23SM0801.pdf

Stengård, L., 2009. *Mätning av kall- och varmevattenanvändning i 44 hushåll*. Acessed in 2009/10 from http://webbshop.cm.se/System/ViewResource.aspx?p=Energimyndigheten&rl=default:/Resources/Permanent/Static/b9a064ece4d747868b5c20d1a03ab0a2/2124W.pdf

Swedish Building Regulation, 2008. *Regelsamling för byggande, BBR 2008*. ISBN 978-91-86045-03-6. Download available at http://online.sis.se/pdf/bbr.pdf

Swedish Energy Agency, 2009a. *Energy statistics for one- and two- dwelling buildings in 2008*. Accessed in 2010/02 from http://webbshop.cm.se/System/ViewResource.aspx?p=Energimyndigheten&rl=default:/Resources/Permanent/Static/60373ee0cdc743898284fec420067527/2128W.pdf

Swedish Energy Agency, 2009b. *FEBY – Krav Specifikation för Minienergihus.* Download available at http://www.energieffektivabyggnader.se/download/18.712fb31f12497ed09a58000141/Kravspecifikation_Minienergihus_version_2009_oktober.pdf

Widén, J., Lundh, M., Vassileva, I., Dahlquist, E., Ellegård, K. and Wäckelgård, E., 2009. *Constructing load profiles for household electricity and hot water from time-use data—Modelling approach and validation.* Energy and Buildings 41(7), pp 753-768.

LUND UNIVERSITY

ISSN 1671-8136
ISBN 978-91-85147-47-2